

TESTING STATIONARITY AND CHANGE POINT DETECTION IN REINFORCEMENT LEARNING

BY MENGBING LI^{*1,a}, CHENGCHUN SHI^{*2,c} AND ZHENKE WU^{1,b} PIOTR FRYZLEWICZ^{2,d}

¹*Department of Biostatistics, University of Michigan, mengbing@umich.edu; zhenkewu@umich.edu*

²*Department of Statistics, London School of Economics and Political Science, c.shi7@lse.ac.uk; p.fryzlewicz@lse.ac.uk*

We consider offline reinforcement learning (RL) methods in possibly nonstationary environments. Many existing RL algorithms in the literature rely on the stationarity assumption that requires the system transition and the reward function to be constant over time. However, this assumption is restrictive in practice and is likely to be violated in a number of applications, including traffic signal control, robotics and mobile health. In this paper, we develop a model-free test to assess the stationarity of the optimal Q-function based on pre-collected historical data, without additional online data collection. Based on the proposed test, we further develop a sequential change point detection method that can be naturally coupled with existing state-of-the-art RL methods designed in stationary environments for policy optimization in nonstationary environments. The usefulness of our method is illustrated by theoretical results, simulation studies, and a real data example from the 2018 Intern Health Study. A Python implementation of the proposed procedure is available at <https://github.com/limengbinggz/CUSUM-RL>.

1. Introduction. Reinforcement learning (RL, see [Sutton and Barto, 2018](#), for an overview) is a powerful machine learning technique that allows an agent to learn and interact with a given environment, to maximize the cumulative reward the agent receives. It has been one of the most popular research topics in the machine learning and computer science literature over the past few years. Significant progress has been made in solving challenging problems across various domains using RL, including games, recommender systems, finance, healthcare, robotics, transportation, among many others (see [Li, 2019](#), for an overview). In contrast, statistics as a field has only begun to engage with RL both in depth and in breadth. Most RL works in the statistics literature focused on developing data-driven methodologies for precision medicine (see e.g., [Murphy, 2003](#); [Robins, 2004](#); [Chakraborty, Murphy and Strecher, 2010](#); [Qian and Murphy, 2011](#); [Zhang et al., 2013](#); [Zhao et al., 2015](#); [Wallace and Moodie, 2015](#); [Song et al., 2015](#); [Luedtke and van der Laan, 2016](#); [Zhu et al., 2017](#); [Zhang et al., 2018](#); [Shi et al., 2018](#); [Wang et al., 2018](#); [Qi et al., 2020](#); [Nie, Brunskill and Wager, 2021](#); [Fang, Wang and Wang, 2022](#)). See also [Tsiatis et al. \(2019\)](#) and [Kosorok and Laber \(2019\)](#) for overviews. These aforementioned methods were primarily motivated by applications in precision medicine with only a few treatment stages. They require a large number of patients in the observed data to achieve consistent estimation and become ineffective in the long or infinite horizon setting where the number of decision stages diverges with the number of observations. The latter setting is widely studied in the computer science literature to formulate many sequential decision making problems in games, robotics, ridesharing, etc. Recently, several algorithms have been proposed in the statistics literature for policy optimization or evaluation in long horizon settings ([Ertefaie and Strawderman, 2018](#); [Luckett et al., 2020](#); [Liao et al., 2022](#); [Hu et al., 2021](#); [Liao, Klasnja and Murphy, 2021](#); [Ramprasad](#)

*The first two authors contribute equally to this paper.

Keywords and phrases: Reinforcement learning, Nonstationarity, Hypothesis testing, Change point detection.

et al., 2021; Chen, Song and Jordan, 2022; Shi et al., 2022; Zhou, Zhu and Qu, 2022; Hu and Wager, 2023; Li et al., 2023; Liu et al., 2023; Wang, Qi and Wong, 2023).

Central to the empirical validity of most existing state-of-the-art RL algorithms is the stationarity assumption that requires the state transition and reward functions to be constant functions of time. Although this assumption is valid in online video games, it can be violated in a number of other applications, including traffic signal control (Padakandla, Prabuchandran and Bhatnagar, 2020), robotic navigation (Niroui et al., 2019), mobile health (mHealth, Liao et al., 2020), e-commerce (Chen, Wang and Zhou, 2020) and infectious disease control (Cazelles, Champagne and Dureau, 2018). According to Sutton and Barto (2018), “*nonstationarity is the case most commonly encountered in reinforcement learning*”. We consider a few examples to elaborate.

One motivating example considered in our paper comes from the Intern Health Study (IHS; NeCamp et al., 2020). The period of medical internship, which marks the initial phase of professional medical training in the United States, is a highly demanding and stressful time for physicians. During this phase, residents are confronted with challenging decisions, extended work hours, and sleep deprivation. In this ongoing prospective longitudinal study, one primary objective is to determine the optimal timing for providing smartphone-delivered interventions. These interventions involve sending mobile prompts through a customized study app, aimed at offering timely tips to encourage interns to adopt anti-sedentary routines that may enhance their physical well-being. Nonstationarity poses a significant challenge within the context of the mHealth study. Specifically, as individuals receive mobile-delivered interventions for longer duration, they may habituate to the prompts or become overwhelmed, resulting in reduced responsiveness to the contents of the suggestions (Klasnja et al., 2019; Qian et al., 2022). Consequently, the treatment effect of activity suggestions may transition from positive to negative over time. To maximize the effectiveness of interventions, ideal treatment policies would be those adapting swiftly to the current circumstances of the subjects based on the most recent data collected. Failing to recognize potential nonstationarity in treatment effects over time may lead to policies that overburden medical interns, resulting in app deletion and study dropouts.

As another example, the coronavirus disease 2019 (COVID-19) emerged as one of the most severe global pandemics in history and infected hundreds of millions of people worldwide. In response to this crisis, there was a growing interest in utilizing RL to develop data-driven intervention policies to contain the spread of the virus (see e.g., Eftekhari et al., 2020; Kompella et al., 2020; Wan, Zhang and Song, 2020). However, the dynamics of COVID-19 transmission were highly intricate and exhibited nonstationary over time. Initially, strict lockdown measures were proven to be highly effective in controlling the spread of the virus (Kharroubi and Saleh, 2020). However, these measures had significant economic costs (Eichenbaum, Rebelo and Trabandt, 2020). As effective vaccines were developed and a substantial proportion of the population became vaccinated, a natural inclination was to ease these lockdown restrictions. Nonetheless, the efficacy of the vaccine was likely to diminish over time, particularly in the presence of new viral variants. To summarize, policymakers needed to dynamically adapt public health policies by taking the nonstationary nature of the COVID-19 spread into consideration, in order to enhance global health outcomes while carefully balancing the negative impacts on the economy and society.

In this paper, we consider situations where the optimal Q-function Q^{opt} (the expected cumulative reward under the optimal policy, see Section 2.3 for its detailed definition) is possibly nonstationary, as a result of potential changes in the state transition or reward functions. These functions can change at an arbitrarily unknown time point (referred to as a change point), and the changes can be abrupt or smooth. A number of time series works have focused on testing the stationarity of a given time series and detecting the change point locations in

various models, ranging from the simple piecewise-constant signal plus noise setting (Killick, Fearnhead and Eckley, 2012; Fryzlewicz, 2014) to complex high-dimensional panel data and time series (Cho and Fryzlewicz, 2015; Wang and Samworth, 2018); see Aminikhanghahi and Cook (2017) and Truong, Oudre and Vayatis (2020) for comprehensive reviews. Different from the aforementioned works in time series, Q^{opt} takes some value of the state-action pair as input. To test its stationarity, we need to check whether it is constant over time, for each possible value of the state-action pair.

Our methodological contributions are summarized as follows:

1. We propose a novel test to assess the stationarity of the optimal Q-function. To the best of our knowledge, this is the first work on developing statistically sound tests for stationarity in offline RL – a domain where policies are learned from previously collected datasets, instead of actively collected data in real-time as in online RL. Our proposal is an example of harnessing the power of classical statistical inferential tools such as hypothesis testing to help address an important practical issue in RL.
2. We apply our proposed test to compute p -values and identify the most recent historical change point location from a set of potential change point candidates for subsequent policy learning in nonstationary environments.

Our technical contributions are summarized as follows:

1. We present and systematically examine various types of stationarity assumptions, analyzing their interrelationships.
2. We establish the size and power properties of the proposed tests under a bidirectional asymptotic framework that allows either the number of data trajectories or the number of decision points per trajectory to diverge to infinity. This is useful for different types of applications. For example, disease management studies using registry data (e.g., Cooperberg et al., 2004) or infectious disease control studies (e.g., Lopes-Júnior et al., 2020) often involve a large number of subjects and the objective is to develop an optimal policy at the population level to maximize the overall long-term reward. Conversely, there are other applications where the number of subjects is limited yet the number of decision points is large (see e.g., Marling and Bunesco, 2020), as in our real data application.
3. We develop a matrix concentration inequality for nonstationarity Markov decision processes (see Lemma 18 in the supplementary article) in order to establish the consistency of the proposed test. The derivation is non-trivial and naively applying the concentration inequality designed for scalar random variables (Alquier, Doukhan and Fan, 2019) would yield a loose error bound. See Section C.5 for details.
4. We derive the limiting distribution of the estimated optimal Q-function computed via the fitted Q-iteration (FQI, Ernst, Geurts and Wehenkel, 2005) algorithm, one of the most popular Q-learning type algorithms. See Theorem 5 in Appendix B; see also Equation (12).

The proposed test and change point detection procedure are useful in practical situations. In particular, the proposed test is useful in identifying nonstationary environments. Existing RL algorithms designed for stationary environments are no longer valid in nonstationary environments. While some recent proposals (see e.g., Domingues et al., 2021) allow for nonstationarity, they may be less efficient in stationary settings. By examining the stationarity assumption, our proposed test provides valuable insights into the system’s dynamics, enabling practitioners to select the most suitable state-of-the-art RL algorithms for implementation. Specifically, if the stationarity assumption is not rejected, standard RL algorithms (e.g., Q-learning, policy gradient methods) can be implemented to ensure efficiency of policy learning. Otherwise, RL algorithms designed for nonstationary environments (e.g., Domingues et al., 2021) should be preferred.

Additionally, the proposed change point detection procedure identifies the most recent “best data segment of stationarity”. It can be integrated with state-of-the-art RL algorithms for policy learning in nonstationary environments; see Section 3.4 for details. We apply this procedure to both synthetic and real datasets in Sections 5 and 6, respectively. Results show that the estimated policy based on our constructed data segment is comparable or often superior to baseline methods that either ignore nonstationarity or do not perform change point detection. In the motivating IHS study, the proposed method reveals the benefit of nonstationarity detection for optimizing population physical activities for interns in some medical specialties. The promotion of healthy behaviors and the mitigation of negative chronic health outcomes typically require continuous monitoring over a long term where nonstationarity is likely to occur. As RL continues to drive development of optimal interventions in mHealth studies, this paper substantiates the need and effectiveness of incorporating a simple statistical solution to accommodate nonstationarity.

The rest of the paper is organized as follows. In Section 2, we introduce the offline RL problem and review some existing algorithms. In Section 3, we detail our procedures for hypothesis testing and change point detection. We establish the theoretical properties of our procedure in Section 4, conduct simulation studies in Section 5, and apply the proposed procedure to the IHS data in Section 6.

2. Problem Formulation. We start by introducing the data generating process and the concept of policy in RL. We next review Q-learning (Watkins and Dayan, 1992), a widely recognized RL algorithm useful in our proposed approach. Finally, we discuss five types of stationarity assumptions and introduce our testing hypotheses.

2.1. *Data.* We consider an offline setting to learn an optimal policy based on a pre-collected dataset from a randomized trial or observational study. The offline dataset is summarized as $\mathcal{D} = \{(S_{i,t}, A_{i,t}, R_{i,t})\}_{1 \leq i \leq N, 0 \leq t \leq T}$, where $(S_{i,t}, A_{i,t}, R_{i,t})$ denotes the state-action-reward triplet at time t of the i th subject. Without loss of generality, we assume all subjects share the same termination time T , which is reasonable in many mHealth studies. In Section A.2 of the supplementary article, we extend our proposal to settings where subjects have different termination times. In IHS, the state corresponds to some time-varying covariates associated with each medical intern, such as their mood score, step counts, and sleep minutes. The action is a binary variable, corresponding to whether to send a certain text message to the intern or not. The immediate reward is the step counts. We assume all rewards are uniformly bounded, as commonly adopted in the RL literature to simplify theoretical analysis (see e.g., Fan et al., 2020).

The trajectories of the N interns $\{(S_{i,t}, A_{i,t}, R_{i,t})\}_{1 \leq i \leq N, t \geq 0}$ are assumed to be i.i.d copies of an infinite horizon Markov decision process (MDP, Puterman, 2014) $\{(S_t, A_t, R_t)\}_{t \geq 0}$ whose data generating process can be described as follows:

1. **State Presentation:** At each time t , the environment (represented as an intern in our example) is in a state $S_t \in \mathcal{S}$ where $\mathcal{S} \in \mathbb{R}^d$ denotes the state space and d denotes the dimension.
2. **Action Selection:** The agent (or decision maker) then selects an action A_t from the action space \mathcal{A} based on the observed data history H_t including S_t and the state-action-reward triplets up to time $t - 1$.
3. **Reward Generation:** The agent receives an immediate reward $R_t \in \mathbb{R}$ with its expected value specified by an unknown reward function r_t :

$$(1) \quad \mathbb{E}(R_t | H_t, A_t) = r_t(S_t, A_t).$$

4. **State Transition:** Subsequently, the environment transitions to the next state S_{t+1} , determined by an unknown transition function \mathcal{T}_t :

$$(2) \quad S_{t+1} = \mathcal{T}_t(S_t, A_t, \delta_t),$$

where $\{\delta_t\}_t$ is a sequence of i.i.d. random noises, with each δ_t being independent of $\{(S_j, A_j, R_j)\}_{j \leq t}$.

REMARK 1. *By definition, \mathcal{T}_t specifies the conditional distribution of the future state given the current state-action pair, and r_t is the conditional mean function of the reward. Both (1) and (2) impose certain Markov or conditional independence assumptions on the data trajectories, implying that the future state and the conditional mean of the current reward are independent of the H_t given the current state-action pair. These assumptions are testable from the observed data (Chen and Hong, 2012; Shi et al., 2020; Zhou et al., 2023).*

2.2. *Policy.* A policy defines how actions are chosen at each decision time. In particular:

1. A **history-dependent policy** π is a sequence of decision rules $\{\pi_t\}_{t \geq 0}$ such that each π_t takes H_t as input, and outputs a probability distribution on the action space, denoted by $\pi_t(\bullet|H_t)$. Under π , the decision maker will set $A_t = a$ with probability $\pi_t(a|H_t)$ at time t .
2. A **Markov policy** π is a special history-dependent policy where each π_t depends on H_t only through the current state S_t .
3. A **stationary policy** π is a special Markov policy where $\{\pi_t\}_t$ are time-invariant, i.e., there exists some function π^* such that $\pi_t(\bullet|H_t) = \pi^*(\bullet|S_t)$ almost surely for any t , and we use $\pi(\bullet|S_t)$ to denote the resulting decision rule.
4. An **optimal policy** $\pi^{opt} = \{\pi_t^{opt}\}_t$ maximizes the expected γ -discounted cumulative reward $J_\gamma(\pi) = \sum_{t \geq 0} \gamma^t \mathbb{E}^\pi(R_t)$ among all history-dependent policies π , given a discount factor $0 < \gamma \leq 1$ which balances the trade-off between the immediate and future rewards. The expectation \mathbb{E}^π is calculated under the assumption that the agent makes decisions in accordance with the policy π .
5. The **behavior policy**, denoted as $b = \{b_t\}_t$, denotes the policy the agent adopted for all individuals in the offline dataset. This policy is not necessarily optimal and may be a purely random policy in scenarios like sequential multiple assignment randomized trials (SMARTs, Collins, Murphy and Strecher, 2007).

REMARK 2. *Under (1) and (2), there exists an optimal Markov policy π^{opt} whose $J_\gamma(\pi^{opt})$ is no worse than that of any history-dependent policy; see Theorem 6.2.10 of Puterman (2014). This substantially simplifies the calculation of the optimal policy. Hence, throughout this paper, ‘optimal policy’ specifically refers to the optimal Markov policy, meaning that each π_t^{opt} is a function of the current state S_t only. Note that the proof in Puterman (2014) relies on the assumption that the reward is a deterministic function of the state-action-next-state triplet. However, this assumption can be effectively relaxed to (1) while still preserving the validity of the proof.*

2.3. *Q-Learning.* We review Q-learning, one of the most popular RL algorithms. It is model-free in that the optimal policy is derived without directly estimating the MDP model (i.e., transition and reward functions). Central to Q-learning is the state-action value function, commonly known as the Q-function. Given a policy π , its Q-function $Q^\pi = \{Q_t^\pi\}_{t \geq 0}$ is defined such that each Q_t^π is the expected cumulative reward given a state-action pair following π , i.e., $Q_t^\pi(a, s) = \mathbb{E}^\pi \left(\sum_{k \geq 0} \gamma^k R_{t+k} | A_t = a, S_t = s \right)$. The optimal Q-function, denoted by

$Q^{\pi^{opt}}$ or simply Q^{opt} , corresponds to the Q-function under the optimal policy. The optimal Q-function possesses two key properties¹: (i) π^{opt} is greedy with respect to Q^{opt} , i.e., for any $t \geq 0$,

$$(3) \quad \pi_t^{opt}(a|s) = \begin{cases} 1, & \text{if } a = \arg \max_{a'} Q_t^{opt}(a', s); \\ 0, & \text{otherwise.} \end{cases}$$

(ii) The Bellman optimality equation holds, stating that the expected Q-value at time t equals the immediate reward plus the maximum Q-value of the next state:

$$(4) \quad \mathbb{E} \left\{ R_t + \gamma \max_a Q_{t+1}^{opt}(a, S_{t+1}) | A_t, S_t \right\} = Q_t^{opt}(A_t, S_t), \quad \forall t \geq 0.$$

Equations (3) and (4) form the basis of Q-learning, which estimates $\{Q_t^{opt}\}_t$ by solving the Bellman optimality equation (4) and computes π^{opt} based on the estimated optimal Q-function using (3). Assuming the stationarity of the optimal Q-function, i.e., $Q_t^{opt} = Q^{opt}$ for any t , various algorithms have been developed under this framework, such as tabular Q-learning (Watkins and Dayan, 1992), fitted Q-Iteration (FQI), greedy gradient Q-learning (GGQ, Maei et al., 2010; Ertefaie and Strawderman, 2018), double Q-learning (Hasselt, 2010) and deep Q-network (DQN, Mnih et al., 2015). GGQ is based on the stochastic gradient descent algorithm for parameter estimation. It employs the weight-doubling trick (Sutton, Szepesvári and Maei, 2008) to alleviate the potential bias of the sub-gradient. On the other hand, FQI, which our paper implements, iteratively updates the optimal Q-function estimator based on (4). Beginning with an initial Q-function estimator $Q^{(0)}$ (typically set to zero), we compute $Q^{(k+1)}$ by minimizing

$$(5) \quad Q^{(k+1)} = \arg \min_Q \sum_{i,t} \left\{ R_{i,t} + \gamma \max_a Q^{(k)}(a, S_{i,t+1}) - Q(A_{i,t}, S_{i,t}) \right\}^2,$$

during the k th iteration. The above optimization can be cast into a supervised learning problem with $\{R_{i,t} + \gamma \max_a Q^{(k)}(a, S_{i,t+1})\}_{i,t}$ as the responses and $\{(A_{i,t}, S_{i,t})\}_{i,t}$ as the predictors. In Appendix B, we establish the limiting distribution of the resulting Q-function estimator when employing the method of sieves for function approximation in a stationary MDP.

2.4. The Stationarity Assumption. Starting from a given time point $T_0 \geq 0$, we introduce five types of stationarity assumptions:

SA1 (Stationary MDPs): The transition function \mathcal{T}_t and the reward function r_t remain constant over time, for all $t \geq T_0$.

SA2 (Stationary Q-functions): For any stationary policy π (see the definition in Section 2.2), the associated Q-function Q_t^π is constant as a function of t , for all $t \geq T_0$.

SA3 (Stationary optimal Q-functions): $Q_{T_0}^{opt} = Q_{T_0+1}^{opt} = \dots = Q_t^{opt} = \dots$.

SA4 (Stationary optimal policies): $\pi_{T_0}^{opt} = \pi_{T_0+1}^{opt} = \dots = \pi_t^{opt} = \dots$.

SA5 (Stationary behavior policies): $b_{T_0} = b_{T_0+1} = \dots = b_t = \dots$.

The following theorem demonstrates a sequential relationship among the first four assumptions.

¹Typically, these properties are verified in a stationary setting, see e.g., Theorem 1.8 of Agarwal et al. (2019). However, by simply incorporating the time index into the state definition, the proofs of these theorems can be readily adapted to nonstationary MDPs defined in Section 2.1 as well.

THEOREM 1 (Stationarity relationships). *Assume both the state space and the action space are finite, and the rewards are uniformly bounded. Then SA1 implies SA2, SA2 implies SA3, and SA3 implies SA4.*

REMARK 3. *Throughout this paper, stationary MDPs refer to MDP models with stationary transition and reward functions. Therefore, SA1 represents a “model-based” stationarity assumption, as it directly relates to the MDP model. It is the most prevalently employed form of stationarity in the literature (Sutton and Barto, 2018). Importantly, this concept does not require the stationarity of the behavior policy (SA5), which characterizes the decisions or strategies put forth by the agent and operates independently of the environmental factors. Moreover, SA5 does not influence SA2 – SA4. As a result, the optimal policy may be stationary or nonstationary, regardless of the stationarity status of the behavior policy.*

REMARK 4. *SA2 and SA3 are characterized as model-free stationary assumptions, as they are defined without direct reference to the transition or reward functions. Theorem 1 suggests that these assumptions are automatically satisfied under SA1. Furthermore, it is a well-established fact that in stationary MDPs, the optimal policy is stationary as well (Puterman, 2014). The proof that SA2 leads to SA3, however, is not straightforward. Drawing inspiration from the policy iteration algorithm (Sutton and Barto, 2018, Section 4.3), we define a sequence of policies whose Q-functions converge to the optimal Q-function. This approach enables us to establish the connection between a non-optimal Q-function and its optimal counterpart, thereby proving the stationarity of the optimal Q-function in a potentially non-stationary MDP (i.e., when SA2 holds, but SA1 does not). We refer readers to Appendix C.1 for details.*

2.5. Hypothesis Testing under Nonstationarity. As commented in the introduction, the stationarity assumption can be restrictive in practice. This motivates us to test stationarity based on offline datasets. Given the five different types of stationarity assumptions we have identified, there are correspondingly five different hypotheses to test. In this paper, we focus on testing SA3 due to the following considerations:

- Testing SA1 poses considerable challenges in scenarios with moderate to high-dimensional states, as the transition function’s outputs are multidimensional with dimension matching that of the state.
- Testing SA2 is extremely difficult due to the need to enumerate over all possible policies, whose number increases exponentially with the cardinality of the state space.
- Based on (3), the optimal policy is intrinsically tied to the optimal Q-function. Theorem 1 further implies that SA4 follows from SA3. Thus, by testing SA3, we can effectively assess the stationarity of the optimal policy.
- Optimal testing of SA4 is complex since the optimal policy is a highly nonlinear functional of the observed data, complicating the derivation of its estimator’s limiting distribution. Moreover, π^{opt} may lack uniqueness even when $\{Q_t^{opt}\}_t$ is uniquely determined.
- Testing SA5 is meaningless because the stationarity of the behavior policy does not influence that of the optimal policy.

Thus, our testing hypotheses are formulated as follows:

$$(6) \quad \mathcal{H}_0 : Q_t^{opt} = Q^{opt}, \forall t \geq T_0, \text{ versus } \mathcal{H}_1 : Q_t^{opt} \text{ has at least one smooth} \\ \text{or abrupt change point for } t \geq T_0 \text{ (see Figure 7).}$$

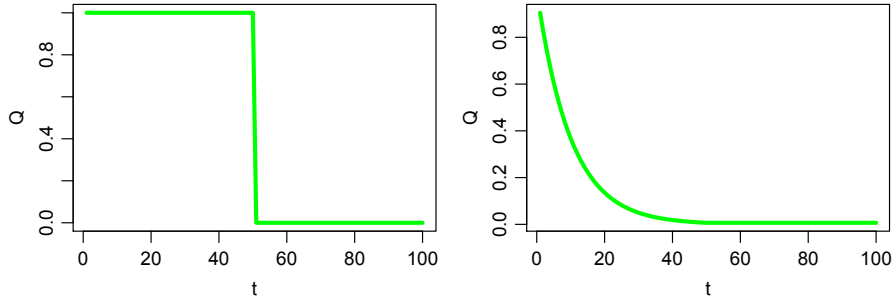


Fig 1: Examples of Q^{opt} at a given state-action pair with an abrupt change point (left panel) and a gradual change point (right panel). $T_0 = 0$ in both examples.

Algorithm 1 Testing Stationarity of the Optimal Policy via the Optimal Q-Function.

Input: The offline data $\{(S_{i,t}, A_{i,t}, R_{i,t})\}_{1 \leq i \leq N, T_0 \leq t \leq T}$, and the significance level $0 < \alpha < 1$.

Step 1. For each $u \in [T_0 + \epsilon T, (1 - \epsilon)T]$, employ the fitted Q-iteration or gradient Q-learning algorithm to compute the estimated Q-functions $\hat{Q}_{[T_0, u]}$ and $\hat{Q}_{[u, T]}$ on separate time segments.

Step 2. Construct one of the CUSUM-type test statistics TS_1 , TS_∞ or TS_n , according to (7), (8) or (9).

Step 3. Employ multiplier bootstrap to compute the bootstrapped test statistics TS_1^b , TS_∞^b or TS_n^b , and calculate the p -value according to (14).

Output: Reject the null hypothesis if the p -value is smaller than α .

3. Proposed Stationarity Test and Change Point Detection. In this section, we start by proposing three types of test statistics for testing (6). Next, we present key computation steps in constructing these tests. Finally, we present our change point detection method, built upon the proposed test.

3.1. Test Statistics. All test statistics we propose require an estimated optimal Q-function, denoted as $\hat{Q}_{[T_1, T_2]}(a, s)$ (here we drop the superscript opt in Q^{opt} for simplicity), using data collected in the interval $[T_1, T_2] \subseteq [T_0, T]$. For any candidate change point $u \in (T_0 + \epsilon T, (1 - \epsilon)T)$, where $\epsilon > 0$ is a pre-specified boundary-removal constant, we use $\hat{Q}_{[u, T]}(a, s) - \hat{Q}_{[T_0, u]}(a, s)$ to measure the difference in the optimal Q-function after and before the candidate. Based on this measure, we introduce three test statistics: an ℓ_1 -type, a maximum-type, and a normalized maximum-type, given by

$$(7) \quad TS_1 = \max_{T_0 + \epsilon T < u < (1 - \epsilon)T} \tau_u \left[\frac{1}{N(T - T_0)} \sum_{i,t} |\hat{Q}_{[T_0, u]}(A_{i,t}, S_{i,t}) - \hat{Q}_{[u, T]}(A_{i,t}, S_{i,t})| \right],$$

$$(8) \quad TS_\infty = \max_{T_0 + \epsilon T < u < (1 - \epsilon)T} \max_{a,s} \tau_u |\hat{Q}_{[T_0, u]}(a, s) - \hat{Q}_{[u, T]}(a, s)|,$$

$$(9) \quad TS_n = \max_{T_0 + \epsilon T < u < (1 - \epsilon)T} \max_{a,s} \tau_u \hat{\sigma}_u^{-1}(a, s) |\hat{Q}_{[T_0, u]}(a, s) - \hat{Q}_{[u, T]}(a, s)|,$$

respectively, where $\tau_u = \sqrt{\frac{(u - T_0)(T - u)}{(T - T_0)^2}}$ is the scale factor being dependent on the proximity of u to the interval boundary, $\hat{\sigma}_u^2(a, s)$ denotes a consistent variance estimator of $\hat{Q}_{[T_0, u]}(a, s) - \hat{Q}_{[u, T]}(a, s)$ whose detailed form is given in Appendix C.2.2.

Under a given significance level α , the critical values and p -values for TS_1 , TS_∞ and TS_n are computed using a multiplier bootstrap method (detailed in Section 3.3) to approximate their asymptotic distributions. This multiplier bootstrap is easy to implement. Unlike

other methods such as the nonparametric bootstrap, it does not require to re-estimate the Q -function, thereby simplifying the estimation procedure. We reject the null hypothesis when the test statistic exceeds its corresponding critical value (or equivalently, the p -value falls below α).

REMARK 5. *The three test statistics (7)–(9) are very similar to the classical cumulative sum (CUSUM) statistic in change point analysis (Csörgő, Csörgő and Horváth, 1997). The weight scale τ_u assigns smaller weights on data points near the boundary of the interval $(T_0 + \epsilon T, (1 - \epsilon)T)$. Removing the boundary is necessary as it is difficult to accurately estimate the Q -function when close to the boundary. Such practice is commonly employed in the time series literature for change point detection in non-Gaussian settings (see e.g., Cho and Fryzlewicz, 2012; Yu and Chen, 2021).*

REMARK 6. *In addition, the three test statistics differ in how they aggregate the estimated changes $|\widehat{Q}_{[T_0, u]} - \widehat{Q}_{[u, T]}|$ across different state-action pairs. The ℓ_1 -type test (7) computes the average of the changes, weighted by the empirical state-action distribution. The two maximum-type tests (8) and (9) focus on the largest change in the (normalized) absolute value. Normalization can enhance efficiency, especially in cases where some state-action pairs (a, s) are less frequently visited. In these cases, the standard error of the difference $\widehat{Q}_{[T_0, u]}(a, s) - \widehat{Q}_{[u, T]}(a, s)$ tends to be large. As a consequence, the estimated maximizer $\arg \max_{a, s} |\widehat{Q}_{[T_0, u]}(a, s) - \widehat{Q}_{[u, T]}(a, s)|$ may differ significantly from the oracle maximizer $\arg \max_{a, s} |Q_{[T_0, u]}^{opt}(a, s) - Q_{[u, T]}^{opt}(a, s)|$, leading to reduced power in the unnormalized test. Additionally, the normalized test requires weaker conditions to control the type I error and detect the alternative hypothesis, as discussed in Section 4. We also remark that the studentized supremum-type statistics have been commonly employed in the econometrics literature (see e.g., Belloni et al., 2015; Chen and Christensen, 2015, 2018).*

REMARK 7. *To conclude this section, we remark that the proposed test is model-free, as it constructs the test statistic without directly estimating the reward and transition functions. Alternatively, one may consider model-based tests. We provide a detailed comparison of model-free and model-based tests in Section A.1 of the supplementary article.*

3.2. *Estimation of the Q -Function.* We provide more details on estimating Q^{opt} in this section. In particular, we focus on a discrete action space $\mathcal{A} = \{0, 1, \dots, m - 1\}$ with m available actions. We advocate the use of the sieve method (Grenander, 1981) to model Q^{opt} , primarily for two benefits. First, the sieve method ensures the resulting Q -estimator has a tractable limiting distribution (see Theorem 5), which allows us to derive the asymptotic distribution of the test statistic. Second, the sieve method is useful in mitigating bias caused by model misspecification, achievable by increasing the number of basis functions.

Specifically, we propose to model $Q^{opt}(a, s)$ by $\phi_L^\top(a, s)\beta^*$ for some $\beta^* \in \mathbb{R}^{m \times L}$ where

$$(10) \quad \phi_L(a, s) = [\mathbb{I}(a = 0)\Phi^\top(s), \mathbb{I}(a = 1)\Phi^\top(s), \dots, \mathbb{I}(a = m - 1)\Phi^\top(s)]^\top,$$

is an mL -dimensional vector constructed using products between the action indicator $\mathbb{I}(a = \bullet)$ and a vector of L basis functions Φ on the state space. Several choices can be considered here for Φ . For continuous state spaces, options for Φ include power series, Fourier series, splines or wavelets (see e.g., Judd, 1998). For discrete state spaces, one could use a lookup table and set $\phi_L(a, s) = [\mathbb{I}\{(a, s) = (a', s')\}; a' \in \mathcal{A}, s' \in \mathcal{S}]^\top$. In Section 4.2, we show that the proposed test is not overly sensitive to the choice of the number of basis functions L . In practice, we can determine L using cross-validation, as illustrated in our simulation studies.

For a given time interval $[T_1, T_2] \subseteq [T_0, T]$, we compute an estimator $\widehat{\beta}_{[T_1, T_2]}$ for β^* using data collected from this interval. A key observation is that, when $Q^{opt}(a, s) = \phi_L^\top(a, s)\beta^*$, the Bellman optimality equation (4) implies that β^* satisfies

$$\mathbb{E} \left[R_t + \gamma \max_a \phi_L^\top(a, S_{t+1})\beta^* - \phi_L(A_t, S_t)^\top \beta^* \mid A_t, S_t \right] = 0.$$

To derive the mL estimating equations, we multiply both sides of the equation by $\nabla_{\beta^*} Q^{opt}(A_t, S_t) = \phi_L(A_t, S_t)$ as in [Ertefaie and Strawderman \(2018\)](#) and take the expectation, resulting in

$$\mathbb{E} \left[R_t + \gamma \max_a \phi_L^\top(a, S_{t+1})\beta^* - \phi_L(A_t, S_t)^\top \beta^* \right] \phi_L(A_t, S_t) = 0.$$

Consequently, $\widehat{\beta}_{[T_1, T_2]}$ can be computed by solving the following estimating equation,

$$(11) \quad \sum_{i=1}^N \sum_{t=T_1}^{T_2-1} \left\{ R_{i,t} + \gamma \max_a \phi_L^\top(a, S_{i,t+1})\beta - \phi_L^\top(A_{i,t}, S_{i,t})\beta \right\} \frac{\phi_L(A_{i,t}, S_{i,t})}{N(T_2 - T_1)} = 0.$$

Under the null hypothesis, equation (11) has zero mean on the left-hand-side (LHS) when $\beta = \beta^*$. The solution to (11) is also unique under certain matrix invertibility condition (see Assumption A5(ii) in Section 4.2). Hence, $\widehat{\beta}_{[T_1, T_2]}$ is consistent. However, computation of $\widehat{\beta}_{[T_1, T_2]}$ is challenging due to the non-smooth max operator in the curly bracket. To address this, several estimation algorithms, including FQI and GGQ, are available. We employ the former in our implementation.

3.3. Bootstrap Approach to Critical Value. We employ a multiplier bootstrap method ([Wu, 1986](#); [Chernozhukov, Chetverikov and Kato, 2014](#)) to obtain the p -values. The idea is to simulate Gaussian random noises to approximate the limiting distribution of the Q-function estimator, and subsequently to approximate that of the test statistic. A key observation is that, under the null hypothesis, when the Q-function is well-approximated and the optimal policy is unique, the estimated Q-function $\phi_L(a, s)^\top \widehat{\beta}_{[T_1, T_2]}$ has the following linear representation:

$$(12) \quad \begin{aligned} & \phi_L(a, s)^\top \widehat{\beta}_{[T_1, T_2]} - Q^{opt}(a, s) \\ &= \frac{1}{N(T_2 - T_1)} \phi_L^\top(a, s) W_{[T_1, T_2]}^{-1} \sum_{i=1}^N \sum_{t=T_1}^{T_2-1} \phi_L(A_{i,t}, S_{i,t}) \delta_{i,t}^* + o_p(1), \end{aligned}$$

where

$$W_{[T_1, T_2]} = \frac{1}{T_2 - T_1} \sum_{t=T_1}^{T_2-1} \mathbb{E} \phi_L(A_{i,t}, S_{i,t}) \{ \phi_L(A_{i,t}, S_{i,t}) - \gamma \phi_L(\pi^{opt}(S_{i,t+1}), S_{i,t+1}) \}^\top,$$

$\delta_{i,t}^* = R_{i,t} + \gamma \max_a Q^{opt}(a, S_{i,t+1}) - Q^{opt}(A_{i,t}, S_{i,t})$ is the temporal difference error. By the Bellman optimality equation (4), the leading term on the right-hand-side (RHS) of (12) forms a mean-zero martingale. When its quadratic variation process converges, it follows from the martingale central limit theorem ([McLeish, 1974](#)) that $\widehat{\beta}_{[T_1, T_2]}$ is asymptotically normal. As such, the estimated Q-function is asymptotically normal as well. Refer to Theorem 4 in the supplementary article for details.

REMARK 8. *To the best of our knowledge, the limiting distribution of the Q-function estimated via FQI has not been established in the existing RL literature. Most papers focus on establishing non-asymptotic error bound of the estimated Q-function (see e.g., [Munos and](#)*

(Szepesvári, 2008; Chen and Jiang, 2019; Fan et al., 2020; Uehara et al., 2021). One exception is a recent proposal by Hao et al. (2021) that studied the asymptotics of Q -estimators computed via the fitted Q -evaluation (FQE, Le, Voloshin and Yue, 2019) algorithm. We note that FQE is similar to FQI but is designed for the purpose of policy evaluation.

In addition, it follows from (12) that

$$(13) \quad \begin{aligned} \widehat{Q}_{[T_0,u]}(a, s) - \widehat{Q}_{[u,T]}(a, s) &= \frac{1}{N(u - T_0)} \phi_L^\top(a, s) W_{[T_0,u]}^{-1} \sum_{i=1}^N \sum_{t=T_0}^{u-1} \phi_L(A_{i,t}, S_{i,t}) \delta_{i,t}^* \\ &\quad - \frac{1}{N(T - u)} \phi_L^\top(a, s) W_{[u,T]}^{-1} \sum_{i=1}^N \sum_{t=u}^{T-1} \phi_L(A_{i,t}, S_{i,t}) \delta_{i,t}^* + o_p(1). \end{aligned}$$

This motivates us to construct B bootstrap samples to approximate the asymptotic distribution of the leading term on the RHS of (13). Specifically, at the b th iteration, $b = 1, \dots, B$, we compute a bootstrap sample $\widehat{Q}_{[T_0,u]}^b(a, s) - \widehat{Q}_{[u,T]}^b(a, s)$ where

$$\widehat{Q}_{[T_1,T_2]}^b(a, s) = \frac{1}{N(T_2 - T_1)} \phi_L^\top(a, s) \widehat{W}_{[T_1,T_2]}^{-1} \sum_{i=1}^N \sum_{t=T_1}^{T_2-1} \phi_L(A_{i,t}, S_{i,t}) \delta_{i,t}(\widehat{\beta}_{[T_1,T_2]}^b) e_{i,t}^b, \forall T_1, T_2,$$

where $\widehat{W}_{[T_1,T_2]}$ denotes a consistent estimator for $W_{[T_1,T_2]}$ (refer to Lemma 18 for a detailed upper bound on the estimation error) given by

$$\widehat{W}_{[T_1,T_2]} = \frac{1}{N(T_2 - T_1)} \sum_{i=1}^N \sum_{t=T_1}^{T_2-1} \phi_L(A_{i,t}, S_{i,t}) \{ \phi_L(A_{i,t}, S_{i,t}) - \gamma \phi_L(\pi_{\widehat{\beta}_{[T_1,T_2]}}(S_{i,t+1}), S_{i,t+1}) \}^\top,$$

$\delta_{i,t}(\beta) = R_{i,t} + \gamma \max_a \beta^\top \phi_L(a, S_{i,t+1}) - \beta^\top \phi_L(A_{i,t}, S_{i,t})$, $\{e_{i,t}^b\}_{i,t}$ is a sequence of i.i.d. standard Gaussian random variables independent of the observed data, and $\pi_{\widehat{\beta}_{[T_1,T_2]}}$ denotes the greedy policy with respect to the estimated Q -function (see (3)), $\pi_{\widehat{\beta}_{[T_1,T_2]}}(s) = \arg \max_a \phi_L^\top(a, s) \widehat{\beta}_{[T_1,T_2]}$. This yields the bootstrapped statistics,

$$\text{TS}_1^b = \max_{T_0 + \epsilon T < u < (1 - \epsilon)T} \tau_u \left[\frac{1}{N(T - T_0)} \sum_{i,t} |\widehat{Q}_{[T_0,u]}^b(A_{i,t}, S_{i,t}) - \widehat{Q}_{[u,T]}^b(A_{i,t}, S_{i,t})| \right],$$

$$\text{TS}_\infty^b = \max_{T_0 + \epsilon T < u < (1 - \epsilon)T} \max_{a,s} \tau_u |\widehat{Q}_{[T_0,u]}^b(a, s) - \widehat{Q}_{[u,T]}^b(a, s)|,$$

$$\text{TS}_n^b = \max_{T_0 + \epsilon T < u < (1 - \epsilon)T} \max_{a,s} \tau_u \widehat{\sigma}_u^{-1}(a, s) |\widehat{Q}_{[T_0,u]}^b(a, s) - \widehat{Q}_{[u,T]}^b(a, s)|.$$

The random noise $e_{i,t}^b$ in $\widehat{Q}_{[T_1,T_2]}^b$ plays a crucial role in the approximation of the asymptotic distribution. In particular, in Step 4 of the proof of Theorem 2 (see Section C.2.1 of the supplementary article), we show that the conditional variance of the difference in the bootstrap sample $\widehat{Q}_{[T_0,u]}^b(a, s) - \widehat{Q}_{[u,T]}^b(a, s)$ given the data, is asymptotically equivalent to the asymptotic variance of the difference in the actual Q -function estimator $\widehat{Q}_{[T_0,u]}(a, s) - \widehat{Q}_{[u,T]}(a, s)$. Meanwhile, $\widehat{Q}_{[T_0,u]}^b(a, s) - \widehat{Q}_{[u,T]}^b(a, s)$ follows a normal distribution given the data, due to the injected Gaussian noises $\{e_{i,t}^b\}_{i,t}$, while $\widehat{Q}_{[T_0,u]}(a, s) - \widehat{Q}_{[u,T]}(a, s)$ is asymptotically normal. These alignments justify the use of the multiplier bootstrap. We thus set the critical value

of each test to the α th upper quantile of the bootstrapped samples. The p -values can be computed by

$$(14) \quad \frac{1}{B} \sum_{b=1}^B \mathbb{I}(\text{TS}_1^b > \text{TS}_1), \frac{1}{B} \sum_{b=1}^B \mathbb{I}(\text{TS}_\infty^b > \text{TS}_\infty) \text{ and } \frac{1}{B} \sum_{b=1}^B \mathbb{I}(\text{TS}_n^b > \text{TS}_n),$$

respectively.

3.4. Change Point Detection. Given the offline data collected from N subjects up to time T , we aim to learn an optimal “warm-up” policy – the optimal policy assuming the environment’s dynamics at time T remain constant afterwards – that can be used for treatment recommendation for these subjects. This goal aligns with our motivating mHealth study setting where the researchers want to design the best policy based on pre-collected data and extends the policy to the same group of subjects after the study ends. To this end, we focus on identifying the most recent change point T^* such that $Q_{T^*}^{\text{opt}} = Q_{T^*+1}^{\text{opt}} = \dots = Q_T^{\text{opt}}$ and apply state-of-the-art Q-learning to the data subset $\{(S_{i,t}, A_{i,t}, R_{i,t})\}_{1 \leq i \leq N, T^* \leq t \leq T}$ to learn $\pi_{T^*}^{\text{opt}}$.

To estimate T^* , we apply any of the three proposed tests to a sequence of candidate change points from the back. We start by specifying a monotonically increasing sequence $\{\kappa_j\}_j \subseteq (0, T)$ and apply the test to intervals $[T - \kappa_j, T]$. The estimator \hat{T}^* is then set as the candidate change point before the first rejection, i.e., $\hat{T}^* = T - \kappa_{j_0-1}$ where the test is first rejected at κ_{j_0} . If no changes are detected, we propose to use all the observed data for policy optimization.

4. Consistency of the Test. We proceed by first investigating the size (i.e., the rejection probability or type I error) of the proposed test, and next establishing its power property. To save space, we derive the asymptotic distribution of the Q-function estimator based on FQI in Appendix B. To simplify the theoretical analysis, we focus on the setting where the state space $\mathcal{S} = [0, 1]^d$, and Φ denotes the tensor product of B-spline basis functions – a choice motivated by their popularity in the sieve estimation literature (see e.g., Section 6 of [Chen and Christensen, 2015](#), for a review). We use $p_t(\bullet | a, s)$ to denote the probability density function of $\mathcal{T}_t(a, s, \delta_1)$. In other words, p_t corresponds to the density function of S_{t+1} given $(A_t, S_t) = (a, s)$. For each s and t , we use $\pi_t^{\text{opt}}(s)$ to denote the greedy action $\arg \max_a Q_t^{\text{opt}}(a, s)$ that π_t^{opt} picks (see (3)). As commented in the introduction, all the theories in this section are established under a bidirectional asymptotic framework, which is to say that they are valid as either N or T diverges to infinity.

4.1. Size of the Test. We introduce the following assumptions:

A1 (Uniform consistency under \mathcal{H}_0): Under the null defined in (6) that $Q_t^{\text{opt}} = Q^{\text{opt}}$ for all $t \geq T_0$, the set of Q-estimators $\{\phi_L^\top(a, s) \hat{\beta}_{[T_1, T_2]}\}$ are uniformly consistent in ℓ_∞ norm,

$$\max_{[T_1, T_2] \subseteq [T_0, T]} \sup_{a, s} |\phi_L^\top(a, s) \hat{\beta}_{[T_1, T_2]} - Q^{\text{opt}}(a, s)| = o_p(1),$$

where $\hat{\beta}_{[T_1, T_2]}$ is defined in (11).

A2 (CUSUM statistics): The boundary removal parameter ϵ in the proposed test statistics (7), (8) and (9), is proportional to $\log^{-c_1}(NT)$ for some $c_1 \geq 0$.

A3 (Reward): The reward functions $\{r_t\}_t$ (see (1)) are p -smooth (Hölder smooth) functions of s for some $p > d/2$; see the supplementary article for the detailed definition.

A4 (Transition): (i) $\sup_{a, t} \mathbb{E} \|\mathcal{T}_t(s, a, \delta) - \mathcal{T}_t(s', a, \delta)\|_2 \leq \rho \|s - s'\|_2$ for some $0 \leq \rho < 1$, $\sup_{t, a, s} \|\mathcal{T}_t(s, a, \delta) - \mathcal{T}_t(s, a, \delta')\|_2 = O(\|\delta - \delta'\|_2)$, where $\|\cdot\|$ denotes the ℓ_2 norm of a vector; (ii) Suppose δ_1 has sub-exponential tails, i.e., for any j th element $\delta_{1,j}$, $\mathbb{E}|\delta_{1,j}|^k \leq k! c_2 c_3^{k-2}$ for some constants $c_2, c_3 > 0$; (iii) $\mathcal{T}_t(s, a, \delta)$ are p -smooth functions of s as well.

A5 (Behavior policy): (i) π^b is a Markov policy; (ii) $\min_t \lambda_{\min}[\mathbb{E}\phi_L(A_t, S_t)\phi_L(A_t, S_t)^\top - \gamma^2\mathbb{E}\phi_L(\pi_t^{\text{opt}}(S_{t+1}), S_{t+1})\phi_L^\top(\pi_t^{\text{opt}}(S_{t+1}), S_{t+1})]$ is uniformly bounded away from zero where $\lambda_{\min}[\bullet]$ denotes the minimum eigenvalue of a given square matrix.

A6 (Optimal policy): The optimal policy π_t^{opt} is unique for all t .

A7 (Optimal Q-function): The margin $Q_t^{\text{opt}}(\pi_t^{\text{opt}}(s), s) - \max_{a \in \mathcal{A} \setminus \pi_t^{\text{opt}}(s)} Q_t^{\text{opt}}(a, s)$ is bounded away from zero, uniformly for all s and t .

A8 (Basis functions): L is proportional to $(NT)^{c_4}$ for some $0 < c_4 < 1/4$. Under the null SA3 (see (6)), we additionally require $c_4 > d/(2p)$ for all three types of tests. For the unnormalized test (8), it is further required that $c_4 > d/(2p - d)$. However, these lower bound requirements are not needed under SA1 and SA5.

REMARK 9. *A1 requires to select a consistent Q-learning algorithm to solve the Bellman optimality equation. In Appendix B, we show that A1 holds when FQI is used to compute $\hat{\beta}_{[T_1, T_2]}$. Additionally, as commented earlier, the elimination of boundary effects is essential and assumptions similar to A2 are commonly adopted in the literature (Yu and Chen, 2021).*

REMARK 10. *The smoothness conditions in A3 and A4(iii) are commonly imposed in the sieve estimation literature (see e.g. Huang, 1998; Chen and Christensen, 2015). These conditions are used to bound the approximation error of the Q-function. When p is an integer, the p -smoothness requires a function to have bounded derivatives up to the p th order. Under this condition, the Q-function at each time is p -smooth as a function of the state as well (Fan et al., 2020; Shi et al., 2022; Chen and Qi, 2022).*

REMARK 11. *Conditions A4(i) and (ii) are needed to establish concentration inequalities for nonstationary Markov chains (Alquier, Doukhan and Fan, 2019). They allow us to develop a matrix concentration inequality with nonstationary transition functions, which is needed to prove the validity of the bootstrap method (see Lemma 18 in the supplementary article for details). These assumptions are automatically satisfied when the state satisfies a time-varying AR(1) process:*

$$S_{t+1} = \rho_t S_t + \beta_t A_t + \delta_t,$$

for some $\{\rho_t\}_t$ and $\{\beta_t\}$ such that $\sup_t |\rho_t| < 1$, and δ_t has sub-exponential tails. More generally, it also holds when the auto-regressive model is given by

$$S_{t+1} = f_t(A_t, S_t) + \delta_t,$$

with $\sup_{a, t} |f_t(a, s) - f_t(a, s')| \leq \rho \|s - s'\|_2$ for some $\rho < 1$. When the transition functions are stationary over time, it essentially requires the Markov chain to possess the exponential forgetting property (Dedecker and Fan, 2015).

REMARK 12. *A5(i) allows the behavior policy that generates the data to be nonstationary over time. It is automatically satisfied in randomized studies where the behavior policy is usually a constant function of the state. A5(ii) is commonly imposed in the statistics literature on RL (see e.g., Ertefaie and Strawderman, 2018; Luckett et al., 2020). It is automatically satisfied when the behavior policy that determines A_t is ε -greedy with respect to π_t^{opt} for some $\varepsilon \leq 1 - \gamma^2$ (Shi et al., 2022).*

REMARK 13. *A6 is a necessary condition for establishing the limiting distribution of $\hat{\beta}_{[T_1, T_2]}$ computed based on FQI. It is imposed in the statistics literature (Ertefaie and Strawderman, 2018; Luckett et al., 2020). It is violated in nonregular settings where the optimal policy is not uniquely defined (Chakraborty, Laber and Zhao, 2013; Luedtke and van der*

Laan, 2016; Shi, Lu and Song, 2020; Guo and He, 2021). Our proposal could be further coupled with data splitting to derive a valid test in nonregular settings. However, the resulting test might suffer from a loss of power, due to the use of data splitting.

REMARK 14. The margin $Q_t^{\text{opt}}(\pi_t^{\text{opt}}(s), s) - \max_{a \in \mathcal{A} \setminus \{\pi_t^{\text{opt}}(s)\}} Q_t^{\text{opt}}(a, s)$ in A7 measures the difference between the state-action value under the best action and the second best action. This condition is imposed to simplify the theoretical analysis. It could be potentially relaxed to require the margin to converge to zero at certain rate or to require the probability that the margin approaches zero at certain rate (see e.g., *Qian and Murphy, 2011; Luedtke and van der Laan, 2016; Hu, Kallus and Uehara, 2021; Shi et al., 2022*).

REMARK 15. As shown in A8, the ℓ_1 -type test (7) and normalized maximum-type test (9) require weaker conditions than the unnormalized test (8). Specifically, for the former two tests, the condition $d/(2p) < c_4 < 1/2$ is sufficient. In contrast, the unnormalized test demands a more stringent condition, namely $d/(2p - d) < c_4 < 1/3$. Further, under SA1 and SA5, the lower bound requirements on c_4 become unnecessary. In such cases, it suffices for the sieve approximation error to simply tend towards zero, as opposed to being $o\{(NT)^{-1/2}\}$. The latter is required to ensure the bias of the Q -estimator converge to zero at a faster rate than its standard deviation. Our CUSUM-type test statistics ensure that the proposed tests remain valid under weaker assumptions about the approximation error and are not overly sensitive to the number of basis functions L . This is because at each hypothesized error location, the test statistics implement scaled differencing, requiring the difference in approximation errors, instead of these errors themselves, to converge at a specific order. Such an order requirement is automatically satisfied under SA1 and SA5.

THEOREM 2 (Size). Recall that \mathcal{D} denote the observed data. Suppose A1-A8 and the null hypothesis SA3 hold, we have

$$\begin{aligned} \sup_z |\mathbb{P}(\sqrt{NT} TS_1^b \leq z | \mathcal{D}) - \mathbb{P}(\sqrt{NT} TS_1 \leq z)| &\xrightarrow{p} 0, \\ \sup_z |\mathbb{P}(\sqrt{NT} TS_n^b \leq z | \mathcal{D}) - \mathbb{P}(\sqrt{NT} TS_n \leq z)| &\xrightarrow{p} 0, \\ \sup_z |\mathbb{P}(\sqrt{NT} TS_\infty^b \leq z | \mathcal{D}) - \mathbb{P}(\sqrt{NT} TS_\infty \leq z)| &\xrightarrow{p} 0, \end{aligned}$$

as either N or T tends to infinity.

Theorem 2 implies that the limiting distribution of the proposed test can be well-approximated by the conditional distribution of the bootstrapped statistic given the data. It in turn implies that the size of the proposed test approaches the nominal level as the total number of observations diverges to infinity. As commented in the introduction, the derivation of the consistency of the proposed test is complicated due to that we allow L to grow with the number of observations. Specifically, when L is fixed, the test statistic's limiting distribution can typically be derived using classical weak convergence theorems (*van der Vaart and Wellner, 1996*). However, these theorems become inapplicable as L diverges with the sample size. This complexity arises because the dimension of the estimator $\hat{\beta}$ also expands with L . To prove its asymptotic normality, it is necessary to demonstrate that $\hat{\beta}$ converges to a Gaussian vector despite the growth of its dimension. To address this challenge, we develop a matrix concentration inequality for nonstationary MDP in Lemma 18.

4.2. *Power of the Test.* We next establish the power property of the proposed test. In our theoretical analysis, we focus on a particular type of alternative hypothesis \mathcal{H}_a where there is a single change point $T^* \in (T_0, T)$ such that

$$(15) \quad Q_{T_0}^{opt} = Q_{T_0+1}^{opt} = \dots = Q_{T^*-1}^{opt} \neq Q_{T^*}^{opt} = Q_{T^*+1}^{opt} = \dots = Q_T^{opt}.$$

Let $\Delta_1 = T^{-1} \sum_{t=0}^{T-1} \mathbb{E}|Q_{T_0}^{opt}(A_t, S_t) - Q_T^{opt}(A_t, S_t)|$ and $\Delta_\infty = \sup_{a,s} |Q_{T_0}^{opt}(a, s) - Q_T^{opt}(a, s)|$ characterize the degree of nonstationarity. Specifically, the null holds if Δ_1 or Δ_∞ equals zero and the alternative hypothesis \mathcal{H}_a holds if Δ_1 or Δ_∞ is positive. However, we remark that the proposed test is consistent against more general alternative hypothesis as well. See Section 5 for details. For any two positive sequences $\{a_{N,T}\}_{N,T}$ and $\{b_{N,T}\}_{N,T}$, the notation $a_{N,T} \gg b_{N,T}$ means that $b_{N,T}/a_{N,T} \rightarrow 0$ as $NT \rightarrow \infty$.

A1' (Uniform consistency under \mathcal{H}_a): Under the alternative hypothesis defined in (15), both sets of Q-estimators $\{\phi_L^\top(a, s)\hat{\beta}_{[T_0, T_1]} : T_1 < T^*\}$ and $\{\phi_L^\top(a, s)\hat{\beta}_{[T_1, T]} : T_1 \geq T^*\}$ are uniformly consistent in ℓ_∞ norm.

A9 (Change point): $T_0 + \epsilon T < T^* < (1 - \epsilon)T$ given the boundary removal parameter ϵ .

THEOREM 3 (Power). *Suppose A1', and A2-A9 hold.*

- If $\Delta_1 \gg \{\sqrt{L(NT)^{-1} \log(NT)} + L^{-p/d}\} \log^{c_1/2}(NT)$, then the power of the test based on TS_1 (7) approaches 1, as either N or T diverges to infinity;
- If $\Delta_\infty \gg \sqrt{L} \{\sqrt{L(NT)^{-1} \log(NT)} + L^{-p/d}\} \log^{c_1/2}(NT)$, then the power of the test based on TS_∞ (8) approaches 1, as either N or T diverges to infinity.
- If $\Delta_\infty \gg \{\sqrt{L(NT)^{-1} \log(NT)} + L^{-p/d}\} \log^{c_1/2}(NT)$, then the power of the test based on TS_n (9) approaches 1, as either N or T diverges to infinity.

Assumption A9 is reasonable as we allow ϵ to decay to zero as the number of observations grows to infinity (see A2). Under the given assumptions, the bias and standard deviation of the Q-function estimator are proportional to $O(\sqrt{L(NT)^{-1}})$ and $O(L^{-p/d})$, respectively, up to some logarithmic factors. The conditions on Δ_1 and Δ_∞ essentially require the signal under \mathcal{H}_a to be much larger than the estimation error. Similar to the findings in Theorem 2, the unnormalized maximum-type test (8) requires a stronger condition on L to detect the alternative hypothesis. To guarantee the proposed three tests have good power properties, we use cross-validation to select the number of basis functions, as discussed in Section D.2. This ensures the bias and standard deviation of the Q-function estimator are approximately of the same order of magnitude. In A1', we further require the Q-estimators before and after the change to be consistent. Similar to Theorem 4, we can show that it holds when FQI is employed for estimating the optimal Q-function.

5. Simulations. In this section, we conduct simulation studies to evaluate the finite sample performance of the proposed method and compare against common alternatives. Section 5.1 presents results of the proposed offline testing and change point detection methods based on four generative models with different nonstationarity scenarios (see Table 1). Section 5.2 further demonstrates the usefulness of the proposed method in an online setting as data accumulate. In Section D.1 of the supplementary article, we simulate data to mimic the data setup in the motivating application of IHS. We detail our implementation in Section D.2 of the supplementary article. All simulation results are aggregated over 100 replications.

	State transition function	Reward function
(1)	Time-homogeneous	Piecewise constant
(2)	Time-homogeneous	Smooth
(3)	Piecewise constant	Time-homogeneous
(4)	Smooth	Time-homogeneous

TABLE 1

Simulation scenarios with different types of nonstationarity in Sections 5.1 and 5.2.

5.1. *Offline Testing and Change Point Detection.* We consider four nonstationary data generating mechanisms with one-dimensional states and binary actions where the nonstationarity occurs in either the state transition function or the reward function, as listed in Table 1. Specifically, in the first two scenarios, the transition function \mathcal{T}_t is stationary whereas the reward function r_t varies over time. The last two scenarios are concerned with stationary reward functions and nonstationary transition functions. For nonstationary functions, both abrupt (e.g., the underlying function is piece-wise constant) and smooth changes are considered. See Section D.3 of the supplementary article for more details about the data generating processes in these four scenarios.

In all scenarios, we set $T = 100$ and simulate offline data with sample sizes $N = 25, 100$. The true location of the change point T^* was set to 50. We first apply each of the proposed three tests to the time interval $[T - \kappa, T]$ to detect nonstationarity, where κ takes value from a equally-spaced sequence between 25 and 75 with increments of 5. According to our true data generating mechanisms, when $\kappa \leq 50$, the null of no change point over $[T - \kappa, T]$ holds; the alternative hypothesis holds if $\kappa > 50$. The actions are generated i.i.d. according to a Bernoulli random variable with a success probability of 0.5.

Figure 2 and Figure 8 in the supplementary article show the empirical rejection probabilities of each proposed test, when $N = 25$ and 100 respectively. First, in all settings, each test properly controls the type I error. Second, the power increases with κ due to inclusion of more pre-change-point data into the interval $[T - \kappa, T]$. The power also increases with the sample size N , demonstrating the consistency of our tests. Third, as expected, gradual changes are more difficult to detect than abrupt changes. This observation is evident in Figure 2, where when $\kappa = 55$, the power of the proposed test in scenarios with a smooth reward or state transition function is smaller than scenarios with a piecewise constant function. Finally, the maximum-type tests (8) and (9) achieve slightly higher power than the ℓ_1 -type test (7) when $N = 25$, whereas the powers of the three tests become indistinguishable when $N = 100$.

Next, we investigate the finite sample performance of the estimated change point location \hat{T}^* . Figure 3 and Figure 9 in the supplementary article depict the distribution of \hat{T}^* in each simulation scenario. It can be seen that in the first two scenarios with abrupt changes, the estimated change points concentrate at 50, which is the true change point location, yielding a minimal detection delay. In the last two scenarios with smooth changes, the estimated change points have a wider spread especially when $N = 25$. This results in a marginally extended detection delay. However, in the majority of cases, these estimators are still close to 50.

5.2. *Online Evaluation.* Finally, we illustrate how the proposed change point detection method can be coupled with existing state-of-the-art RL algorithms for policy learning in nonstationary environments. In each simulation, we first simulate an offline dataset as discussed earlier with $T = 100$ and $N = 200$. We next apply our proposal to identify the most recent change point location \hat{T}^* and estimate the optimal policy using the data subset $\{(S_{i,t}, R_{i,t}, A_{i,t}) : 1 \leq i \leq N, \hat{T}^* \leq t \leq T\}$. As commented earlier, the resulting estimated policy can be used for treatment recommendation after study end time T . Specifically, we

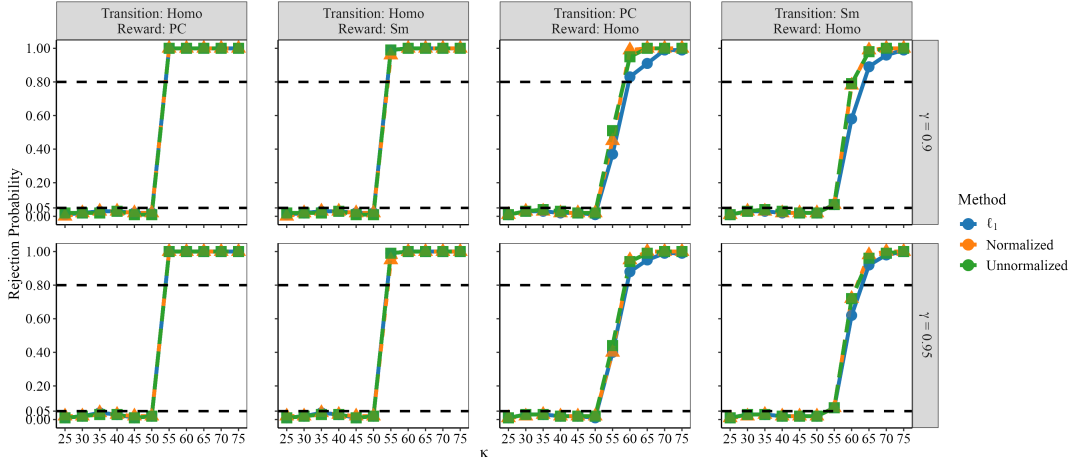


Fig 2: Empirical type I errors and powers of the proposed test and their associated 95% confidence intervals under settings described in Section 5.1, with $N = 25$. Abbreviations: Homo for homogeneous, PC for piecewise constant, and Sm for smooth.

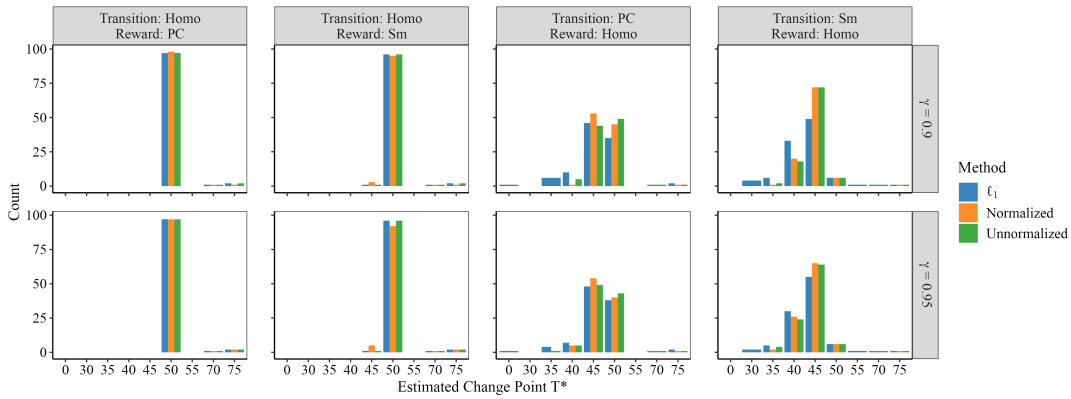


Fig 3: Distribution of detected change points under simulation settings in Section 5.1 with $N = 25$.

use a decision tree model (Myles et al., 2004) to approximate Q^{opt} to obtain interpretable policies for healthcare researchers. Through FQI, we transform the Q^{opt} estimation into an iterative regression problem (see Equation 5) and employ decision tree regression to update the Q-estimator at each iteration. The decision tree model involves hyperparameters such as the maximum tree depth and the minimum number of samples on each leaf node. We use 5-fold cross validation to select these hyperparameters from $\{3, 5, 6\}$ and $\{50, 60, 80\}$, respectively (see Section D.2 in the supplementary article).

Next, for each of the 200 subjects, we sequentially apply our procedure for online policy learning as data accumulate to maximize their cumulative reward. Specifically, we consider an online setting and assume the number of change points after $T = 100$ follow a Poisson process with rate $1/50$. In other words, we expect a new change point to occur every 50 time points. We set the termination time $T_{end} = 300$, yielding 3 to 4 change points in most simulations. We similarly consider four different types of change points listed in Table 1. Whenever a new change point occurs, the effect of the action on the state transition or reward function is reversed. We further consider three different settings with strong, moderate and

weak signals by varying the magnitude of treatment effect. For instance, suppose we have two change points T_1 and T_2 after $T = 100$. In Scenario (1) with a piecewise constant reward function, we set $r(a, s)$ to $1.5\delta as$ when $t \in [100, T_1]$ or $[T_2, 300]$ and $-1.5\delta as$ when $t \in (T_1, T_2]$ where δ measures the treatment effect equals 1, 0.5 and 0.2 in strong-, moderate- and weak-signal settings, respectively.

Finally, we assume that online data come in batches regularly at every $L = 25$ time points starting from $T = 100$. This yields a total of $K = 8$ batches of data. The first online data batch is generated according to an ϵ -greedy policy that selects actions using the estimated optimal policy $\hat{\pi}$ computed based on the data subset in the time interval $[\hat{T}^*, T]$ with probability $1 - \epsilon$ and a uniformly random policy with probability ϵ . Let $T^{*(0)} = \hat{T}^*$. Suppose we have received k batches of data. We first apply the proposed change point detection method on the data subset in $[T^{*(k-1)}, T + kL]$ to identify a new change point $T^{*(k)}$. If no changes are detected, we set $T^{*(k)} = T^{*(k-1)}$. We next update the optimal policy based on the data subset in $[T^{*(k)}, T + kL]$ and use this estimated optimal policy (combined with the ϵ -greedy algorithm) to generate the $(k + 1)$ -th data batch. We repeat this procedure until all 8 batches of data are received. Finally, we aggregate all immediate rewards obtained from time T to T_{end} over the 200 subjects to estimate the average value. Comparison is made among the following methods:

Proposed: The proposed ℓ_1 -type test (7) (the other two tests yield similar change points and policies. Their results are not reported to save space);

Overall: Standard policy optimization method that uses all the data;

Random: Policy optimization with a randomly assigned change point location;

Kernel: The kernel-based approach developed by [Domingues et al. \(2021\)](#);

Oracle: The ‘‘oracle’’ policy optimization method as if the oracle change point location were known in advance.

For fair comparisons, we use FQI and decision tree regression to compute the optimal Q-function for all methods. To implement the random method, after a new batch of data arrives, we randomly pick a time point uniformly from the interval $[T^{*(k-1)}, T + kL]$ as the next change point location $T^{*(k)}$ and compute the optimal Q-function based on the observations that occur after time $T^{*(k)}$. To implement the kernel-based method, at the l -th FQI iteration, we consider the following objective function,

$$(16) Q^{(l+1)} = \arg \min_Q \sum_{i,t} K \left(\frac{T-t}{Th} \right) \left\{ R_{i,t} + \gamma \max_a Q^{(l)}(a, S_{i,t+1}) - Q(A_{i,t}, S_{i,t}) \right\}^2,$$

where $K(\cdot)$ denotes the Gaussian RBF basis and h denotes the associated bandwidth parameter taken from the set $\{0, 0.1, 0.2, 0.4, 0.8, 1.6\}$. According to (16), the kernel-based method assigns larger weights to more recent observations to deal with nonstationarity. After we receive the k th data batch, we sample $B \gg T$ data slices across all individuals from $\{(S_{i,t}, A_{i,t}, R_{i,t}, S_{i,t+1}; 1 \leq i \leq N)\}_{0 \leq t < T+kL}$ with weights proportional to $K((T-t)/(Th))$ and apply the decision tree regression to these samples to solve (16). To implement the oracle method, we repeatedly use observations that occur after the oracle change point to update the optimal policy.

Figure 4 reports the difference between the average value under the proposed policy and those under policies estimated based on these baseline methods in the ‘‘strong signal’’ setting (i.e., the treatment effect $\delta = 1$). Additional simulation results with moderate and weak signals are available in Section D.4 of the supplementary article. We briefly summarize a few notable findings. First, the proposed method achieves much larger average values compared to the ‘‘overall’’ method, demonstrating the inferiority of the best policy learned without acknowledging the nonstationarity. Second, the proposed method outperforms the ‘‘random’’

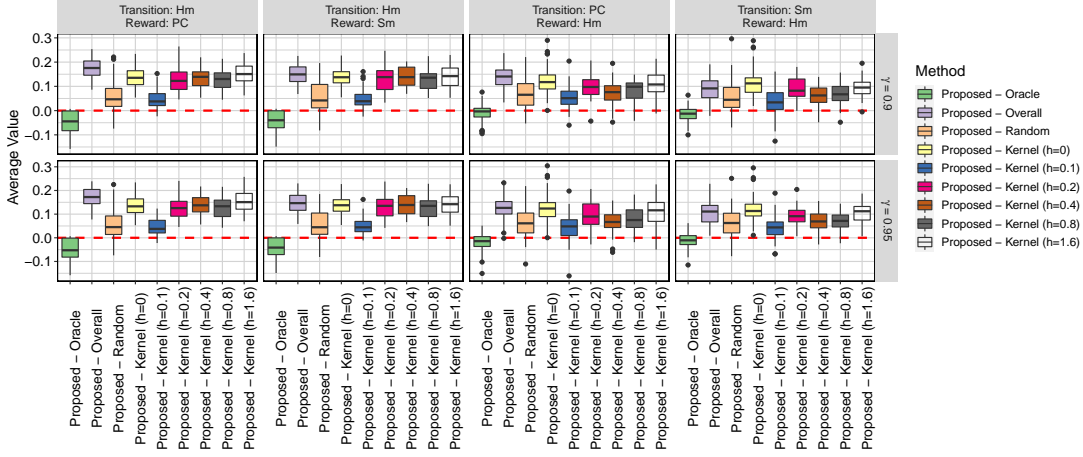


Fig 4: Distribution of the difference between the average value $(T_{end} - T)^{-1} \sum_{t=T+1}^{T_{end}} \mathbb{E}R_t$ under the proposed policy and those under policies computed by other baseline methods, under settings in Section 5.1 with strong signal-to-noise ratio. The proposed policy is based on the change point detected by the ℓ_1 -type test (7). In all scenarios, we find the normalized or unnormalized tests (8) and (9) yield similar average values.

method in all cases. This implies that correctly identifying the change point location is essential to policy optimization in nonstationary environment. Third, the proposed method is no worse and often better than kernel-based approaches in all cases, again highlighting the necessity of change point detection in policy learning. In addition, as shown in Figure 4, kernel-based method can be sensitive to the choice of the kernel bandwidth and it remains unclear how to determine this tuning parameter in practice.

6. Application to Intern Health Study. The 2018 Intern Health Study (IHS) is a micro-randomized trial (MRT) that seeks to evaluate the efficacy of push notifications sent via a customized study app upon proximal physical and mental health outcomes (NeCamp et al., 2020), a critical first step for designing effective just-in-time adaptive interventions. Over the 26 weeks, each study subject was re-randomized weekly to receive or not to receive activity suggestions; daily self-reported mood scores were assessed via ecological momentary assessments, a research method repeatedly recording subjects’ behaviors in real time and in their natural environment; step count and sleep duration in minutes were measured by wearables (Fitbit). In this paper, we focus on policy optimization for improving time-discounted cumulative step counts under the infinite horizon setting. As discussed in Section 1, determining the optimal policy for delivering prompts is challenging due to potential nonstationarity that results in changes in the treatment effects. Here we demonstrate how to use the proposed method to detect change point and perform optimal policy estimation in the presence of potential temporal nonstationarity.

6.1. Data and method: Setup. Let the state vector S_t be comprised of the following: square root of average step count in week t , cubic root of average sleep minutes in week t , average mood score in week t , and square root of average step count in week $t - 1$; all state variables are centered by mean and scaled by standard deviation after transformation (NeCamp et al., 2020). The reward R_t is defined as the average step count in week t . The binary action $A_t = 1$ (0) corresponds to pushing (not pushing) an activity message in week t . The randomization probabilities are known under MRT: $\mathbb{P}(A_t = 1) = 1 - \mathbb{P}(A_t = 0) = 1/4$.

To resemble a real-time evaluation scenario, we divide the data of 26 weeks into two trunks: we perform change point detection and estimate the optimal policy based on data collected in the first $T = 22$ weeks (training data batch), and then evaluate the estimated policy on data in the remaining 4 weeks (testing data batch) assuming that there is no change point in the final 4 weeks. To implement change point detection, we set the boundary removal parameter $\epsilon = 0.08$ and search for change points within $[5, 18]$. The number of basis functions is selected via 5-fold cross validation (see Section D.2 of the supplementary article for implementation details). We focus on three specialties: emergency ($N = 141$), pediatrics ($N = 211$), and family practice ($N = 125$). One consideration is that work schedules and activity levels vary greatly across different specialties, and thus medical interns might experience distinct change points. Stratification by specialty may improve homogeneity of the study groups so that the assumption of a common change point is more plausible.

6.2. *Results.* Figure 5 plots the trajectories of p -values using ℓ_1 -type test statistic (7); the results are similar when maximum-type tests (8) and (9) were applied to the data (not reported here). We consider $\gamma = 0.9$ or 0.95 , which produce similar results. First, we notice that in the pediatrics and family practice specialties, many p -values are close to 1. This is due to the use of the p -value aggregation method (Meinshausen, Meier and Bühlmann, 2009, see Section D.2 of the supplementary article for details), which tends to increase insignificant p -values and reduce the type I error. Second, the emergency specialty displays roughly monotonically decreasing p -values over time, whereas at the largest few κ values the p -values rise up due to the limited effective sample size at the boundary. Third, the U-shaped p -value trajectory of the pediatrics specialty shows evidence for multiple change points. Specifically, when only a single change point exists, the significant p -values are likely to decrease with κ . The U-shaped p -value trajectory can occur only when the data interval contains at least two change points and the system dynamics after the second change point is similar to that before the first change occurs, yielding a small CUSUM statistics. Because we focus on the latest detected change point (first κ_{j_0-1} where κ_{j_0} results in a rejection of the null) to inform the latest data segment to use for optimal policy estimation, we find $\kappa_{j_0-1} = 6$ for the emergency specialty and $\kappa_{j_0-1} = 5$ for the pediatrics specialty, for both choices of γ . Fourth, the p -value trajectories of the family practice specialty (mostly close to 1) are above the significance threshold, indicating the stationarity assumption is compatible with this data subset. We therefore estimate the optimal policy using data from all the time points for family practice specialty.

We next compare the proposed policy optimization method with three other methods: 1) overall, 2) random, which were described in Section 5.1) and 3) behavior, which is the treatment policy used in the completed MRT. The data of the first 22 weeks are used to learn an optimal policy $\hat{\pi}^{opt}$ through FQI and decision tree regression. In particular, the proposed method uses data after the estimated change point location whereas the overall method uses all the training data. Similar to simulations, hyperparameters of the decision tree regression are selected via 5-fold cross-validation. Next, based on the evaluation data, we applied FQE to the testing data of the remaining 4 weeks to evaluate the γ -discounted values (i.e., $J_\gamma(\pi)$) of these estimated optimal policies. Results are reported in Table 2. It can be seen that the proposed method achieves larger values when compared to “random” and “behavior” in all cases, demonstrating the need for change point detection and data-driven decision making. In the following, we focus on comparing the proposed method against “overall”. In the emergency specialty, the optimal policy estimated using data after the detected change point improves weekly average step count per day by about 130 \sim 170 steps relative to the estimated policy based on the overall method. In the pediatrics specialty, however, the overall method achieves a larger weekly average step count by about 40 \sim 112 steps per day. Recall that the proposed method only uses data on $t \in [T - \kappa_{j_0-1}, T] = [17, 22]$ for policy learning. As commented

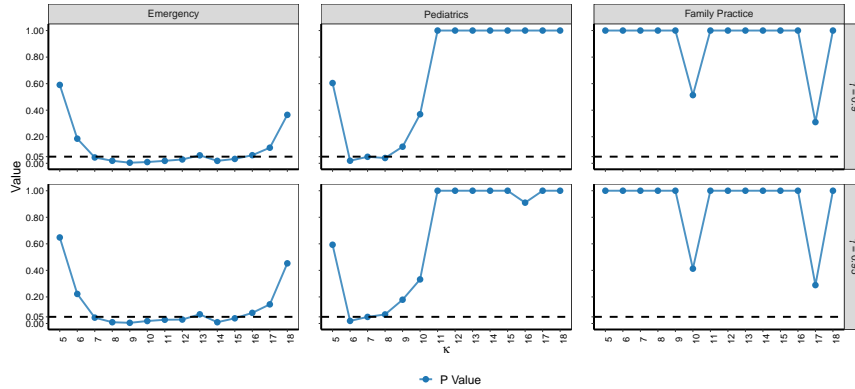


Fig 5: p -values over different values of κ (the number of time points from the last time point T) under $\gamma = 0.9$ (top) and 0.95 (bottom). The specialties are emergency (left), pediatrics (middle) and family practice (right). Many insignificant p -values are close to 1, due to the use of the aggregation method (see Section D.2), which tends to increase insignificant p -values.

earlier, there are likely two change points in the pediatrics specialty and according to Fig 5, the system dynamics after the first most recent change point are very similar to those before the second most recent change point. As a result, the overall method pools over more data from similar dynamics, resulting in a better policy. This represents a bias-variance trade-off. In settings with a U-shaped p -value trajectory and the most recent change point is close to the second most recent one, it might be sensible to borrow more information from the historical data. Finally, the proposed and overall methods have equal values in the family practice specialty since no change point is identified.

Number of Change Points	Specialty	Method	$\gamma = 0.9$	$\gamma = 0.95$
≥ 1	Emergency	Proposed	8237.16	8295.99
		Overall	8108.13	8127.55
		Behavior	7823.75	7777.32
		Random	8114.78	8080.27
≥ 2	Pediatrics	Proposed	7883.08	7848.57
		Overall	7925.44	7960.12
		Behavior	7730.98	7721.29
		Random	7807.52	7815.30
0	Family Practice	Proposed	8062.50	7983.69
		Overall	8062.50	7983.69
		Behavior	7967.67	7957.24
		Random	7983.52	7969.31

TABLE 2

Mean value estimates using decision tree in analysis of IHS. Values are normalized by multiplying $1 - \gamma$. All values are evaluated over 10 splits of data.

7. Discussion. We consider testing stationarity and change point detection based on a pre-collected offline dataset. Meanwhile, our proposal can be adopted for policy learning in nonstationary environments, as shown in the numerical study. Recently, there have been some works on online nonstationary RL in the machine learning literature (see e.g., Lecarpentier

and Rachelson, 2019; Cheung, Simchi-Levi and Zhu, 2020; Fei et al., 2020; Xie, Harrison and Finn, 2021; Wei and Luo, 2021; Zhong, Yang and Szepesvári, 2021; Alami, Mahfoud and Moulines, 2023). Nonetheless, offline hypothesis testing and change point detection have not been studied in these papers. Our paper is also related to the literature on sequential learning and nonstationary bandits; refer to Section A.3 of the supplementary article for details.

REFERENCES

- ADAMS, R. P. and MACKAY, D. J. (2007). Bayesian online changepoint detection. *arXiv preprint arXiv:0710.3742*.
- AGARWAL, A., JIANG, N., KAKADE, S. M. and SUN, W. (2019). Reinforcement learning: Theory and algorithms. *CS Dept., UW Seattle, Seattle, WA, USA, Tech. Rep* **32**.
- ALAMI, R., MAHFOUD, M. and MOULINES, E. (2023). Restarted Bayesian online change-point detection for non-stationary Markov decision processes. *arXiv preprint arXiv:2304.00232*.
- ALAMI, R., MAILLARD, O. and FÉRAUD, R. (2020). Restarted bayesian online change-point detector achieves optimal detection delay. In *International conference on machine learning* 211–221. PMLR.
- ALQUIER, P., DOUKHAN, P. and FAN, X. (2019). Exponential inequalities for nonstationary Markov chains. *Dependence Modeling* **7** 150–168.
- AMINIKHANGHAHI, S. and COOK, D. (2017). A survey of methods for time series change point detection. *Knowledge and Information Systems* **51** 339–367.
- BELLONI, A. and OLIVEIRA, R. I. (2018). A high dimensional central limit theorem for martingales, with applications to context tree models. *arXiv preprint arXiv:1809.02741*.
- BELLONI, A., CHERNOZHUKOV, V., CHETVERIKOV, D. and KATO, K. (2015). Some new asymptotic theory for least squares series: Pointwise and uniform results. *Journal of Econometrics* **186** 345–366.
- BIRNBAUM, Z. W. (1942). An inequality for Mill’s ratio. *The Annals of Mathematical Statistics* **13** 245–246.
- BORUVKA, A., ALMIRALL, D., WITKIEWITZ, K. and MURPHY, S. A. (2018). Assessing time-varying causal effect moderation in mobile health. *J. Amer. Statist. Assoc.* **113** 1112–1121. <https://doi.org/10.1080/01621459.2017.1305274>
- BURMAN, P. and CHEN, K.-W. (1989). Nonparametric estimation of a regression function. *The Annals of Statistics* **17** 1567–1596.
- CAO, Y., WEN, Z., KVETON, B. and XIE, Y. (2019). Nearly optimal adaptive procedure with change detection for piecewise-stationary bandit. In *The 22nd International Conference on Artificial Intelligence and Statistics* 418–427. PMLR.
- CAZELLES, B., CHAMPAGNE, C. and DUREAU, J. (2018). Accounting for non-stationarity in epidemiology by embedding time-varying parameters in stochastic models. *PLoS Computational Biology* **14** e1006211.
- CHAKRABORTY, B., LABER, E. B. and ZHAO, Y. (2013). Inference for optimal dynamic treatment regimes using an adaptive m-out-of-n bootstrap scheme. *Biometrics* **69** 714–723.
- CHAKRABORTY, B., MURPHY, S. and STRECHER, V. (2010). Inference for non-regular parameters in optimal dynamic treatment regimes. *Statistical Methods in Medical Research* **19** 317–343.
- CHEN, X. and CHRISTENSEN, T. M. (2015). Optimal uniform convergence rates and asymptotic normality for series estimators under weak dependence and weak conditions. *Journal of Econometrics* **188** 447–465.
- CHEN, X. and CHRISTENSEN, T. M. (2018). Optimal sup-norm rates and uniform inference on nonlinear functionals of nonparametric IV regression. *Quantitative Economics* **9** 39–84.
- CHEN, B. and HONG, Y. (2012). Testing for the Markov property in time series. *Econometric Theory* **28** 130–178.
- CHEN, J. and JIANG, N. (2019). Information-theoretic considerations in batch reinforcement learning. In *International Conference on Machine Learning* 1042–1051. PMLR.
- CHEN, X. and QI, Z. (2022). On well-posedness and minimax optimal rates of nonparametric q-function estimation in off-policy evaluation. In *International Conference on Machine Learning* 3558–3582. PMLR.
- CHEN, E. Y., SONG, R. and JORDAN, M. I. (2022). Reinforcement learning with heterogeneous data: estimation and inference. *arXiv preprint arXiv:2202.00088*.
- CHEN, X., WANG, Y. and ZHOU, Y. (2020). Dynamic assortment optimization with changing contextual information. *Journal of machine learning research* **21** 1–44.
- CHERNOZHUKOV, V., CHETVERIKOV, D. and KATO, K. (2014). Gaussian approximation of suprema of empirical processes. *Ann. Statist.* **42** 1564–1597. <https://doi.org/10.1214/14-AOS1230>
- CHEUNG, W. C., SIMCHI-LEVI, D. and ZHU, R. (2020). Reinforcement learning for non-stationary Markov decision processes: The blessing of (more) optimism. In *International Conference on Machine Learning* 1843–1854. PMLR.

- CHO, H. and FRYZLEWICZ, P. (2012). Multiscale and multilevel technique for consistent segmentation of non-stationary time series. *Statistica Sinica* 207–229.
- CHO, H. and FRYZLEWICZ, P. (2015). Multiple change-point detection for high-dimensional time series via sparsified binary segmentation. *Journal of the Royal Statistical Society: Series B* 77 475–507.
- COLLINS, L. M., MURPHY, S. A. and STRECHER, V. (2007). The multiphase optimization strategy (MOST) and the sequential multiple assignment randomized trial (SMART): new methods for more potent eHealth interventions. *American journal of preventive medicine* 32 S112–S118.
- COOPERBERG, M. R., BROERING, J. M., LITWIN, M. S., LUBECK, D. P., MEHTA, S. S., HENNING, J. M., CARROLL, P. R. and INVESTIGATORS, C. (2004). The contemporary management of prostate cancer in the United States: lessons from the cancer of the prostate strategic urologic research endeavor (CapSURE), a national disease registry. *The Journal of urology* 171 1393–1401.
- CSÖRGŐ, M., CSÖRGŐ, M. and HORVÁTH, L. (1997). *Limit theorems in change-point analysis*. John Wiley & Sons.
- DEDECKER, J. and FAN, X. (2015). Deviation inequalities for separately Lipschitz functionals of iterated random functions. *Stochastic Processes and their Applications* 125 60–90.
- DOMINGUES, O. D., MÉNARD, P., PIROTTA, M., KAUFMANN, E. and VALKO, M. (2021). A kernel-based approach to non-stationary reinforcement learning in metric spaces. In *International Conference on Artificial Intelligence and Statistics* 3538–3546. PMLR.
- EFTEKHARI, H., MUKHERJEE, D., BANERJEE, M. and RITOV, Y. (2020). Markovian and non-Markovian processes with active decision making strategies for addressing the COVID-19 pandemic. *arXiv preprint arXiv:2008.00375*.
- EICHENBAUM, M. S., REBELO, S. and TRABANDT, M. (2020). The macroeconomics of epidemics Technical Report, National Bureau of Economic Research.
- ERNST, D., GEURTS, P. and WEHENKEL, L. (2005). Tree-based batch mode reinforcement learning. *Journal of Machine Learning Research* 6 503–556.
- ERTEFAIE, A. and STRAWDERMAN, R. L. (2018). Constructing dynamic treatment regimes over indefinite time horizons. *Biometrika* 105 963–977.
- FAN, J., WANG, Z., XIE, Y. and YANG, Z. (2020). A theoretical analysis of deep Q-learning. In *Learning for Dynamics and Control* 486–489. PMLR.
- FANG, E. X., WANG, Z. and WANG, L. (2022). Fairness-oriented learning for optimal individualized treatment rules. *Journal of the American Statistical Association* **just-accepted** 1–14.
- FEI, Y., YANG, Z., WANG, Z. and XIE, Q. (2020). Dynamic regret of policy optimization in non-stationary environments. In *Advances in Neural Information Processing Systems* 6743–6754.
- FRYZLEWICZ, P. (2014). Wild binary segmentation for multiple change-point detection. *The Annals of Statistics* 42 2243–2281.
- GARIVIER, A. and MOULINES, E. (2008). On Upper-Confidence Bound Policies for Non-Stationary Bandit Problems.
- GARREAU, D., JITKRITUM, W. and KANAGAWA, M. (2017). Large sample analysis of the median heuristic. *arXiv preprint arXiv:1707.07269*.
- GOPALAN, A., LAKSHMINARAYANAN, B. and SALIGRAMA, V. (2021). Bandit quickest changepoint detection. *Advances in Neural Information Processing Systems* 34 29064–29073.
- GRENANDER, U. (1981). *Abstract inference*. Wiley Series, New York.
- GUO, X. and HE, X. (2021). Inference on selected subgroups in clinical trials. *Journal of the American Statistical Association* 116 1498–1506.
- HAO, B., JI, X., DUAN, Y., LU, H., SZEPESVARI, C. and WANG, M. (2021). Bootstrapping fitted Q-evaluation for off-policy inference. In *International Conference on Machine Learning* 4074–4084. PMLR.
- HASSETT, H. V. (2010). Double Q-learning. In *Advances in Neural Information Processing Systems* 2613–2621.
- HU, Y., KALLUS, N. and UEHARA, M. (2021). Fast rates for the regret of offline reinforcement learning. *arXiv preprint arXiv:2102.00479*.
- HU, Y. and WAGER, S. (2023). Off-policy evaluation in partially observed Markov decision processes under sequential ignorability. *The Annals of Statistics* 51 1561–1585.
- HU, X., QIAN, M., CHENG, B. and CHEUNG, Y. K. (2021). Personalized policy learning using longitudinal mobile health data. *Journal of the American Statistical Association* 116 410–420.
- HUANG, J. Z. (1998). Projection estimation in multiple regression with application to functional ANOVA models. *The Annals of Statistics* 26 242–272.
- JUDD, K. L. (1998). *Numerical methods in economics*. MIT press.
- KHARROUBI, S. and SALEH, F. (2020). Are lockdown measures effective against COVID-19? *Frontiers in public health* 8 549692.
- KILLICK, R., FEARNHEAD, P. and ECKLEY, I. (2012). Optimal detection of changepoints with a linear computational cost. *Journal of the American Statistical Association* 107 1590–1598.

- KLASNJA, P., SMITH, S., SEEWALD, N. J., LEE, A., HALL, K., LUERS, B., HEKLER, E. B. and MURPHY, S. A. (2019). Efficacy of contextually tailored suggestions for physical activity: A micro-randomized optimization trial of HeartSteps. *Annals of Behavioral Medicine* **53** 573–582.
- KOMPELLA, V., CAPOBIANCO, R., JONG, S., BROWNE, J., FOX, S., MEYERS, L., WURMAN, P. and STONE, P. (2020). Reinforcement learning for optimization of COVID-19 mitigation policies. *arXiv preprint arXiv:2010.10560*.
- KOSOROK, M. R. and LABER, E. B. (2019). Precision medicine. *Annual review of statistics and its application* **6** 263–286.
- LE, H., VOLOSHIN, C. and YUE, Y. (2019). batch Policy learning under constraints. In *International Conference on Machine Learning* 3703–3712.
- LECARPENTIER, E. and RACHELSON, E. (2019). Non-stationary Markov decision processes, a worst-case approach using model-based reinforcement learning. *Advances in Neural Information Processing Systems* **32**.
- LI, Y. (2019). Reinforcement learning applications. *arXiv preprint arXiv:1908.06973*.
- LI, G., SHI, L., CHEN, Y., CHI, Y. and WEI, Y. (2023). Settling the sample complexity of model-based offline reinforcement learning. *Annals of Statistics* **accepted**.
- LIAO, P., KLASNJA, P. and MURPHY, S. (2021). Off-policy estimation of long-term average outcomes with applications to mobile health. *Journal of the American Statistical Association* **116** 382–391.
- LIAO, P., GREENEWALD, K., KLASNJA, P. and MURPHY, S. (2020). Personalized HeartSteps: A reinforcement learning algorithm for optimizing physical activity. *Proceedings of the ACM on Interactive, Mobile, Wearable and Ubiquitous Technologies* **4** 1–22.
- LIAO, P., QI, Z., WAN, R., KLASNJA, P. and MURPHY, S. A. (2022). Batch policy learning in average reward Markov decision processes. *Annals of statistics* **50** 3364.
- LIU, W., TU, J., ZHANG, Y. and CHEN, X. (2023). Online estimation and inference for robust policy evaluation in reinforcement learning. *arXiv preprint arXiv:2310.02581*.
- LOPES-JÚNIOR, L. C., BOMFIM, E., DA SILVEIRA, D. S. C., PESSANHA, R. M., SCHUAB, S. I. P. C. and LIMA, R. A. G. (2020). Protocol: Effectiveness of mass testing for control of COVID-19: a systematic review protocol. *BMJ open* **10**.
- LUCKETT, D. J., LABER, E. B., KAHKOSKA, A. R., MAAHS, D. M., MAYER-DAVIS, E. and KOSOROK, M. R. (2020). Estimating dynamic treatment regimes in mobile health using V-learning. *Journal of the American Statistical Association* **115** 692–706.
- LUEDTKE, A. R. and VAN DER LAAN, M. J. (2016). Statistical inference for the mean outcome under a possibly non-unique optimal treatment strategy. *The Annals of Statistics* **44** 713–742.
- MAEI, H. R., SZEPESVÁRI, C., BHATNAGAR, S. and SUTTON, R. S. (2010). Toward off-policy learning control with function approximation. In *ICML* 719–726.
- MANEGUEU, A. G., CARPENTIER, A. and YU, Y. (2021). Generalized non-stationary bandits. *arXiv preprint arXiv:2102.00725*.
- MARLING, C. and BUNESCU, R. (2020). The OhioT1DM dataset for blood glucose level prediction: Update 2020. In *CEUR Workshop Proceedings* **2675** 71.
- MCLEISH, D. L. (1974). Dependent central limit theorems and invariance principles. *Ann. Probability* **2** 620–628.
- MEINSHAUSEN, N., MEIER, L. and BÜHLMANN, P. (2009). P-values for high-dimensional regression. *Journal of the American Statistical Association* **104** 1671–1681.
- MENDELSON, S., PAJOR, A. and TOMCZAK-JAEGERMANN, N. (2008). Uniform uncertainty principle for Bernoulli and sub-Gaussian ensembles. *Constructive Approximation* **28** 277–289.
- MNIH, V., KAVUKCUOGLU, K., SILVER, D., RUSU, A. A., VENESS, J., BELLEMARE, M. G., GRAVES, A., RIEDMILLER, M., FIDJELAND, A. K., OSTROVSKI, G. et al. (2015). Human-level control through deep reinforcement learning. *Nature* **518** 529–533.
- MUNOS, R. and SZEPESVÁRI, C. (2008). Finite-time bounds for fitted value iteration. *Journal of Machine Learning Research* **9**.
- MURPHY, S. A. (2003). Optimal dynamic treatment regimes. *Journal of the Royal Statistical Society. Series B. Statistical Methodology* **65** 331–366.
- MYLES, A. J., FEUDALE, R. N., LIU, Y., WOODY, N. A. and BROWN, S. D. (2004). An introduction to decision tree modeling. *Journal of Chemometrics: A Journal of the Chemometrics Society* **18** 275–285.
- NECAMP, T., SEN, S., FRANK, E., WALTON, M. A., IONIDES, E. L., FANG, Y., TEWARI, A. and WU, Z. (2020). Assessing real-time moderation for developing adaptive mobile health interventions for medical interns: micro-randomized trial. *Journal of Medical Internet Research* **22** e15033.
- NIE, X., BRUNSKILL, E. and WAGER, S. (2021). Learning when-to-treat policies. *Journal of the American Statistical Association* **116** 392–409.

- NIROUI, F., ZHANG, K., KASHINO, Z. and NEJAT, G. (2019). Deep reinforcement learning robot for search and rescue applications: Exploration in unknown cluttered environments. *IEEE Robotics and Automation Letters* **4** 610–617.
- PADAKANDLA, S., PRABUCHANDRAN, K. and BHATNAGAR, S. (2020). Reinforcement learning algorithm for non-stationary environments. *Applied Intelligence* **50** 3590–3606.
- PIKE-BURKE, C. and GRÜNEWÄLDER, S. (2019). Recovering Bandits.
- PUTERMAN, M. L. (2014). *Markov decision processes: discrete stochastic dynamic programming*. John Wiley & Sons.
- QI, Z., LIU, D., FU, H. and LIU, Y. (2020). Multi-armed angle-based direct learning for estimating optimal individualized treatment rules with various outcomes. *Journal of the American Statistical Association* **115** 678–691.
- QIAN, M. and MURPHY, S. A. (2011). Performance guarantees for individualized treatment rules. *The Annals of Statistics* **39** 1180–1210.
- QIAN, T., WALTON, A. E., COLLINS, L. M., KLASNJA, P., LANZA, S. T., NAHUM-SHANI, I., RABBI, M., RUSSELL, M. A., WALTON, M. A., YOO, H. et al. (2022). The microrandomized trial for developing digital interventions: Experimental design and data analysis considerations. *Psychological Methods*.
- RAHIMI, A. and RECHT, B. (2007). Random features for large-scale kernel machines. In *Advances in Neural Information Processing Systems* (J. PLATT, D. KOLLER, Y. SINGER and S. ROWEIS, eds.) **20**. Curran Associates, Inc.
- RAMPRASAD, P., LI, Y., YANG, Z., WANG, Z., SUN, W. W. and CHENG, G. (2021). Online bootstrap inference for policy evaluation in reinforcement learning. *arXiv preprint arXiv:2108.03706*.
- ROBINS, J. M. (2004). Optimal structural nested models for optimal sequential decisions. In *Proceedings of the Second Seattle Symposium in Biostatistics* 189–326. Springer.
- SHI, C., LU, W. and SONG, R. (2020). Breaking the curse of nonregularity with dubagging—inference of the mean outcome under optimal treatment regimes. *Journal of Machine Learning Research* **21** 1–67.
- SHI, C., SONG, R., LU, W. and FU, B. (2018). Maximin projection learning for optimal treatment decision with heterogeneous individualized treatment effects. *Journal of Royal Statistical Society: Series B* **80** 681–702.
- SHI, C., WAN, R., SONG, R., LU, W. and LENG, L. (2020). Does the Markov decision process fit the data: testing for the Markov property in sequential decision making. In *International Conference on Machine Learning* 8807–8817. PMLR.
- SHI, C., ZHANG, S., LU, W. and SONG, R. (2022). Statistical inference of the value function for reinforcement learning in infinite-horizon settings. *Journal of the Royal Statistical Society Series B: Statistical Methodology* **84** 765–793.
- SONG, R., WANG, W., ZENG, D. and KOSOROK, M. R. (2015). Penalized Q-learning for dynamic treatment regimens. *Statistica Sinica* **25** 901–920.
- SUTTON, R. S. and BARTO, A. G. (2018). *Reinforcement Learning: An Introduction*, second ed. *Adaptive Computation and Machine Learning*. MIT Press, Cambridge, MA.
- SUTTON, R. S., SZEPESVÁRI, C. and MAEI, H. R. (2008). A convergent $O(n)$ algorithm for off-policy temporal-difference learning with linear function approximation. *Advances in Neural Information Processing Systems* **21** 1609–1616.
- TROPP, J. (2011). Freedman’s inequality for matrix martingales. *Electronic Communications in Probability* **16** 262–270.
- TRUONG, C., OUDRE, L. and VAYATIS, N. (2020). Selective review of offline change point detection methods. *Signal Processing* **167**. 107299.
- TSIATIS, A. A., DAVIDIAN, M., HOLLOWAY, S. T. and LABER, E. B. (2019). *Dynamic Treatment Regimes: Statistical Methods for Precision Medicine*. CRC press.
- UEHARA, M., IMAIZUMI, M., JIANG, N., KALLUS, N., SUN, W. and XIE, T. (2021). Finite sample analysis of minimax offline reinforcement learning: Completeness, fast rates and first-order efficiency. *arXiv preprint arXiv:2102.02981*.
- VAN DER VAART, A. W. and WELLNER, J. A. (1996). *Weak convergence and empirical processes*. *Springer Series in Statistics*. Springer-Verlag, New York.
- WALLACE, M. P. and MOODIE, E. E. M. (2015). Doubly-robust dynamic treatment regimen estimation via weighted least squares. *Biometrics* **71** 636–644.
- WAN, R., ZHANG, X. and SONG, R. (2020). Multi-objective reinforcement learning for infectious disease control with application to COVID-19 spread. *arXiv preprint arXiv:2009.04607*.
- WANG, J., QI, Z. and WONG, R. K. (2023). Projected state-action balancing weights for offline reinforcement learning. *The Annals of Statistics* **51** 1639–1665.
- WANG, T. and SAMWORTH, R. (2018). High dimensional change point estimation via sparse projection. *Journal of the Royal Statistical Society: Series B* **80** 57–83.

- WANG, L., ZHOU, Y., SONG, R. and SHERWOOD, B. (2018). Quantile-optimal treatment regimes. *J. Amer. Stat. Assoc.* **113** 1243–1254.
- WATKINS, C. J. and DAYAN, P. (1992). Q-learning. *Machine learning* **8** 279–292.
- WEI, C.-Y. and LUO, H. (2021). Non-stationary reinforcement learning without prior knowledge: An optimal black-box approach. In *Conference on Learning Theory* 4300–4354. PMLR.
- WU, C.-F. J. (1986). Jackknife, bootstrap and other resampling methods in regression analysis. *the Annals of Statistics* **14** 1261–1295.
- XIE, A., HARRISON, J. and FINN, C. (2021). Deep reinforcement learning amidst continual structured non-stationarity. In *International Conference on Machine Learning* 11393–11403. PMLR.
- YU, M. and CHEN, X. (2021). Finite sample change point inference and identification for high-dimensional mean vectors. *Journal of the Royal Statistical Society: Series B* **83** 247–270.
- ZHANG, B., TSIATIS, A. A., LABER, E. B. and DAVIDIAN, M. (2013). Robust estimation of optimal dynamic treatment regimes for sequential treatment decisions. *Biometrika* **100** 681–694.
- ZHANG, Y., LABER, E. B., DAVIDIAN, M. and TSIATIS, A. A. (2018). Estimation of optimal treatment regimes using lists. *Journal of American Statistical Association* **113** 1541–1549.
- ZHAO, Y.-Q., ZENG, D., LABER, E. B. and KOSOROK, M. R. (2015). New statistical learning methods for estimating optimal dynamic treatment regimes. *Journal of American Statistical Association* **110** 583–598.
- ZHONG, H., YANG, Z. and SZEPESVÁRI, Z. W. C. (2021). Optimistic policy optimization is provably efficient in non-stationary MDPs. *arXiv preprint arXiv:2110.08984*.
- ZHOU, W., ZHU, R. and QU, A. (2022). Estimating optimal infinite horizon dynamic treatment regimes via pt-learning. *Journal of the American Statistical Association* **accepted**.
- ZHOU, Y., SHI, C., LI, L. and YAO, Q. (2023). Testing for the Markov property in time series via deep conditional generative learning. *Journal of the Royal Statistical Society: Series B* **accepted**.
- ZHU, R., ZHAO, Y.-Q., CHEN, G., MA, S. and ZHAO, H. (2017). Greedy outcome weighted tree learning of optimal personalized treatment rules. *Biometrics* **73** 391–400.

Supplement to “Testing Stationarity and Change Point Detection in Reinforcement Learning”

This supplement is organised as follows. We begin with a list of commonly used notations in the supplement, and introduce some technical definitions. We next compare model-free tests against model-based tests, and discuss some extensions and related work in Section A. We establish the asymptotic properties of the Q-function estimator in Section B. In Section C, we present the proofs of our theorems. Finally, in Appendix D, we detail the simulation setting and present some additional simulation results.

We introduce the class of p -smoothness functions. For a J -tuple $\alpha = (\alpha_1, \dots, \alpha_J)^\top$ of nonnegative integers and a given function h on \mathcal{S} , let D^α denote the differential operator:

$$D^\alpha h(s) = \frac{\partial^{|\alpha|} h(s)}{\partial s_1^{\alpha_1} \dots \partial s_J^{\alpha_J}}.$$

Here, s_j denotes the j th element of s . For any $p > 0$, let $\lfloor p \rfloor$ denote the largest integer that is smaller than p . The class of p -smooth functions is defined as follows:

$$\Lambda(p, c) = \left\{ h : \sup_{\|\alpha\|_1 \leq \lfloor p \rfloor} \sup_{s \in \mathcal{S}} |D^\alpha h(s)| \leq c, \sup_{\|\alpha\|_1 = \lfloor p \rfloor} \sup_{\substack{s_1, s_2 \in \mathcal{S} \\ s_1 \neq s_2}} \frac{|D^\alpha h(s_1) - D^\alpha h(s_2)|}{\|s_1 - s_2\|_2^{p - \lfloor p \rfloor}} \leq c \right\},$$

for some constant $c > 0$.

APPENDIX A: ADDITIONAL DISCUSSIONS

A.1. Model-free Tests vs. Model-based Tests. As commented in the main text, we focus on model-free tests in this paper, constructing the test statistic without directly estimating the reward and transition functions. Alternatively, one may study model-based tests, which directly evaluate the stationarity of the MDP model (i.e., reward and transition functions). Both model-based and model-free methods offer distinct advantages in RL. For example, model-free RL focuses on learning a one-dimensional optimal Q-function, eliminating the need to model a complex transition function that has an output dimension equal to the state’s. This is particularly relevant given the challenges in modeling transition functions, which can be prone to misspecification, especially in high-dimensional state spaces. Consider the case where the future state follows a conditional Gaussian distribution. Specifying the d -dimensional mean and $d \times d$ -dimensional covariance functions of the state-action pair can be quite complex. Conversely, the estimation the Q-function is challenging. A limited number of visits to certain state-action pairs can lead to inaccurate estimations of the Q-function’s value across other pairs.

A.2. Extensions to Settings with Varying Termination Times. Our proposed method is readily adaptable to scenarios where subjects have varying termination times. To elaborate, let $T^{(i)}$ represent the termination time for the i th subject, and $T = \max_i T^{(i)}$ be the maximum of these times. In estimating $\hat{\beta}_{[T_1, T_2]}$, we can modify the empirical sum operator $\sum_{i=1}^N \sum_{t=T_1}^{T_2-1}$ to $\sum_{i:1 \leq i \leq N, T^{(i)} > T_1} \sum_{t=T_1}^{T^{(i)}-1}$. Similarly, for the construction of the ℓ_1 -type test, the empirical average operator $1/(N(T - T_0)) \sum_{i=1}^N \sum_{t=T_0}^{T-1}$ is substituted with $n^{-1}(T_0) \sum_{i:1 \leq i \leq N, T^{(i)} > T_0} \sum_{t=T_0}^{T^{(i)}-1}$, where $n(T_0)$ denotes the total count of observations in the interval between T_0 and T .

A.3. Additional Related Works. Our proposal is related to a growing literature on multi-armed bandits and/or contextual bandits in nonstationary environments (see e.g., [Garivier and Moulines, 2008](#); [Cao et al., 2019](#); [Pike-Burke and Grünewälder, 2019](#); [Gopalan, Lakshminarayanan and Saligrama, 2021](#); [Manegueu, Carpentier and Yu, 2021](#)). In bandits, the system does not involve state transitions, which implies that past actions do not influence future outcomes through state variables, thereby negating any carryover effects over time. This assumption is often not applicable in mobile health ([Boruvka et al., 2018](#); [NeCamp et al., 2020](#); [Liao, Klasnja and Murphy, 2021](#)).

Change point detection has also been studied in online settings (see e.g., [Adams and MacKay, 2007](#); [Alami, Maillard and Féraud, 2020](#)). However, these works primarily concentrate on changes within a single time series. In contrast, our study is focused on detecting changes in the optimal Q-function.

APPENDIX B: ASYMPTOTIC PROPERTIES OF THE Q-FUNCTION ESTIMATOR

In this section, we focus on investigating the asymptotic properties of the estimated Q-function computed by FQI.

THEOREM 4 (Uniform consistency). *Suppose SA1, A2-A8 hold. Suppose the maximum number of iterations K in FQI satisfies $\log(NT) \ll K = O(N^{c_5} T^{c_5})$ for any $c_5 > 0$. Then A1 is satisfied for sufficiently large NT .*

THEOREM 5 (Asymptotic normality). *Suppose the conditions in Theorem 4 hold. Then*

$$\widehat{Q}_{[T_1, T_2]}(a, s) - Q^{opt}(a, s) = \frac{\phi_L^\top(a, s)}{N(T_2 - T_1)} \sum_{i=1}^N \sum_{t=T_1}^{T_2-1} \delta_L^\top(a, s) W_{[T_1, T_2]}^{-1} \phi_L(A_{i,t}, S_{i,t}) \delta_{i,t}^* + \phi_L^\top(a, s) \text{residual}_{[T_1, T_2]},$$

where the residual term (whose closed-form is given in Equation 38) is $O(L^{-p/d})$, with probability approaching 1 (WPA1).

We again make a few remarks. First, Theorem 5 implies that the FQE estimator has an asymptotic linear representation under SA1. It follows from the high-dimensional martingale central limit theorem ([Belloni and Oliveira, 2018](#)) that the set of the estimated Q-functions $\{\widehat{Q}_{[T_1, T_2]}\}_{T_1, T_2}$ are jointly asymptotically normal.

Second, as stated in Theorem 4, we require SA1, which is a stronger stationarity assumption compared to SA3. This is because FQI iteratively updates the Q-function using supervised learning. It thus requires the stationarity of the supervised learning target at each iteration. In contrast, such a condition is not needed when GGQ is employed to learn the optimal Q-function. However, it is worth mentioning that FQI is much easier to implement in practice, as it suffices to implement OLS during each iteration. It could be further extended to employ more general supervised learning algorithms to fit more complicated nonlinear models (e.g., neural networks).

APPENDIX C: PROOFS

Throughout the proof, we use c, \bar{c}, C, \bar{C} to denote some generic constants whose values are allowed to vary from place to place. Recall that for any two positive sequences $\{a_{N,T}\}_{N,T}, \{b_{N,T}\}_{N,T}$, the notation $a_{N,T} \preceq b_{N,T}$ means that there exists some constant $C > 0$ such that $a_{N,T} \leq C b_{N,T}$ for any N and T .

C.1. Proof of Theorem 1. The implication of SA1 leading to SA2 is apparent, given the definition of Q_t^π . Similarly, the transition from SA3 to SA4 is straightforward, as it directly follows from Equation (3). Therefore, we aim to show SA3 under SA2 in the rest of the proof.

Without loss of generality, assume $T_0 = 0$. The main idea of our proof lies in the use of policy iteration to establish the connection between a (non-optimal) Q-function and its optimal counterpart. We initiate this process with an arbitrarily chosen stationary policy π_1 . Subsequently, we define π_2 as the greedy policy with respect to $Q_t^{\pi_1}$, i.e.,

$$\pi_{2,t}(a|s) = \begin{cases} 1, & \text{if } a = \arg \max_{a'} Q_t^{\pi_1}(a', s); \\ 0, & \text{otherwise.} \end{cases}$$

When the argmax is non-unique, we select the smallest maximizer. Under SA2, $Q_t^{\pi_1}$ is stationary, so is π_2 . We next repeat this process by defining π_k to the greedy policy with respect to $Q_t^{\pi_{k-1}}$ for $k = 3, 4, \dots$. Similarly, we can show that all these policies and Q-functions are stationary. To ease the notation, we remove the subscript t from $\pi_{k,t}$ and $Q_t^{\pi_{k-1}}$. Thus, they are represented as π_k and $Q^{\pi_{k-1}}$, respectively.

According to the policy improvement theorem (see e.g., Sutton and Barto, 2018, Equation 4.8), we obtain $V_t^{\pi_k}(s) \geq V_t^{\pi_{k-1}}(s)$ for any k, t and s . Here, $V_t^\pi(\bullet)$ denotes the (state) value function $\mathbb{E}^\pi(\sum_{k \geq t} \gamma^{k-t} R_k | S_t = s)$ starting from a given state s at time t . Additionally, the Q-function is connected to the value function through the following equation:

$$(17) \quad Q_t^\pi(a, s) = \mathbb{E}[R_t + \gamma V_{t+1}^\pi(S_{t+1}) | A_t = a, S_t = s].$$

As such, we obtain that $Q^{\pi_k}(a, s) \geq Q^{\pi_{k-1}}(a, s)$ for any k, a and s . For a given state-action pair, the sequence $\{Q^{\pi_k}(a, s)\}_k$ is monotonically non-decreasing. Since all rewards are uniformly bounded, so are these Q-function. Consequently, Q^{π_k} converges to a bounded function Q^* . The convergence is uniform given that the state-action space is finite.

To complete the proof, we aim to show that $Q^* = Q_t^{opt}$ for any t . According to Theorem 6.2.10 of Puterman (2014), π^{opt} maximizes the value function among all policies, i.e., $V_t^{\pi^{opt}}(s) \geq V_t^\pi(s)$ for any t, s and π . This together with (17) yields

$$(18) \quad Q^{\pi_k} \leq Q_t^{opt},$$

for any k, t . Additionally, it follows from (17) that

$$Q^{\pi_k}(a, s) = \mathbb{E}[R_t + \gamma Q^{\pi_k}(\pi_k(S_{t+1}), S_{t+1}) | A_t = a, S_t = s].$$

Since Q^{π_k} is monotonically non-decreasing, we obtain

$$\begin{aligned} Q^{\pi_k}(a, s) &\geq \mathbb{E}[R_t + \gamma Q^{\pi_{k-1}}(\pi_k(S_{t+1}), S_{t+1}) | A_t = a, S_t = s] \\ &= \mathbb{E}[R_t + \gamma \max_{a'} Q^{\pi_{k-1}}(a', S_{t+1}) | A_t = a, S_t = s]. \end{aligned}$$

This together with the Bellman optimality equation yields,

$$Q^{\pi_k}(a, s) - Q_t^{opt}(a, s) \geq \gamma \mathbb{E}[\max_{a'} Q^{\pi_{k-1}}(a', S_{t+1}) - \max_{a'} Q_{t+1}^{opt}(a', S_{t+1}) | A_t = a, S_t = s].$$

In view of (18), we obtain

$$\begin{aligned} |Q^{\pi_k}(a, s) - Q_t^{opt}(a, s)| &\leq \gamma \mathbb{E}[|\max_{a'} Q^{\pi_{k-1}}(a', S_{t+1}) - \max_{a'} Q_{t+1}^{opt}(a', S_{t+1})| | A_t = a, S_t = s] \\ &\leq \gamma \max_{a', s'} |Q^{\pi_{k-1}}(a', s') - Q_{t+1}^{opt}(a', s')|, \end{aligned}$$

and hence

$$\max_{a, s} |Q^{\pi_k}(a, s) - Q_t^{opt}(a, s)| \leq \gamma \max_{a, s} |Q^{\pi_{k-1}}(a, s) - Q_{t+1}^{opt}(a, s)|.$$

Notice that Q^{π^k} converges uniformly to Q^* . By letting $k \rightarrow \infty$, we obtain

$$\max_{a,s} |Q^*(a,s) - Q_t^{\text{opt}}(a,s)| \leq \gamma \max_{a,s} |Q^*(a,s) - Q_{t+1}^{\text{opt}}(a,s)| \leq \gamma^K \max_{a,s} |Q^*(a,s) - Q_{t+K}^{\text{opt}}(a,s)|,$$

for any $K > 1$. Under the bounded reward assumption, by letting $K \rightarrow \infty$, we obtain $Q^* = Q_t^{\text{opt}}$ for any t . This yields SA3. The proof is hence completed.

C.2. Proof of Theorem 2. We begin by introducing the following auxiliary lemmas. Specifically, Lemma 16 lists the properties of B-spline basis function. Lemma 17 derives the uniform rate of convergence of $\{\hat{\beta}_{[T_1, T_2]}\}_{T_1, T_2}$. Lemma 18 provides a uniform upper error bound on $|\widehat{W}_{[T_1, T_2]} - W_{[T_1, T_2]}|$. Without loss of generality, assume $T_0 = 0$. Their proofs are provided in Sections C.3, C.4 and C.5, respectively.

LEMMA 16. *Under the null hypothesis, there exists some $\beta^* \in \mathbb{R}^L$ such that*

$$(19) \quad \sup_{a,s} |Q^{\text{opt}}(a,s) - \phi_L^\top(a,s)\beta^*| = O(L^{-p/d}).$$

Additionally, we have

$$(20) \quad \max_a \lambda_{\max} \left[\int_s \phi_L(a,s)\phi_L^\top(a,s)ds \right] = O(1), \quad \sup_{a,s} \|\phi_L(a,s)\|_1 = O(\sqrt{L}),$$

and

$$(21) \quad \max_a \sup_{s_1 \neq s_2} \frac{\|\phi_L(a,s_1) - \phi_L(a,s_2)\|_2}{\|s_1 - s_2\|_2} = O(\sqrt{L}).$$

LEMMA 17. *Under the null hypothesis, there exists some constant $c > 0$ such that*

$$\sup_{T_2 - T_1 \geq \epsilon T} \|\hat{\beta}_{[T_1, T_2]} - \beta^*\|_2 = O(L^{-\kappa}),$$

for some $\kappa > 1/2$ WPA1, where β^* corresponds to the least-false parameter defined in Lemma 16. Here, the exponent κ can be set to $\min(p/d, 0.5c_4^{-1} - 0.5 - \epsilon^*)$ for any sufficiently small $\epsilon^* > 0$.

LEMMA 18. *Under the null hypothesis, there exists some constant $\bar{c} > 0$ such that $\|W_{[T_1, T_2]}^{-1}\|_2 \leq \bar{c}$ and that $\max_{T_2 - T_1 \geq \epsilon T} \|\widehat{W}_{[T_1, T_2]} - W_{[T_1, T_2]}\| = O\{(\epsilon NT)^{-1/2} \sqrt{L \log(NT)}\}$ with probability at least $1 - O(N^{-1}T^{-1})$. Here, $\|W_{[T_1, T_2]}^{-1}\|_2$ corresponds to the matrix operator norm of $W_{[T_1, T_2]}^{-1}$.*

C.2.1. ℓ_1 Type Test. We begin with an outline of the proof of Theorem 2. The proof is divided into four steps.

In Step 1, we show there exist some constants $c, C > 0$ such that

$$(22) \quad \mathbb{P}(|\sqrt{NT}(\text{TS}_1 - \text{TS}_1^*)| \leq C(NT)^{-c}) \rightarrow 1,$$

where

$$\text{TS}_1^* = \max_{\epsilon T < u < (1-\epsilon)T} \sqrt{\frac{u(T-u)}{T^2}} \left\{ \frac{1}{T} \sum_{t=0}^{T-1} \sum_a \int_s |\widehat{Q}_{[0,u]}(a,s) - \widehat{Q}_{[u,T]}(a,s)| \pi_t^b(a|s) p_t^b(s) ds \right\},$$

where π_t^b denotes the behavior policy at time t and p_t^b denotes the marginal distribution of S_t under the behavior policy. By definition, TS_1^* corresponds to a version of TS_1 assuming the marginal distribution of the observed state-action pairs is known to us.

In the second step, we define

$$\widehat{Q}_{[T_1, T_2]}^{b,0}(a, s) = \frac{1}{N(T_2 - T_1)} \phi_L^\top(a, s) W_{[T_1, T_2]}^{-1} \sum_{i=1}^N \sum_{t=T_1}^{T_2-1} \phi_L(A_{i,t}, S_{i,t}) \delta_{i,t}(\widehat{\beta}_{[T_1, T_2]}) e_{i,t}, \quad \forall T_1, T_2,$$

a version of $\widehat{Q}_{[T_1, T_2]}^b(a, s)$ with $\widehat{W}_{[T_1, T_2]}^{-1}$ replaced by its oracle value, and establish a uniform upper error bound for $\max_{i,t,T_1,T_2} |\widehat{Q}_{[T_1, T_2]}^b(A_{i,t}, S_{i,t}) - \widehat{Q}_{[T_1, T_2]}^{b,0}(A_{i,t}, S_{i,t})|$. Specifically, we show that there exists some constant $\epsilon_0 > 0$ such that the uniform upper error bound decays to zero at a rate of $O\{(NT)^{-1/2-\epsilon_0}\}$, WPA1. By triangle inequality, we can show that

$$(23) \quad \mathbb{P}(|\sqrt{NT}(\text{TS}_1^b - \text{TS}_1^{b,0})| \leq C(NT)^{-c}) \rightarrow 1,$$

for some constant $C > 0$, where

$$\text{TS}_1^{b,0} = \max_{\epsilon T < u < (1-\epsilon)T} \sqrt{\frac{u(T-u)}{T^2}} \left\{ \frac{1}{NT} \sum_{t=0}^{T-1} \sum_{i=1}^N |\widehat{Q}_{[0,u]}^{b,0}(A_{i,t}, S_{i,t}) - \widehat{Q}_{[u,T]}^{b,0}(A_{i,t}, S_{i,t})| \right\}.$$

Using similar arguments as in the proof of (22) in Step 1 (see Pages 9 – 11), we can show that $|\text{TS}_1^{b,0} - \text{TS}_1^{b,*}|$ is upper bounded by $C(NT)^{-c}$ for some $c, C > 0$, WPA1, where

$$\text{TS}_1^{b,*} = \max_{\epsilon T < u < (1-\epsilon)T} \sqrt{\frac{u(T-u)}{T^2}} \left\{ \frac{1}{T} \sum_{t=0}^{T-1} \sum_a \int_s |\widehat{Q}_{[0,u]}^{b,0}(a, s) - \widehat{Q}_{[u,T]}^{b,0}(a, s)| \pi_t^b(a|s) p_t^b(s) ds \right\}.$$

This together with (23) yields that

$$\mathbb{P}(|\sqrt{NT}(\text{TS}_1^b - \text{TS}_1^{b,*})| \leq C(NT)^{-c}) \rightarrow 1,$$

for some constants $c, C > 0$. It also implies that

$$(24) \quad \mathbb{P}(|\sqrt{NT}(\text{TS}_1^b - \text{TS}_1^{b,*})| \leq C(NT)^{-c} | \text{Data}) \xrightarrow{P} 1.$$

In the third step, we define TS_1^{**} to be a version of TS_1^* with $\widehat{Q}_{[T_1, T_2]}(a, s)$ replaced by

$$\frac{1}{N(T_2 - T_1)} \sum_{i=1}^N \sum_{t=T_1}^{T_2-1} \phi_L^\top(a, s) W_{[T_1, T_2]}^{-1} \phi_L(A_{i,t}, S_{i,t}) \delta_{i,t}^*$$

Similarly, we define $\text{TS}_1^{b,**}$ to be a version of $\text{TS}_1^{b,*}$ with $\delta_{i,t}(\widehat{\beta}_{[T_1, T_2]})$ replaced by the oracle value $\delta_{i,t}^*$. We will show that

$$(25) \quad \mathbb{P}(|\sqrt{NT}(\text{TS}_1^* - \text{TS}_1^{**})| \leq C(NT)^{-c}) \rightarrow 1,$$

$$\mathbb{P}(|\sqrt{NT}(\text{TS}_1^{b,*} - \text{TS}_1^{b,**})| \leq C(NT)^{-c} | \text{Data}) \xrightarrow{P} 1.$$

Combining the results in (22)-(25), we have shown that

$$(26) \quad \mathbb{P}(|\sqrt{NT}(\text{TS}_1 - \text{TS}_1^{**})| \leq C(NT)^{-c}) \rightarrow 1,$$

$$\mathbb{P}(|\sqrt{NT}(\text{TS}_1^b - \text{TS}_1^{b,**})| \leq C(NT)^{-c} | \text{Data}) \xrightarrow{P} 1.$$

In the last step, we aim to show the proposed test controls the type-I error. A key step in our proof is to bound the Kolmogorov distance between TS_1^{**} and $\text{TS}_1^{b,**}$. This together with (26) yields the validity of the proposed test. Notice that TS_1^{**} can be viewed as a function of the set of mean zero random vectors

$$(27) \left\{ Z_u \equiv \frac{W_{[0,u]}^{-1}}{Nu} \sum_{i=1}^N \sum_{t=0}^{u-1} \phi_L(A_{i,t}, S_{i,t}) \delta_{i,t}^* - \frac{W_{[u,T]}^{-1}}{N(T-u)} \sum_{i=1}^N \sum_{t=u}^{T-1} \phi_L(A_{i,t}, S_{i,t}) \delta_{i,t}^* : u \right\}.$$

Similarly, $\text{TS}_1^{b,**}$ can be represented as a function of the bootstrapped samples

$$\left\{ \mathbb{E}_u^b \equiv \frac{W_{[0,u]}^{-1}}{Nu} \sum_{i=1}^N \sum_{t=0}^{u-1} \phi_L(A_{i,t}, S_{i,t}) \delta_{i,t}^* e_{i,t} - \frac{W_{[u,T]}^{-1}}{N(T-u)} \sum_{i=1}^N \sum_{t=u}^{T-1} \phi_L(A_{i,t}, S_{i,t}) \delta_{i,t}^* e_{i,t} : u \right\}.$$

When T and L are fixed, the classical continuous mapping theorem can be applied to establish the weak convergence results. However, in our setting, L needs to diverge with the number of observations to alleviate the model misspecification error. We also allow T to approach infinity. Hence, classical weak convergence results cannot be applied. Toward that end, we establish a nonasymptotic error bound for the Kolmogorov distance as a function of N, T and L , and show that this bound decays to zero under the given conditions. The proof is based on the high-dimensional martingale central limit theorem developed by [Belloni and Oliveira \(2018\)](#); see also the high-dimensional CLT by [Chernozhukov, Chetverikov and Kato \(2014\)](#).

We next detail the proof for each step.

Step 1. For each u , we aim to develop a concentration inequality to bound the difference

$$(29) \quad \left| \sqrt{\frac{u(T-u)}{T^2}} \left\{ \frac{1}{NT} \sum_{t=0}^{T-1} \sum_{i=1}^N \sum_a \int_s \left[|\widehat{Q}_{[0,u]}(A_{i,t}, S_{i,t}) - \widehat{Q}_{[u,T]}(A_{i,t}, S_{i,t})| \right. \right. \right. \\ \left. \left. \left. - |\widehat{Q}_{[0,u]}(a, s) - \widehat{Q}_{[u,T]}(a, s)| \right] \pi_t^b(a|s) p_t^b(s) ds \right\} \right|.$$

According to Lemma 17, we have that $\sup_{T_1, T_2} \|\widehat{\beta}_{[T_1, T_2]} - \beta^*\|_2 = O(L^{-\kappa})$ for some constant $\kappa > 1/2$, WPA1.

Define the set $\mathcal{B}(C) = \{\beta \in \mathbb{R}^L : \|\beta - \beta^*\|_2 \leq CL^{-\kappa}\}$. It follows that there exists some sufficiently large constant $C > 0$ such that $\widehat{\beta}_{[T_1, T_2]} \in \mathcal{B}(C)$ WPA1. (29) can thus be upper bounded by

$$(30) \quad \sup_{\substack{\beta_1 \in \mathcal{B}(C) \\ \beta_2 \in \mathcal{B}(C)}} \left| \frac{1}{2NT} \sum_{t=0}^{T-1} \sum_{i=1}^N \left\{ |\phi_L^\top(A_{i,t}, S_{i,t})(\beta_1 - \beta_2)| - \mathbb{E} |\phi_L^\top(A_{i,t}, S_{i,t})(\beta_1 - \beta_2)| \right\} \right|.$$

The upper bound for (30) can be established using similar arguments as in the proof of Lemma 18. To save space, we only provide a sketch of the proof here. Please refer to the proof of Lemma 18 for details.

Notice that the suprema in (30) are taken with respect to infinitely many β s. As such, standard concentration inequalities are not applicable to bound (30). Toward that end, we first take an ε -net of $\mathcal{B}(C)$ for some sufficiently small $\varepsilon > 0$, denote by $\mathcal{B}^*(C)$, such that for any $\beta \in \mathcal{B}(C)$, there exists some $\beta^* \in \mathcal{B}^*(C)$ that satisfies $\|\beta - \beta^*\|_2 \leq \varepsilon$. The purpose of introducing an ε -net is to approximate these sets by collections of finitely many β s so that concentration inequalities are applicable to establish the upper bound. Set $\varepsilon = C(NT)^{-2}L^{-\kappa}$. It follows from Lemma 2.2 of [Mendelson, Pajor and Tomczak-Jaegermann \(2008\)](#) that there exist some $\mathcal{B}^*(C)$ with number of elements upper bounded by $5^L(NT)^{2L}$.

By Lemma 16, we have $\sup_{a,s} \|\phi_L(a, s)\|_2 = O(\sqrt{L})$. Thanks to this uniform bound, the quantity within the absolute value symbol in (30) is a Lipschitz continuous function of (β_1, β_2) , with the Lipschitz constant upper bounded by $O(\sqrt{L})$. As such, (30) can be approximated by

$$(31) \quad \sup_{\beta_1, \beta_2 \in \mathcal{B}^*(C)} \left| \underbrace{\frac{1}{2NT} \sum_{t=0}^{T-1} \sum_{i=1}^N \sum_a \left\{ |\phi_L^\top(A_{i,t}, S_{i,t})(\beta_1 - \beta_2)| - \mathbb{E} |\phi_L^\top(A_{i,t}, S_{i,t})(\beta_1 - \beta_2)| \right\}}_{I(\beta_1, \beta_2) \text{ (without absolute value)}} \right|,$$

with the approximation error given by $O(C\sqrt{LN}^{-2}T^{-2}L^{-\kappa})$.

It remains to develop a concentration inequality for (31). Since the number of elements in $\mathcal{B}^*(C)$ are bounded, we could develop a tail inequality for the quantity within the absolute value symbol in (31) for each combination of β_1 and β_2 , and then apply Bonferroni inequality to establish a uniform upper error bound. More specifically, for each pair (β_1, β_2) , let

$$I^*(\beta_1, \beta_2) = \frac{1}{2NT} \sum_{t=0}^{T-1} \sum_{i=1}^N [\mathbb{E}\{\phi_L^\top(A_{i,t}, S_{i,t})(\beta_1 - \beta_2) | S_{i,t-1}\} - \mathbb{E}\phi_L^\top(A_{i,t}, S_{i,t})(\beta_1 - \beta_2)],$$

with the convention that $S_{i,-1} = \emptyset$. Notice that $I(\beta_1, \beta_2) - I^*(\beta_1, \beta_2)$ forms a mean-zero martingale under the conditional (mean) independence assumptions in (1) and (2) (e.g., the future state and the conditional mean of the immediate reward are independent of the history given the current state-action pair), we can first apply the martingale concentration inequality (see e.g., [Tropp, 2011](#)) to show that

$$(32) \quad |I(\beta_1, \beta_2) - I^*(\beta_1, \beta_2)| = O(L^{-\varepsilon_0} \sqrt{N^{-1}T^{-1} \log(NT)}),$$

for some $\varepsilon_0 > 0$, with probability at least $1 - O\{(NT)^{-CL}\}$ for some sufficiently large constant $C > 0$. Here, the upper bound $O(L^{-\varepsilon_0} \sqrt{N^{-1}T^{-1} \log(NT)})$ decays faster than the parametric rate, due to the fact that the variance of the summand decays to zero. Specifically, notice that $\text{Var}\{\phi_L^\top(A_t, S_t)(\beta_1 - \beta_2) | S_{t-1}\}$ is upper bounded by

$$\max_{a, a', s} \lambda_{\max} \left\{ \int_{s'} \phi_L(a', s') \phi_L^\top(a', s') p(s' | a, s) ds' \right\} \|\beta_1 - \beta_2\|_2^2 = O(L^{-2\kappa}),$$

where the equality is due to Lemma 16 and the fact that p is uniformly bounded (see A4(iii) and the definition of the p -smoothness function class).

Next, under A4(i) and (ii), the transition functions $\{\mathcal{T}_t\}_t$ satisfies the conditions in the statement of Theorem 3.1 in [Alquier, Doukhan and Fan \(2019\)](#). In addition, each summand in the definition of $I^*(\beta_1, \beta_2)$ is upper bounded by $O(L^{-\kappa})$ for some $\kappa > 1/2$. We can apply the concentration inequality for non-stationary Markov chains developed therein to show that $|I^*(\beta_1, \beta_2)| = O(L^{-\varepsilon_0} \sqrt{N^{-1}T^{-1} \log(NT)})$, with probability at least $1 - O\{(NT)^{-CL}\}$ for some sufficiently large constant $C > 0$. This together with the upper bound for $|I(\beta_1, \beta_2) - I^*(\beta_1, \beta_2)|$ in (32), Bonferroni inequality and the condition that L is proportional to $(NT)^{c_4}$ yields the desired uniform upper bound for (31). This completes Step 1 of the proof.

Step 2. By definition, $\widehat{Q}_{[T_1, T_2]}^{b,0}(A_{i,t}, S_{i,t}) - \widehat{Q}_{[T_1, T_2]}^b(A_{i,t}, S_{i,t})$ is equal to the sum of

$$(33) \quad \frac{1}{N(T_2 - T_1)} \phi_L^\top(A_{i,t}, S_{i,t}) (\widehat{W}_{[T_1, T_2]}^{-1} - W_{[T_1, T_2]}^{-1}) \sum_{i'=1}^N \sum_{t'=T_1}^{T_2-1} \phi_L(A_{i', t'}, S_{i', t'}) \delta_{i', t'} (\widehat{\beta}_{[T_1, T_2]}) e_{i', t'}.$$

and

$$(34) \quad \frac{1}{N(T_2 - T_1)} \phi_L^\top(A_{i,t}, S_{i,t}) W_{[T_1, T_2]}^{-1} \sum_{i'=1}^N \sum_{t'=T_1}^{T_2-1} \phi_L(A_{i', t'}, S_{i', t'}) (\delta_{i', t'} (\widehat{\beta}_{[T_1, T_2]}) - \delta_{i', t'}^*) e_{i', t'}.$$

Consider the first term. In Lemma 18, we establish a uniform upper error bound for $\|\widehat{W}_{[T_1, T_2]} - W_{[T_1, T_2]}\|_2$ and show that $\|W_{[T_1, T_2]}^{-1}\|_2$ is upper bounded by some constant. Using similar arguments in Part 3 of the proof of Lemma 3 in [Shi et al. \(2022\)](#), we can show that $\|\widehat{W}_{[T_1, T_2]}^{-1} - W_{[T_1, T_2]}^{-1}\|_2$ is of the same order of magnitude as $\|\widehat{W}_{[T_1, T_2]} - W_{[T_1, T_2]}\|_2$. The boundedness assumption of R_t implies that the Q-function is bounded. This together with

Lemma 17 implies the estimated Q-function is bounded as well, and so is $\delta_{i',t'}(\widehat{\beta}_{[T_1, T_2]})$. By (20), the conditional variance of (33) given the data is upper bounded by

$$\frac{CL^2}{\epsilon^2 N^2 T^2} \lambda_{\max} \left\{ \frac{1}{N(T_2 - T_1)} \sum_{i=1}^N \sum_{t=T_1}^{T_2-1} \phi_L(A_{i,t}, S_{i,t}) \phi_L^\top(A_{i,t}, S_{i,t}) \right\}.$$

Similar to Lemma 18, we can show that the maximum eigenvalue of the matrix inside the curly brackets converges to $\lambda_{\max}\{(T_2 - T_1)^{-1} \sum_{t=T_1}^{T_2-1} \mathbb{E} \phi_L(A_t, S_t) \phi_L^\top(A_t, S_t)\}$, which is bounded by some finite constant according to (20). Under the given conditions on ϵ and L , the conditional variance of (33) given the data is of the order $(NT)^{-2c-1}$, for some constant $c > 0$, WPA1. Notice that the probability of a standard normal random variable exceeding z is bounded by $\exp(-z^2/2)$ for any $z > 1$; see e.g., the inequality for the Gaussian Mill's ratio (Birnbaum, 1942). Since (33) is a mean-zero Gaussian random variable given the data, it is of the order $O\{(NT)^{-c-1/2} \sqrt{\log(NT)}\}$, with probability at least $1 - O\{(NT)^{-C}\}$ for any sufficiently large constant $C > 0$. This together with Bonferroni inequality yields the desired uniform upper error bound for the first term. As for the second term, notice that by Lemma 17, the difference $\delta_{i,t}(\widehat{\beta}_{[T_1, T_2]}) - \delta_{i,t}^*$ decays at a rate of $(NT)^{-c}$ for some constant $c > 0$, uniformly in i, t, T_1, T_2 , WPA1. Based on this result, we can similarly derive the upper error bound for the second term. This completes the proof.

Step 3. We first bound the difference between TS_1^* and TS_1^{**} . Let m_0 denote the margin defined in A7. Under A1, it is clear that

$$(35) \quad \mathbb{P} \left(\max_{[T_1, T_2] \subseteq [0, T]} \sup_{a, s} |\phi_L^\top(a, s) \widehat{\beta}_{[T_1, T_2]} - Q^{opt}(a, s)| \leq \frac{m_0}{3} \right) \rightarrow 1.$$

Under the event defined in (35), it follows from the uniqueness of the optimal policy (see A6) that

$$\begin{aligned} & \phi_L^\top(\pi^{opt}(s), s) \widehat{\beta}_{[T_1, T_2]} - \max_{a \neq \pi^{opt}(s)} \phi_L^\top(a, s) \widehat{\beta}_{[T_1, T_2]} \\ & \geq Q^{opt}(\pi^{opt}(s), s) - \max_{a \neq \pi^{opt}(s)} Q^{opt}(a, s) - \frac{2m_0}{3} \geq \frac{m_0}{3}, \end{aligned}$$

for any a, s, T_1 and T_2 . This leads to

$$(36) \quad \pi^{opt}(s) = \arg \max_a \phi_L^\top(a, s) \widehat{\beta}_{[T_1, T_2]}.$$

By definition, $\widehat{\beta}_{[T_1, T_2]}$ solves the estimating equation in (11). This together with (36) yields

$$(37) \quad \sum_{i=1}^N \sum_{t=T_1}^{T_2-1} \left\{ R_{i,t} + \gamma \phi_L^\top(\pi^{opt}(S_{i,t+1}), S_{i,t+1}) \widehat{\beta}_{[T_1, T_2]} - \phi_L^\top(A_{i,t}, S_{i,t}) \widehat{\beta}_{[T_1, T_2]} \right\} \\ \times \frac{\phi_L(A_{i,t}, S_{i,t})}{N(T_2 - T_1)} = 0.$$

Additionally,

$$\begin{aligned} & \frac{1}{N(T_2 - T_1)} \sum_{i=1}^N \sum_{t=T_1}^{T_2-1} \left\{ R_{i,t} + \gamma \phi_L^\top(\pi^{opt}(S_{i,t+1}), S_{i,t+1}) \beta^* - \phi_L^\top(A_{i,t}, S_{i,t}) \beta^* \right\} \phi_L(A_{i,t}, S_{i,t}) \\ & = \frac{1}{N(T_2 - T_1)} \sum_{i=1}^N \sum_{t=T_1}^{T_2-1} \delta_{i,t}^* \phi_L(A_{i,t}, S_{i,t}) + \text{residual}_{[T_1, T_2]}, \end{aligned}$$

where the residual term is given by

$$(38) \sum_{i=1}^N \sum_{t=T_1}^{T_2-1} \frac{\phi_L(A_{i,t}, S_{i,t})}{N(T_2 - T_1)} \left\{ \gamma \phi_L^\top(\pi^{opt}(S_{i,t+1}), S_{i,t+1}) \beta^* - \gamma Q^{opt}(\pi^{opt}(S_{i,t+1}), S_{i,t+1}) \right. \\ \left. - \phi_L^\top(A_{i,t}, S_{i,t}) \beta^* + Q^{opt}(A_{i,t}, S_{i,t}) \right\}.$$

We first consider the mean of (38). According to (19), the term inside the curly bracket is $O(L^{-p/d})$. Consequently, the ℓ_2 norm of the mean of (38) is upper bounded by

$$\frac{O(L^{-p/d})}{T_2 - T_1} \sum_{t=T_1}^{T_2-1} \sup_{\nu \in \mathbb{R}^L: \|\nu\|_2=1} \sum_a \int_s |\phi_L^\top(a, s) \nu| \pi_t^b(a|s) p_t^b(s) ds.$$

Under A4(iii), $\{p_t\}_t$ is uniformly bounded. So is $\{p_t^b\}_t$. It follows from (20) that the above expression is of the order

$$O \left\{ L^{-p/d} \max_a \lambda_{\max} \left[\int_s \phi_L(a, s) \phi_L^\top(a, s) ds \right] \right\} = O(L^{-p/d}).$$

Additionally, using similar arguments in Step 2, we can show that the difference between (38) and its mean is upper bounded by $O(L^{1/2-p/d} \sqrt{(\epsilon NT)^{-1} \log(NT)})$, WPA1. Under the conditions on ϵ and L in A2 and A8, the residual term is bounded by $O(L^{-p/d})$, WPA1. It follows from (37) that

$$(39) \hat{\beta}_{[T_1, T_2]} - \beta^* = \frac{\widehat{W}_{[T_1, T_2]}^{-1}}{N(T_2 - T_1)} \sum_{i=1}^N \sum_{t=T_1}^{T_2-1} \delta_{i,t}^* \phi_L(A_{i,t}, S_{i,t}) + \widehat{W}_{[T_1, T_2]}^{-1} \text{residual}_{[T_1, T_2]}.$$

By Lemma 18, $\|\widehat{W}_{[T_1, T_2]}^{-1}\|_2$ is upper bounded, WPA1. This together with $\|\text{residual}_{[T_1, T_2]}\|_2 = O(L^{-p/d})$ implies that the second term on the right-hand-side (RHS) of (39) is $O(L^{-p/d})$. As for the first term, it can be approximated by

$$(40) \text{leading}_{[T_1, T_2]} = \frac{W_{[T_1, T_2]}^{-1}}{N(T_2 - T_1)} \sum_{i=1}^N \sum_{t=T_1}^{T_2-1} \delta_{i,t}^* \phi_L(A_{i,t}, S_{i,t}),$$

with approximation error bound from above by

$$\left\| \frac{\widehat{W}_{[T_1, T_2]}^{-1} - W_{[T_1, T_2]}^{-1}}{N(T_2 - T_1)} \right\| \left\| \sum_{i=1}^N \sum_{t=T_1}^{T_2-1} \delta_{i,t}^* \phi_L(A_{i,t}, S_{i,t}) \right\|_2.$$

Notice that $\|\widehat{W}_{[T_1, T_2]}^{-1} - W_{[T_1, T_2]}^{-1}\|_2$ is of the same order of magnitude as $\|\widehat{W}_{[T_1, T_2]} - W_{[T_1, T_2]}\|_2$. Additionally, the mean zero residual $\|\sum_{i=1}^N \sum_{t=T_1}^{T_2-1} \delta_{i,t}^* \phi_L(A_{i,t}, S_{i,t})\|_2 = O(\sqrt{L \epsilon NT \log(NT)})$, WPA1. It follows from (39) that $\hat{\beta}_{[T_1, T_2]} - \beta^*$ can be well-approximated by (40), with the approximation error upper bounded by $O(L^{-p/d}) + O(L(\epsilon NT)^{-1} \log(NT))$, WPA1. This allows us to bound the difference between TS_1^* and TS_1^{**} by

$$(41) \frac{O(L^{-p/d}) + O(L(\epsilon NT)^{-1} \log(NT))}{T} \sum_{t=0}^{T-1} \sup_{\nu \in \mathbb{R}^L: \|\nu\|_2=1} \sum_a \int_s |\phi_L^\top(a, s) \nu| \pi_t^b(a|s) p_t^b(s) ds,$$

which is of the order $O(L^{-p/d}) + O(L(\epsilon NT)^{-1} \log(NT))$. Under the conditions on c_4 and ϵ (see A2 and A8), it verifies the first equation in (25).

As commented in A8, the lower bound requirement on L is not needed under SA1 and SA5. This is because both $W_{[T_1, T_2]}$ and the mean of the residual term $\mathbb{E}(\text{residual}_{[T_1, T_2]})$ are constant over all combinations of T_1 and T_2 . Using similar arguments, we can show that the difference between $\widehat{\beta}_{[0, u]} - \widehat{\beta}_{[u, T]}$ can be well approximated by $\text{leading}_{[0, u]} - \text{leading}_{[u, T]}$ with the approximation error bounded by $O(L(\epsilon NT)^{-1} \log(NT))$, WPA1. This establishes the equivalence between TS_1^* and TS_1^{**} .

Next, consider the difference between $\text{TS}_1^{b,*}$ and $\text{TS}_1^{b,**}$. By triangle inequality, $|\text{TS}_1^{b,*} - \text{TS}_1^{b,**}|$ can be upper bounded by the sum of

$$\max_{u > \epsilon T} \frac{1}{2T} \sum_{t=0}^{T-1} \sum_a \int_s \left| \phi_L^\top(a, s) \left(\frac{1}{Nu} \sum_{i=1}^N \sum_{t=0}^{u-1} W_{[0, u]}^{-1} \phi_L(A_{i,t}, S_{i,t}) [\delta_{i,t}(\widehat{\beta}_{[0, u]}) - \delta_{i,t}^*] e_{i,t} \right) \right| \pi_t^b(a|s) p_t^b(s) ds,$$

and

$$\max_{u < (1-\epsilon)T} \frac{1}{2T} \sum_{t=0}^{T-1} \sum_a \int_s \left| \phi_L^\top(a, s) \left(\frac{1}{N(T-u)} \sum_{i=1}^N \sum_{t=u}^{T-1} W_{[0, u]}^{-1} \phi_L(A_{i,t}, S_{i,t}) [\delta_{i,t}(\widehat{\beta}_{[0, u]}) - \delta_{i,t}^*] e_{i,t} \right) \right| \times \pi_t^b(a|s) p_t^b(s) ds.$$

By (39), using similar arguments in Step 2 of the proof, we can show that

$$\left\| \frac{1}{N(T_2 - T_1)} \sum_{i=1}^N \sum_{t=T_1}^{T_2-1} W_{[T_1, T_2]}^{-1} \phi_L(A_{i,t}, S_{i,t}) [\delta_{i,t}(\widehat{\beta}_{[T_1, T_2]}) - \delta_{i,t}^*] e_{i,t} \right\|_2$$

can be upper bounded by $O\{(NT)^{-c}\}$ for some constant $c > 1/2$, WPA1. Consequently, using similar arguments in bounding $|\text{TS}_1^* - \text{TS}_1^{**}|$ (see e.g., 41), we can show that $|\text{TS}_1^{b,*} - \text{TS}_1^{b,**}|$ can be upper bounded by $O\{(NT)^{-c}\}$ as well. This completes the proof of Step 3.

Step 4. As we have commented, the proof is based on the high-dimensional martingale central limit theorem developed by Belloni and Oliveira (2018). Let Z and Z^b denote the high-dimensional random vectors formed by stacking the random vectors in the set (27) and (28), respectively. Notice that Z can be represented as $\sum_{i,t} Z_{i,t}$ where each $Z_{i,t}$ depends on the data tuple $(S_{i,t}, A_{i,t}, R_{i,t}, S_{i,t+1})$. We first observe that it corresponds to a sum of high-dimensional martingale difference. Specifically, for any integer $1 \leq g \leq NT$, let $i(g)$ and $t(g)$ be the quotient and the remainder of $g + T - 1$ divided by T that satisfy

$$g = \{i(g) - 1\}T + t(g) + 1 \quad \text{and} \quad 0 \leq t(g) < T.$$

Let $\mathcal{F}^{(0)} = \{S_{1,0}, A_{1,0}\}$. Then we recursively define $\{\mathcal{F}^{(g)}\}_{1 \leq g \leq NT}$ as follows:

$$\mathcal{F}^{(g)} = \begin{cases} \mathcal{F}^{(g-1)} \cup \{R_{i(g), t(g)}, S_{i(g), t(g)+1}, A_{i(g), t(g)+1}\}, & \text{if } t(g) < T - 1; \\ \mathcal{F}^{(g-1)} \cup \{R_{i(g), T-1}, S_{i(g), T}, S_{i(g)+1, 0}, A_{i(g)+1, 0}\}, & \text{otherwise.} \end{cases}$$

This allows us to rewrite Z as $\sum_{g=1}^{NT} Z^{(g)} = \sum_{g=1}^{NT} Z_{i(g), t(g)}$. Similarly, we can rewrite Z^b as $\sum_{g=1}^{NT} Z^{b,(g)}$. Under the conditional (mean) independence assumptions in (1) and (2), it forms a sum of martingale difference sequence with respect to the filtration $\{\sigma(\mathcal{F}^{(g)})\}_{g \geq 0}$ where $\sigma(\mathcal{F})$ denotes the σ -algebra generated by \mathcal{F} . Similarly, we can represent $Z_u = \sum_{g=1}^{NT} Z_u^{(g)}$. The test statistic can be represented as

$$\text{TS}_1^{**} = \max_{\epsilon T < u < (1-\epsilon)T} \underbrace{\sqrt{\frac{u(T-u)}{T^2}} \frac{1}{T} \sum_{t=0}^{T-1} \sum_a \int_s \left| \phi_L^\top(a, s) Z_u | p_t^b(s) \pi_t^b(a|s) ds \right|}_{\psi_u}.$$

Due to the existence of the max operator and the absolute value function, TS_1^{**} is a non-smooth function of Z . We next approximate the maximum and absolute value functions using a smooth surrogate. Let θ be a sufficiently large real number. Consider the following smooth approximation of the maximum function, $F_\theta(\{\psi_u\}_u)$, defined as

$$\frac{1}{\theta} \log\left(\sum_u \exp(\theta\psi_u)\right).$$

It can be shown that

$$(42) \quad \max_{\epsilon T < u < (1-\epsilon)T} \psi_u \leq F_\theta(\{\psi_u\}_{\epsilon T < u < (1-\epsilon)T}) \leq \max_{\epsilon T < u < (1-\epsilon)T} \psi_u + \frac{\log T}{\theta}.$$

See e.g., Equation (37) of [Chernozhukov, Chetverikov and Kato \(2014\)](#).

Similarly, we can approximate the absolute value function $|x| = \max(x, 0) + \max(-x, 0)$ by $\theta^{-1}\{\log(1 + \exp(\theta x)) + \log(1 + \exp(-\theta x))\}$. Define the corresponding smooth function $f_\theta(Z_u)$ as

$$\sqrt{\frac{u(T-u)}{T^2}} \frac{1}{T\theta} \sum_{t=0}^{T-1} \sum_a \int_s \{\log(1 + \exp(\theta\phi_L^\top(a, s)Z_u)) + \log(1 + \exp(-\theta\phi_L^\top(a, s)Z_u))\} p_t^b(s) \pi_t^b(a|s) ds.$$

Similarly, we have $\psi_u \leq f_\theta(Z_u) \leq \psi_u + \theta^{-1} \log 2$. This together with (42) yields

$$(43) \quad \text{TS}_1^{**} \leq F_\theta(\{f_\theta(Z_u)\}_u) \leq F_\theta(\{\psi_u + \theta^{-1} \log 2\}_u) \leq \text{TS}_1^{**} + \frac{\log(2T)}{\theta}.$$

For a given z , consider the probability $\mathbb{P}(\sqrt{NT}\text{TS}_1^{**} \leq z)$. According to Section B.1 of [Belloni and Oliveira \(2018\)](#), for any $\delta > 0$, there exists a thrice differentiable function h that satisfies $|h'| \leq \delta^{-1}$, $|h''| \leq \delta^{-2}K$ and $|h'''| \leq \delta^{-3}K$ for some universal constant $K > 0$ such that

$$(44) \quad \mathbb{I}(x \leq z/\sqrt{NT} + \delta) \leq h(x) \leq \mathbb{I}(x \leq z/\sqrt{NT} + 4\delta).$$

Define a composite function $m(\{Z_u\}_u) = h \circ F_\theta(\{f_\theta(Z_u)\}_u)$. Combining (44) with (43) yields that

$$(45) \quad \mathbb{P}(\sqrt{NT}\text{TS}_1^{**} \leq z) \leq \mathbb{E}m(\{Z_u\}_u) \leq \mathbb{P}(\sqrt{NT}\text{TS}_1^{**} \leq z + 4\sqrt{NT}\delta).$$

Similarly, we have

$$\mathbb{P}(\sqrt{NT}\text{TS}_1^{b,**} \leq z | \text{Data}) \leq \mathbb{E}[m(\{Z_u^b\}_u) | \text{Data}] \leq \mathbb{P}(\sqrt{NT}\text{TS}_1^{b,**} \leq z + 4\sqrt{NT}\delta | \text{Data}),$$

where Z_u^b is defined in (28). This together with (45) yields that

$$(46) \quad \begin{aligned} & \max_z \{ \max_z |\mathbb{P}(\sqrt{NT}\text{TS}_1^{b,**} \leq z | \text{Data}) - \mathbb{P}(\sqrt{NT}\text{TS}_1^{**} \leq z - 4\sqrt{NT}\delta)|, \\ & \max_z |\mathbb{P}(\sqrt{NT}\text{TS}_1^{b,**} \leq z | \text{Data}) - \mathbb{P}(\sqrt{NT}\text{TS}_1^{**} \leq z + 4\sqrt{NT}\delta)| \} \\ & \leq |\mathbb{E}m(\{Z_u\}) - \mathbb{E}[m(\{Z_u^b\}_u) | \text{Data}]|. \end{aligned}$$

We next apply Corollary 2.1 of [Belloni and Oliveira \(2018\)](#) to establish an upper bound for $|\mathbb{E}m(\{Z_u\}_u) - \mathbb{E}[m(\{Z_u^b\}_u) | \text{Data}]|$. Similar to Lemma 4.3 of [Chernozhukov, Chetverikov and Kato \(2014\)](#), we can show that $c_0 \equiv \sup_{z, z'} |m(z) - m(z')| \leq 1$,

$$c_2 \equiv \sup_z \sum_{j_1, j_2} \left| \frac{\partial^2 m(z)}{\partial z_{j_1} \partial z_{j_2}} \right| \leq \delta^{-2}L + \delta^{-1}\theta L,$$

$$c_3 \equiv \sup_z \sum_{j_1, j_2, j_3} \left| \frac{\partial^3 m(z)}{\partial z_{j_1} \partial z_{j_2} \partial z_{j_3}} \right| \leq \delta^{-3}L^{3/2} + \delta^{-2}\theta L^{3/2} + \delta^{-1}\theta^2 L^{3/2}.$$

In addition, similar to Lemma 18, we can show that the quadratic variation process $\sum_g \mathbb{E}\{Z^{(g)}(Z^{(g)})^\top | \mathcal{F}^{(g-1)}\}$ will converge to some deterministic matrix with elementwise maximum norm bounded by $C\sqrt{\log(NT)}/(\epsilon NT)^{3/2}$ for some constant $C > 0$, with probability at least $1 - O(N^{-2}T^{-2})$. So is the conditional covariance matrix of Z^b given the data, e.g.,

$$\sum_g \mathbb{E}[Z^{b,(g)}(b, Z^{(g)})^\top | \{S_{i,t}, A_{i,t}, R_{i,t}\}_{1 \leq i \leq N, 0 \leq t \leq T}].$$

Moreover, by (20), the third absolute moment of each element in $Z^{(g)}$ is bounded by $O(N^{-3}T^{-3}\sqrt{L})$. Let $\delta = \theta^{-1}$. It follows from Corollary 2.1 of Belloni and Oliveira (2018) that

$$(47) \quad |\mathbb{E}m(\{Z_u\}) - \mathbb{E}[m(\{Z_u^b\}_u) | \text{Data}]| \leq \frac{\theta^2 L \sqrt{\log(NT)}}{(\epsilon NT)^{3/2}} + \frac{\theta^3 L^2}{\epsilon^3 (NT)^2},$$

WPA1. Notice that $\sqrt{NT}TS_1^{**}$ has a bounded probability density function. It follows that

$$(48) \quad \sup_z |\mathbb{P}(\sqrt{NT}TS_1^{**} \leq z - 4\sqrt{NT}\delta) - \mathbb{P}(\sqrt{NT}TS_1^{**} \leq z + 4\sqrt{NT}\delta)| \leq \sqrt{NT}\delta.$$

By setting $\theta = (NT)^c$ for some constant $1/2 < c < 2/3 - 2c_4/3$, both the RHS of (47) and (48) decay to zero. In view of (46), we have shown that

$$\sup_z |\mathbb{P}(\sqrt{NT}TS_1^{b,**} \leq z | \text{Data}) - \mathbb{P}(\sqrt{NT}TS_1^{**} \leq z)| \xrightarrow{p} 0.$$

Similarly, based on (26), we can show that

$$\sup_z |\mathbb{P}(\sqrt{NT}TS_1^b \leq z | \text{Data}) - \mathbb{P}(\sqrt{NT}TS_1 \leq z)| \xrightarrow{p} 0.$$

The proof is hence completed.

C.2.2. Maximum-Type Tests. For any u, a and s , define the variance estimator $\hat{\sigma}_u^2(a, s)$ by

$$\begin{aligned} & \frac{\phi_L^\top(a, s) \widehat{W}_{[T-\kappa, T-u]}^{-1}}{N^2(\kappa - u)^2} \left[\sum_{i=1}^N \sum_{t=T-\kappa}^{T-u-1} \phi_L(A_{i,t}, S_{i,t}) \phi_L^\top(A_{i,t}, S_{i,t}) \delta_{i,t}^2(\widehat{\beta}_{[T-\kappa, T-u]}) \right] \{ \widehat{W}_{[T-\kappa, T-u]}^{-1} \}^\top \phi_L^\top(a, s) \\ & + \frac{1}{N^2 u^2} \phi_L^\top(a, s) \widehat{W}_{[T-u, T]}^{-1} \left[\sum_{i=1}^N \sum_{t=T-u}^{T-1} \phi_L(A_{i,t}, S_{i,t}) \phi_L^\top(A_{i,t}, S_{i,t}) \delta_{i,t}^2(\widehat{\beta}_{[T-u, T]}) \right] \{ \widehat{W}_{[T-u, T]}^{-1} \}^\top \phi_L^\top(a, s). \end{aligned}$$

We next show that both the unnormalized and normalized maximum-type tests have good size property. The proof is very similar to that in Section C.2.1. We provide a sketch of the proof and outline some major key steps only.

Proof for the unnormalized test: The first step in the proof is to show that $\sqrt{NT}(\text{TS}_\infty - \text{TS}_\infty^*) = o_p(1)$, where TS_∞^* is a version of TS_∞ with $\widehat{Q}_{[T_1, T_2]}(a, s)$ replaced by the leading term

$$\frac{1}{N(T_2 - T_1)} \sum_{i=1}^N \sum_{t=T_1}^{T_2-1} \phi_L^\top(a, s) W_{[T_1, T_2]}^{-1} \phi_L(A_{i,t}, S_{i,t}) \delta_{i,t}^*.$$

When either SA1, SA5 hold or the lower bound condition $c_4 > d/(2p - d)$ holds, this can be proven using similar arguments to Step 3 of the proof in Section C.2.1.

The second step in the proof is to show that $\sqrt{NT}(\text{TS}_\infty^b - \text{TS}_\infty^{b,*}) = o_p(1)$ where $\text{TS}_\infty^{b,*}$ is a version of TS_∞^b with $\widehat{W}_{[T_1, T_2]}$ and $\delta_{i,t}(\widehat{\beta}_{[T_1, T_2]})$ replaced by their oracle values $W_{[T_1, T_2]}$ and $\delta_{i,t}^*$, respectively, for any T_1 and T_2 . This can be proven using similar arguments to Steps 2 and 3 of the proof in Section C.2.1.

Notice that in the test statistic, the maximum is taken over all state-action pairs. Recall that the state space is $[0, 1]^d$. Consider an ε -net of $[0, 1]^d$ with $\varepsilon = \sqrt{d}/(NT)^4$. Let TS_∞^{**} and $\text{TS}_\infty^{b,**}$ be versions of TS_∞^* and $\text{TS}_\infty^{b,*}$ where the maximum is taken over the ε -net. Notice that the B-spline basis function is Lipschitz continuous. Using similar arguments to Step 1 of the proof in Section C.2.1, we can show that $\sqrt{NT}(\text{TS}_\infty^* - \text{TS}_\infty^{**}) = o_p(1)$ and $\sqrt{NT}(\text{TS}_\infty^{b,*} - \text{TS}_\infty^{b,**}) = o_p(1)$. This corresponds to the second step of the proof.

Finally, the last step in the proof is to show

$$\sup_z |\mathbb{P}(\sqrt{NT}\text{TS}_\infty^{b,**} \leq z | \text{Data}) - \mathbb{P}(\sqrt{NT}\text{TS}_\infty^{**} \leq z)| \xrightarrow{P} 0.$$

Similar to Step 4 of the proof in Section C.2.1, this step can be proven based on the high-dimensional martingale central limit theorem (CLT) developed by Belloni and Oliveira (2018). Together with the first two steps, we obtain that

$$\sup_z |\mathbb{P}(\sqrt{NT}\text{TS}_\infty^b \leq z | \text{Data}) - \mathbb{P}(\sqrt{NT}\text{TS}_\infty \leq z)| \xrightarrow{P} 0.$$

The proof is hence completed.

Proof for the normalized test: Using similar arguments to Step 2 of the proof in Section C.2.1, we can show that WPA1, (i) $\max_{T_2 - T_1 \geq \varepsilon T} \|\widehat{W}_{[T_1, T_2]}^{-1}\|_2 = O(1)$;

$$(ii) \min_{T_2 - T_1 \geq \varepsilon T} \lambda_{\min} \left\{ \frac{1}{N(T_2 - T_1)} \sum_{i=1}^N \sum_{t=T_1}^{T_2-1} \phi_L(A_{i,t}, S_{i,t}) \phi_L^\top(A_{i,t}, S_{i,t}) \right\} > C,$$

for some constant $C > 0$. In addition, the difference $\delta_{i,t}(\widehat{\beta}_{[T_1, T_2]}) - \delta_{i,t}^*$ decays at a rate of $(NT)^{-c}$ for some constant $c > 0$, uniformly in i, t, T_1, T_2 , WPA1. These together with (i) and (ii) implies that there exists some constant $C > 0$ such that $\widehat{\sigma}_u^2(a, s) > C \|\phi_L(a, s)\|_2^2$ for any u, a, s , WPA1. This allows us to show $\sqrt{NT}(\text{TS}_n - \text{TS}_n^*) = o_p(1)$ under a weaker condition that only require $c_4 > d/(2p)$, where TS_n^* is a version of TS_n with $\widehat{Q}_{[T_1, T_2]}$ replaced by the leading term. When SA1 and SA5 hold, using similar arguments to Step 1 of the proof in Section C.2.1, we can show the lower bound requirement is not needed. The rest of the proof can be established in a similar manner as the proof for the unnormalized test.

C.3. Proof of Lemma 16. Under A2(i), the optimal Q-function Q^{opt} is p -smooth (see e.g., the proof of Lemma 1 in Shi et al., 2022). According to Section 2.2 of Huang (1998), there exists some β^* that satisfies (19). The first part of (20) can be proven based on the proof of Theorem 3.3 of Burman and Chen (1989). The second part follows from the fact that the number of nonzero elements in the vector $\Phi(s)$ is bounded by some universal constant and that each of the basis function is bounded by $O(\sqrt{L})$. Finally, each function in Φ is Lipschitz continuous. This yields (21).

C.4. Proof of Lemma 17. The proof of Lemma 17 is straightforward based on the analyses in Step 3 of the proof of Theorem 2. We omit the details to save space.

C.5. Proof of Lemma 18. We focus on establishing a uniform upper error bound for $\{|\widehat{W}_{[T_1, T_2]} - W_{[T_1, T_2]}| : T_2 - T_1 \geq \epsilon T\}$ in this section. The assertion that $\|W_{[T_1, T_2]}^{-1}\|_2 \leq \bar{c}$ can be proven by Lemma 3 of [Shi et al. \(2022\)](#).

In Step 3 of the proof of Theorem 2, we have shown that $\arg \max_a \phi_L^\top(a, s) \widehat{\beta}_{[T_1, T_2]} = \arg \max_a Q^{opt}(a, s)$ and hence $\pi_{\widehat{\beta}_{[T_1, T_2]}} = \pi^{opt}$, WPA1. It follows that

$$\widehat{W}_{[T_1, T_2]} = \frac{1}{N(T_2 - T_1)} \sum_{i=1}^N \sum_{t=T_1}^{T_2-1} \phi_L(A_{i,t}, S_{i,t}) \{\phi_L(A_{i,t}, S_{i,t}) - \gamma \phi_L(\pi^{opt}(S_{i,t+1}), S_{i,t+1})\}^\top. \quad (49)$$

We next provide an upper bound on the difference between the RHS of (49) and $W_{[T_1, T_2]}$. Define $\widehat{W}_{[T_1, T_2]}^*$ as

$$\frac{1}{N(T_2 - T_1)} \sum_{i=1}^N \sum_{t=T_1}^{T_2-1} \sum_a \pi^b(a|S_{i,t}) \phi_L(a, S_{i,t}) [\phi_L(a, S_{i,t}) - \gamma \mathbb{E}\{\phi_L(\pi^{opt}(S_{i,t+1}), S_{i,t+1}) | A_{i,t} = a, S_{i,t}\}]^\top.$$

The difference $|\widehat{W}_{[T_1, T_2]} - W_{[T_1, T_2]}|$ can be upper bounded by $|\widehat{W}_{[T_1, T_2]} - \widehat{W}_{[T_1, T_2]}^*| + |\widehat{W}_{[T_1, T_2]}^* - W_{[T_1, T_2]}|$.

Under the conditional mean independent assumption on the reward (1), the first term $\widehat{W}_{[T_1, T_2]} - \widehat{W}_{[T_1, T_2]}^*$ corresponds to a sum of martingale difference. Using similar arguments to the proof of Lemma 3 of [Shi et al. \(2022\)](#), we can show that the first term is of the order $O(\sqrt{(\epsilon NT)^{-1} L \log(NT)})$, with probability at least $1 - O\{(NT)^{-3}\}$, under the condition that $T_2 - T_1 \geq \epsilon T$. See also, Freedman's inequality for matrix martingales developed by [Tropp \(2011\)](#). It follows from Bonferroni's inequality that $\sup_{T_1, T_2} \|\widehat{W}_{[T_1, T_2]} - \widehat{W}_{[T_1, T_2]}^*\|_2 = O(\sqrt{(\epsilon NT)^{-1} L \log(NT)})$, with probability at least $1 - O\{(NT)^{-1}\}$.

It remains to bound $\|\widehat{W}_{[T_1, T_2]}^* - W_{[T_1, T_2]}\|_2$. Let Γ_0 be an ϵ -net of the unit sphere in \mathbb{R}^L that satisfies the following: for any $\nu \in \mathbb{R}^L$ with unit ℓ_2 norm, there exists some $\nu_0 \in \Gamma_0$ such that $\|\nu - \nu_0\|_2 \leq \epsilon$. Set $\epsilon = (NT)^{-2}$. According to Lemma 2.3 of [Mendelson, Pajor and Tomczak-Jaegermann \(2008\)](#), there exists such an ϵ -net Γ_0 that belongs to the unit sphere and satisfies $|\Gamma_0| \leq 5^L (NT)^{2L}$.

For any ν_1, ν_2 with unit ℓ_2 norm, define

$$\Psi_t(a, s, \nu_1, \nu_2) = \pi_t^b(a|s) \nu_1^\top \phi_L(a, s) [\phi_L(a, s) - \gamma \mathbb{E}\{\phi_L(\pi^{opt}(S_{t+1}), S_{t+1}) | A_t = a, S_t = s\}]^\top \nu_2.$$

The difference $\|\widehat{W}_{[T_1, T_2]}^* - W_{[T_1, T_2]}\|_2$ can be represented as

$$\sup_{\|\nu_1\|_2 = \|\nu_2\|_2 = 1} \left| \frac{1}{N(T_2 - T_1)} \sum_{i=1}^N \sum_{t=T_1}^{T_2-1} \sum_a \{\Psi_t(a, S_{i,t}, \nu_1, \nu_2) - \mathbb{E}\Psi_t(a, S_{i,t}, \nu_1, \nu_2)\} \right|.$$

We first show that $\Psi_t(a, s, \nu_1, \nu_2)$ is a Lipschitz continuous function of ν_1 and ν_2 . For any $\nu_1, \nu_2, \nu_3, \nu_4$, the difference $\Psi_t(a, s, \nu_1, \nu_2) - \Psi_t(a, s, \nu_3, \nu_4)$ can be decomposed into the sum of the following two terms:

$$\begin{aligned} & \pi_t^b(a|s) (\nu_1 - \nu_3)^\top \phi_L(a, s) [\phi_L(a, s) - \gamma \mathbb{E}\{\phi_L(\pi^{opt}(S_{t+1}), S_{t+1}) | A_t = a, S_t = s\}]^\top \nu_2 \\ & + \pi_t^b(a|s) \nu_3^\top \phi_L(a, s) [\phi_L(a, s) - \gamma \mathbb{E}\{\phi_L(\pi^{opt}(S_{t+1}), S_{t+1}) | A_t = a, S_t = s\}]^\top (\nu_2 - \nu_4). \end{aligned}$$

The first term is $O(L)$ according to (20). Similarly, the second term is $O(L)$ as well. To summarize, we have shown that

$$|\Psi_t(a, s_1, \nu_1, \nu_2) - \Psi_t(a, s_2, \nu_3, \nu_4)| \leq cL(\|\nu_1 - \nu_3\|_2 + \|\nu_2 - \nu_4\|_2),$$

for some constant $c > 0$.

For any ν_1, ν_2 with unit ℓ_2 norm, there exist $\nu_{1,0}, \nu_{2,0} \in \Gamma_0$ that satisfy $\|\nu_1 - \nu_{1,0}\|_2 \leq \varepsilon$ and $\|\nu_2 - \nu_{2,0}\|_2 \leq \varepsilon$. As such, $\Psi_t(a, s_1, \nu_1, \nu_2) - \Psi_t(a, s_2, \nu_1, \nu_2)$ can be upper bounded by

$$\sup_{\nu_{1,0}, \nu_{2,0} \in \Gamma_0} \left| \frac{1}{N(T_2 - T_1)} \sum_{i=1}^N \sum_{t=T_1}^{T_2-1} \sum_a \{\Psi_t(a, S_{i,t}, \nu_{1,0}, \nu_{2,0}) - \mathbb{E}\Psi_t(a, S_{i,t}, \nu_{1,0}, \nu_{2,0})\} \right| + \frac{2cL}{(NT)^2}.$$

It remains to establish a uniform upper bound for the first term. We aim to apply the concentration inequality developed by [Alquier, Doukhan and Fan \(2019\)](#). However, a direct application of Theorem 3.1 in [Alquier, Doukhan and Fan \(2019\)](#) would yield a sub-optimal bound. This is because each summand $\Psi_t(a, S_t, \nu_{1,0}, \nu_{2,0})$ is not bounded, since $\|\phi_L\|_2$ is allowed to diverge with the number of observations. To obtain a sharper bound, we further decompose the first term into the sum of the following two terms:

$$(50) \quad \sup_{\nu_{1,0}, \nu_{2,0} \in \Gamma_0} \left| \frac{1}{N(T_2 - T_1)} \sum_{i=1}^N \sum_{t=T_1}^{T_2-1} \sum_a [\Psi_t(a, S_{i,t}, \nu_{1,0}, \nu_{2,0}) - \mathbb{E}\{\Psi_t(a, S_{i,t}, \nu_{1,0}, \nu_{2,0}) | S_{i,t-1}\}] \right| \\ + \sup_{\nu_{1,0}, \nu_{2,0} \in \Gamma_0} \left| \frac{1}{N(T_2 - T_1)} \sum_{i=1}^N \sum_{t=T_1}^{T_2-1} \sum_a [\mathbb{E}\{\Psi_t(a, S_{i,t}, \nu_{1,0}, \nu_{2,0}) | S_{i,t-1}\} - \mathbb{E}\Psi_t(a, S_{i,t}, \nu_{1,0}, \nu_{2,0})] \right|.$$

The first term corresponds to a sum of martingale difference. Using similar arguments in showing $\sup_{T_1, T_2} \|\widehat{W}_{[T_1, T_2]} - \widehat{W}_{[T_1, T_2]}^*\|_2 = O(\sqrt{(\varepsilon NT)^{-1} L \log(NT)})$, we can show that the first term in (50) is of the order $O(\sqrt{(\varepsilon NT)^{-1} L \log(NT)})$, with probability at least $1 - O(N^{-1}T^{-1})$, where the big- O term is uniform in $\{(T_1, T_2) : T_2 - T_1 \geq \varepsilon T\}$.

As for the second term, notice that by definition, $\mathbb{E}\{\Psi_t(a, S_t, \nu_{1,0}, \nu_{2,0}) | S_{t-1} = s\}$ equals

$$\int_{s'} \pi_t^b(a|s') \nu_{1,0}^\top \phi_L(a, s') [\phi_L(a, s') - \gamma \mathbb{E}\{\phi_L(\pi^{opt}(S_{t+1}), S_{t+1}) | A_t = a, S_t = s'\}]^\top \nu_{2,0} p_{t-1}(s' | a, s) ds'.$$

Under the p -smoothness condition in A4(iii), $\mathbb{E}\{\Psi_t(a, S_t, \nu_{1,0}, \nu_{2,0}) | S_{t-1} = s\}$ is a Lipschitz continuous function of s . However, unlike $\Psi_t(a, s, \nu_{1,0}, \nu_{2,0})$, the integrand

$$|\pi_t^b(a|s') \nu_{1,0}^\top \phi_L(a, s') [\phi_L(a, s') - \gamma \mathbb{E}\{\phi_L(\pi^{opt}(S_{t+1}), S_{t+1}) | A_t = a, S_t = s'\}]^\top \nu_{2,0}|$$

is upper bounded by a constant; see e.g., Equation (E.77) of [Shi et al. \(2022\)](#). As such, the Lipschitz constant is uniformly bounded by some constant. Consequently, the conditions in the statement of Theorem 3.1 in [Alquier, Doukhan and Fan \(2019\)](#) are satisfied. We can apply Theorem 3.1 to the mean zero random variable

$$\frac{1}{N(T_2 - T_1)} \sum_{i=1}^N \sum_{t=T_1}^{T_2-1} \sum_a [\mathbb{E}\{\Psi_t(a, S_{i,t}, \nu_{1,0}, \nu_{2,0}) | S_{i,t-1}\} - \mathbb{E}\Psi_t(a, S_{i,t}, \nu_{1,0}, \nu_{2,0})],$$

for each combination of $\nu_{1,0}, \nu_{2,0}, T_1, T_2$, and show that it is of the order $O(\sqrt{\varepsilon L (NT)^{-1} \log(NT)})$ with probability at least $1 - O(N^{-CL} T^{-CL})$, for some sufficiently large constant $C > 0$. By Bonferroni's inequality, we can show that

$$\sup_{T_2 - T_1 \geq \varepsilon T} \sup_{\nu_{1,0}, \nu_{2,0} \in \Gamma_0} \left| \frac{1}{N(T_2 - T_1)} \sum_{i=1}^N \sum_{t=T_1}^{T_2-1} \sum_a [\Psi_t(a, S_{i,t}, \nu_{1,0}, \nu_{2,0}) - \mathbb{E}\{\Psi_t(a, S_{i,t}, \nu_{1,0}, \nu_{2,0}) | S_{i,t-1}\}] \right|,$$

is upper bounded by $O(\sqrt{L \varepsilon^{-1} (NT)^{-1} \log(NT)})$ with probability at least $1 - O(N^{-1}T^{-1})$.

C.6. Proof of Theorem 3. Without loss of generality, assume $T_0 = 0$. We only consider the ℓ_1 -type test. The proof for the maximum-type tests can be similarly derived. Under the given conditions on T^* , we have

$$(51) \quad \begin{aligned} \text{TS}_1 &\geq \sqrt{\frac{T^*(T - T^*)}{T^2}} \left\{ \frac{1}{NT} \sum_{i,t} |\widehat{Q}_{[0,T^*]}(A_{i,t}, S_{i,t}) - \widehat{Q}_{[T^*,T]}(A_{i,t}, S_{i,t})| \right\} \\ &\geq \sqrt{\epsilon(1 - \epsilon)} \left\{ \frac{1}{NT} \sum_{i,t} |\widehat{Q}_{[0,T^*]}(A_{i,t}, S_{i,t}) - \widehat{Q}_{[T^*,T]}(A_{i,t}, S_{i,t})| \right\}. \end{aligned}$$

Similar to Lemma 16, there exist some β_0^* and β_T^* such that

$$(52) \quad \sup_{a,s} |Q_0^{opt}(a, s) - \phi_L^\top(a, s)\beta_0^*| = O(L^{-p/d}), \sup_{a,s} |Q_T^{opt}(a, s) - \phi_L^\top(a, s)\beta_T^*| = O(L^{-p/d}).$$

Using similar arguments in Step 3 of the proof of Theorem 2, we can show that

$$(53) \quad \max(\|\widehat{\beta}_{[0,T^*]} - \beta_0^*\|_2, \|\widehat{\beta}_{[T^*,T]} - \beta_T^*\|_2) = O(L^{-p/d}) + O(\sqrt{L(\epsilon NT)^{-1} \log(NT)}),$$

WPA1. Using similar arguments in Step 1 of the proof of Theorem 2, we can show that the last line of (51) can be well-approximated by

$$(54) \quad \frac{\sqrt{\epsilon(1 - \epsilon)}}{T} \sum_{t=0}^{T-1} \sum_a \int_s |\widehat{Q}_{[0,T^*]}(a, s) - \widehat{Q}_{[T^*,T]}(a, s)| \pi_t^b(a|s) p_t^b(s) ds,$$

with the approximation error upper bounded by $\sqrt{\epsilon(1 - \epsilon)L(NT)^{-1} \log(NT)}$, WPA1.

By 20 and Cauchy-Schwarz inequality, we have

$$\sum_a \int_s |\phi_L^\top(a, s)\nu| ds \leq \sum_a \sqrt{\int_s |\phi_L^\top(a, s)\nu|^2 ds} = O(\|\nu\|_2).$$

This together with (51), (53) and (54) yields that

$$\begin{aligned} \text{TS}_1 &\geq \frac{\sqrt{\epsilon(1 - \epsilon)}}{T} \sum_{t=0}^{T-1} \sum_a \int_s |\phi_L^\top(a, s)(\beta_0^* - \beta_T^*)| \pi_t^b(a|s) p_t^b(s) ds \\ &\quad + O(\sqrt{L(NT)^{-1} \log(NT)}) + O(L^{-p/d}), \end{aligned}$$

WPA1. Combining this together with (52) yields that

$$\begin{aligned} \text{TS}_1 &\geq \frac{\sqrt{\epsilon(1 - \epsilon)}}{T} \sum_{t=0}^{T-1} \sum_a \int_s |Q_0^{opt}(a, s) - Q_T^{opt}(a, s)| \pi_t^b(a|s) p_t^b(s) ds \\ &\quad + O(\sqrt{L(NT)^{-1} \log(NT)}) + O(L^{-p/d}), \end{aligned}$$

WPA1. In addition, using similar arguments in Step 2 of the proof of Theorem 2, we can show that the bootstrapped test statistic TS_1^b is upper bounded by $O(\sqrt{L(NT)^{-1} \log(NT)})$, WPA1. Under the given condition on Δ_1 , TS_1 is much larger than the upper α th quantile of TS_1^b , WPA1. As such, the power of the proposed test approaches 1 under the alternative hypothesis. This completes the proof.

C.7. Proof of Theorem 4. In FQI, we iteratively update the Q-function according to the formula,

$$Q^{(k+1)} = \arg \min_Q \sum_{i,t} \left\{ R_{i,t} + \gamma \max_a Q^{(k)}(a, S_{i,t+1}) - Q(A_{i,t}, S_{i,t}) \right\}^2.$$

At the k th iteration, we define the population-level Q-function

$$(55) \quad Q^{(k+1),*}(a, s) = r(a, s) + \gamma \int_{s'} \max_{a'} Q^{(k)}(a', s') p(s'|a, s) ds'.$$

According to the Bellman optimality equation,

$$Q^{opt}(a, s) = r(a, s) + \gamma \int_{s'} \max_{a'} Q^{opt}(a', s') p(s'|a, s) ds'.$$

It follows that

$$\begin{aligned} \sup_{a,s} |Q^{opt}(a, s) - Q^{(k+1)}(a, s)| &\leq \sup_{a,s} |Q^{(k+1),*}(a, s) - Q^{(k+1)}(a, s)| + \sup_{a,s} |Q^{opt}(a, s) - Q^{(k+1),*}(a, s)| \\ &\leq \sup_{a,s} |Q^{(k+1),*}(a, s) - Q^{(k+1)}(a, s)| + \gamma \sup_{a,s} |Q^{opt}(a, s) - Q^{(k)}(a, s)|. \end{aligned}$$

Iteratively applying this inequality for $k = K, K-1, \dots, 1$, we obtain that

$$(56) \quad \begin{aligned} \sup_{a,s} |Q^{opt}(a, s) - \widehat{Q}_{[T_1, T_2]}(a, s)| &\leq \sum_k \gamma^{K-k} \sup_{a,s} |Q^{(k+1),*}(a, s) - Q^{(k+1)}(a, s)| \\ &\quad + \gamma^{K+1} \sup_{a,s} |Q^{opt}(a, s) - Q^{(0)}(a, s)|. \end{aligned}$$

As K diverges to infinity, the second term on the RHS decays to zero. The first term is upper bounded by

$$(57) \quad \frac{1}{1-\gamma} \sup_{a,s,k} |Q^{(k+1),*}(a, s) - Q^{(k+1)}(a, s)|.$$

It remains to show this term decays to zero as the sample size approaches to infinity.

Let $\beta^{(k)}$ denote the estimated regression coefficients such that $Q^{(k)}(a, s) = \phi_L^\top(a, s) \beta^{(k)}$. We claim that there exist some constants $C, \bar{C} > 0$ such that

$$(58) \quad \sup_{a,s} \max_{k \in \{0, \dots, j\}} |Q^{(k)}(a, s)| \leq C \text{ and } \max_{k \in \{0, \dots, j\}} \|\beta^{(k)}\|_2 \leq \bar{C},$$

with probability at least $1 - (j+1)/(NT)$, for sufficiently large NT . The values of C and \bar{C} will be specified later.

We will prove this assertion by induction. Using similar arguments in the proof of Lemma 18, we can show that

$$\begin{aligned} \left\| \frac{1}{N(T_2 - T_1)} \sum_{i=1}^N \sum_{t=T_1}^{T_2-1} \phi_L(A_{i,t}, S_{i,t}) \phi_L(A_{i,t}, S_{i,t})^\top - \frac{1}{T_2 - T_1} \sum_{t=T_1}^{T_2-1} \mathbb{E} \phi_L(A_t, S_t) \phi_L(A_t, S_t)^\top \right\|_2 \\ \leq c \sqrt{L(\epsilon NT)^{-1} \log(NT)}, \end{aligned}$$

for some constant $c > 0$, with probability at least $1 - N^{-1}T^{-1}$. Under A5(ii), $\lambda_{\min}\left\{(T_2 - T_1)^{-1} \sum_{t=T_1}^{T_2-1} \mathbb{E} \phi_L(A_t, S_t) \phi_L(A_t, S_t)^\top\right\}$ is uniformly bounded away from zero. On the event set defined by (59), for sufficiently large NT , there exists some $\bar{c} > 0$ such that

$$(60) \quad \lambda_{\min} \left\{ \frac{1}{N(T_2 - T_1)} \sum_{i=1}^N \sum_{t=T_1}^{T_2-1} \phi_L(A_{i,t}, S_{i,t}) \phi_L(A_{i,t}, S_{i,t})^\top \right\} \geq \bar{c}.$$

When $k = 0$, the posit assertion in (58) holds as long as $\sup_{a,s} |Q^{(0)}(a, s)| \leq C$ and $\|\beta^{(0)}\|_2 \leq \bar{C}$. Suppose the assertion holds for $k = 0, 1, \dots, J$. We aim to prove this assertion holds for $k = J + 1$. Since the reward is uniformly bounded, so is $\sup_{a,s} |r(a, s)|$. We will choose C to be such that $C \geq 2(1 - \gamma)^{-1} \sup_{a,s} |r(a, s)|$. It follows from (55) that $\sup_{a,s} |Q^{(k+1),*}(a, s)| \leq (1 + \gamma)C/2$. In addition, define

$$\beta^{(k+1),*} = \left\{ \frac{1}{T_2 - T_1} \sum_{t=T_1}^{T_2-1} \mathbb{E} \phi_L(A_t, S_t) \phi_L(A_t, S_t)^\top \right\}^{-1} \left\{ \frac{1}{T_2 - T_1} \sum_{t=T_1}^{T_2-1} \mathbb{E} \phi_L(A_t, S_t) Q^{(k+1),*}(A_t, S_t) \right\}.$$

Under (20) and (60), it follows from Lemma 18 that there exist some constants $c, C > 0$ such that $\|\beta^{(k+1),*}\|_2 \leq cC$. We choose \bar{C} to be such that $\bar{C} \geq 2cC$. As such, it suffices to show that on the set defined in (60), the estimation errors $\sup_{a,s} |Q^{(k+1)}(a, s) - Q^{(k+1),*}(a, s)| \leq (1 - \gamma)C/2$ and $\|\beta^{(k+1)} - \beta^{(k+1),*}\|_2 \leq cC$, with probability at least $1 - (NT)^{-1}$.

Similar to Lemma 16, there exists some $\beta^{(k+1),**}$ such that $\sup_{a,s} |Q^{(k+1),*}(a, s) - \phi_L^\top(a, s) \beta^{(k+1),**}| \leq c_0 L^{-p/d}$ for some constant $c_0 > 0$. Similar to Lemma 17, we can show that $\sup_k \|\beta^{(k+1),**} - \beta^{(k+1),*}\|_2 = O(L^{-p/d})$. Since L is proportional to $(NT)^{c_4}$ for some $c_4 > 0$, for sufficiently large NT , we have $\|\beta^{(k+1),**} - \beta^{(k+1),*}\|_2 \leq cC/2$ and hence $\|\beta^{(k+1),**}\|_2 \leq 3cC/2$. Therefore, to show $\|\beta^{(k+1)} - \beta^{(k+1),*}\|_2 \leq cC$, it suffices to show $\|\beta^{(k+1)} - \beta^{(k+1),**}\|_2 \leq cC/2$.

By definition, we have

$$\begin{aligned} \beta^{(k+1)} - \beta^{(k+1),**} &= \left\{ \frac{1}{N(T_2 - T_1)} \sum_{i=1}^N \sum_{t=T_1}^{T_2-1} \phi_L(A_{i,t}, S_{i,t}) \phi_L(A_{i,t}, S_{i,t})^\top \right\}^{-1} \\ &\times \left[\frac{1}{N(T_2 - T_1)} \sum_{i=1}^N \sum_{t=T_1}^{T_2-1} \phi_L(A_{i,t}, S_{i,t}) \{R_{i,t} + \gamma \max_a \phi_L^\top(a, S_{i,t+1}) \beta^{(k)} - \phi_L^\top(A_{i,t}, S_{i,t}) \beta^{(k+1),**}\} \right]. \end{aligned}$$

On the set defined in (60), $\|\beta^{(k+1)} - \beta^{(k+1),**}\|_2$ is upper bounded by

$$\begin{aligned} &\sup_{\|\beta_0^{(k)}\|_2 \leq 2cC, \|\beta_0^{(k+1),**}\|_2 \leq 3cC/2} \left| \frac{\bar{c}^{-1}}{N(T_2 - T_1)} \sum_{i=1}^N \sum_{t=T_1}^{T_2-1} \phi_L(A_{i,t}, S_{i,t}) \right. \\ &\left. \sup_{\sup_{a,s} |r(a,s) + \gamma \int_{s'} \max_{a'} \phi_L^\top(a', s') \beta_0^{(j)} p(s'|a,s) ds' - \phi_L^\top(a,s) \beta_0^{(k+1),**}| \leq c_0 L^{-p/d}} \right. \\ &\left. \times \{R_{i,t} + \gamma \max_a \phi_L^\top(a, S_{i,t+1}) \beta_0^{(k)} - \phi_L^\top(A_{i,t}, S_{i,t}) \beta_0^{(k+1),**}\} \right|. \end{aligned}$$

Using similar arguments to Step 3 of the proof of Theorem 2, we can show that the upper bound is of the order $O(L^{-p/d}) + O(\sqrt{L}(\epsilon NT)^{-1} \log(NT))$, with probability at least $1 - (NT)^{-1}$. For sufficiently large NT , the assertion $\|\beta^{(k+1)} - \beta^{(k+1),**}\|_2 \leq cC/2$ is automatically satisfied. Moreover, by (20) and the conditions that L is proportional to $(NT)^{c_4}$ for some $0 < c_4 < 1/4$, $p > d/2$, we obtain that $\sup_{a,s} |Q^{(k+1)}(a, s) - Q^{(k+1),*}(a, s)| = O(L^{1/2-p/d}) + O(L\sqrt{(\epsilon NT)^{-1} \log(NT)}) \ll (1 - \gamma)C/2$. The assertion is thus proven.

Under the given conditions on K , the maximum number of iterations, we obtain that both $\widehat{Q}_{[T_1, T_2]}$ and $\widehat{\beta}_{[T_1, T_2]}$ are uniformly bounded WPA1. In addition, using similar arguments, we can show that the estimation error (57) decays to zero, WPA1. According to (56), we have

$$\max_{K/2 < k \leq K} \sup_{a,s} |Q^{opt}(a, s) - Q^{(k+1)}(a, s)| \xrightarrow{p} 0.$$

Additionally, one can also verify that the convergence is uniform in (T_1, T_2) . The proof is hence completed.

C.8. Proof of Theorem 5. Theorem 5 can be proven based on the uniform consistency in Theorem 4 and similar arguments to Step 3 of the proof of Theorem 2. We omit the details to save space.

APPENDIX D: MORE ON THE NUMERICAL STUDY

D.1. Real-data-based Simulation. To mimic the IHS study, we simulate $N = 100$ subjects, each observed over $T = 50$ time points. Our aim is to estimate an optimal treatment policy to improve these interns' long-term physical activity levels. See Section 6 for more details about the study background. At time t , the state vector $S_{i,t}$ comprises four variables to mimic the actual IHS study: the square root of step count at time t ($S_{i,t,1}$), cubic root of sleep minutes at time t ($S_{i,t,2}$), mood score at time t ($S_{i,t,3}$), and the square root of step count at time $t - 1$ ($S_{i,t,4} = S_{i,t-1,1}$). These power transformations were applied in accordance with the approaches in NeCamp et al. (2020). The actions are binary with $\mathbb{P}(A_{it} = 1) = 0.25$; $A_{it} = 1$ means the subject is randomized to receive activity messages at time t , and $A_{it} = 0$ means any other types of messages or no message at all. Reward $R_{i,t} = S_{i,t,1}$ is defined as the step count at time t . We assume that the state transition function has an abrupt change point at time $T^* = 25$. Specifically, we initiate the state variables as independent normal distributions with $S_{i,0,1} \sim \mathcal{N}(20, 3)$, $S_{i,0,2} \sim \mathcal{N}(20, 2)$, and $S_{i,0,3} \sim \mathcal{N}(7, 1)$, and let them evolve according to

$$\begin{pmatrix} S_{i,t+1,1} \\ S_{i,t+1,2} \\ S_{i,t+1,3} \end{pmatrix} = \mathbf{W}_1(A_{i,t})\tilde{S}_{i,t}I\{t \in [0, T^*)\} + \mathbf{W}_2(A_{i,t})\tilde{S}_{i,t}I\{t \in [T^*, T]\} + \mathbf{z}_{i,t},$$

where the transition matrices are

$$\mathbf{W}_1(A_{i,t}) = \begin{pmatrix} 10 + 0.6A_{i,t} & 0.4 + 0.3A_{i,t} & 0.1 - 0.1A_{i,t} & -0.04 & 0.1 \\ 11 - 0.4A_{i,t} & 0.05 & 0 & 0.4 & 0 \\ 1.2 - 0.5A_{i,t} & -0.02 & 0 & 0.03 + 0.03A_{i,t} & 0.8 \end{pmatrix},$$

$$\mathbf{W}_2(A_{i,t}) = \begin{pmatrix} 10 - 0.6A_{i,t} & 0.4 - 0.3A_{i,t} & 0.1 + 0.1A_{i,t} & 0.04 & -0.1 \\ 11 - 0.4A_{i,t} & 0.05 & 0 & 0.4 & 0 \\ 1.2 + 0.5A_{i,t} & -0.02 & 0 & 0.03 - 0.03A_{i,t} & 0.8 \end{pmatrix},$$

$\tilde{S}_{i,t} = (1, S_{i,t,1}, S_{i,t,2}, S_{i,t,3}, S_{i,t-1,1})^\top$, and $\mathbf{z}_{i,t} \sim \mathcal{N}_3(0, \text{diag}(1, 1, 0.2))$ is random noise.

Under this setting, the state transition function is nonstationary whereas the reward is a stationary function of the state. In addition, the data follow the null hypothesis when $\kappa = 1, \dots, 25$ and follow the alternative hypothesis for $\kappa = 26, \dots, 49$. The discount factor is set to $\gamma = 0.9$ or 0.95 . We test the null hypothesis along a sequence of $\kappa = 10, 15, \dots, 40$ for every five time points. The number of basis functions is chosen among $\{20, 30, 40, 50, 60\}$.

Figure 6 shows the empirical rejection rates of the proposed tests as well as the distribution of the estimated change point location. Similar to the results in Section 5.1, our proposed test controls the type I error at the nominal level (see $\kappa < 25$) and is powerful to detect the alternative hypothesis (see $\kappa > 25$). At the true change point where $\kappa = 25$ however, the proposed test fails to control the type I error. We also remark that the reason the proposed test fails at the boundary is because the marginal distribution of the first few states after the change point is very different from the stationary state distribution. After an initial burn-in period of 5 points, the proposed test is able to control the type I error at $\kappa = 20$. In addition, the distribution of the estimated change point concentrates on 30, which is very close to the oracle change point location 25, implying the consistency of the proposed change point detection procedure. We remark that consistency here requires $T^{-1}|\hat{T}^* - T^*| \xrightarrow{P} 0$ instead of $\mathbb{P}(\hat{T}^* = T^*) \rightarrow 1$, the latter being usually impossible to achieve in change point detection. It also demonstrates the detection delay (i.e., the estimated change point occurs later than its oracle value).

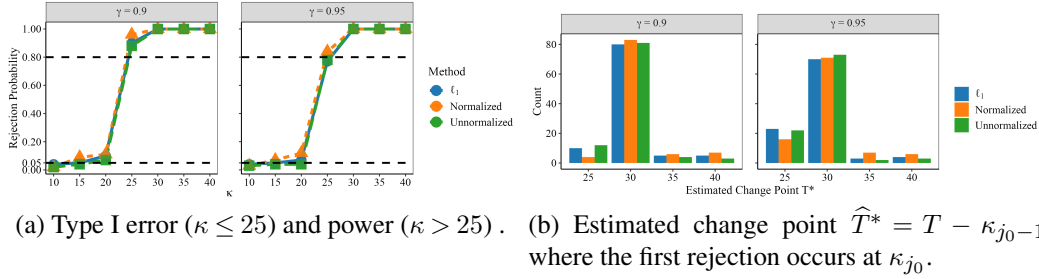


Fig 6: Real-data-based simulation: Empirical rejection rates of the proposed tests (ℓ_1 -type (7), normalized (8), and unnormalized (9)) and the distribution of the estimated change points.

D.2. Implementation Details. To implement the proposed tests, the boundary removal parameter ϵ is set to 0.1; 2000 bootstrap samples are generated to compute p -values. The discount factor γ is chosen from $\{0.9, 0.95\}$. In our simulations, the state variables are continuous. We set the basis function Φ_L (see (10)) to the random Fourier features following the Random Kitchen Sinks (RKS) algorithm (Rahimi and Recht, 2007), using `RBFsampler` function from the Python `scikit-learn` module for implementation. The bandwidth in the radial basis function (RBF) kernel is selected according to the median heuristic (Gareau, Jitkrittum and Kanagawa, 2017). The number of basis functions L is selected via 5-fold cross-validation. Specifically, we first divide all data trajectories into 5 non-overlapping equal-sized data subsets. Let \mathcal{I}_f denote the f -th subsample and \mathcal{I}_f^c denote its complement, $f = 1, 2, 3, 4, 5$. For each combination of f , L and the specified data interval $[T_1, T_2]$, we use FQI to compute an estimated optimal Q-function $\hat{Q}_{f,L,[T_1,T_2]}$ using L basis functions based on the data subsets in $\mathcal{I}_f^c \times [T_1, T_2]$. We next select L that minimizes the FQI objective function,

$$(61) \quad \sum_{f=1}^5 \sum_{i \in \mathcal{I}_f} \sum_{t=T_1}^{T_2-1} \left\{ R_{i,t} + \gamma \max_a \hat{Q}_{f,L,[T_1,T_2]}(a, S_{i,t+1}) - \hat{Q}_{f,L,[T_1,T_2]}(A_{i,t}, S_{i,t}) \right\}^2.$$

When the data is stationary over $[T_1, T_2]$, this criterion balances off the bias and standard deviation of the Q-function estimator.

To mitigate the randomness introduced by the random Fourier features, for each of the 100 simulation replications, we repeat our tests four times with different random seeds. This yields p -values $\{p_r, r = 1, \dots, 4\}$. We then employ the method developed by Meinshausen, Meier and Bühlmann (2009) to combine these p -values by defining

$$(62) \quad p_0 = \min \left(1, q_\tau \left\{ \tau^{-1} p_r, r = 1, \dots, 4 \right\} \right),$$

to be the final p -value. Here, τ is some constant between 0 and 1, and q_τ is the empirical τ -quantile of the p -values. Compared to using a single set of Fourier features, such an aggregation method reduces the type I error and increases the power of the resulting test. Our simulation results hardly change under $\tau = 0.05, 0.1, 0.15, 0.2$; hereafter, we report results under $\tau = 0.1$. All tests are conducted at significance level $\alpha = 0.05$.

D.3. Four Synthetic Nonstationary Settings. The way we generate a smooth transition function is to first define a piecewise constant function, and smoothly connects the constant functions through a transformation. Specifically, let the piecewise constant function with two segments be $f(s, t) = f_1(s)I\{t \leq T^*\} + f_2(s)I\{t > T^*\}$, where f_1 and f_2 are functions not dependent on t .

We now introduce a smooth transformation $\phi(s) = \frac{\psi(s)}{\psi(s) + \psi(1-s)}$, where $\psi(s) = e^{-1/s}I\{s > 0\}$. Then $g(s; f_1, f_2, s_0, s_1) := f_1(s) + (f_2(s) - f_1(s))\phi\left(\frac{s-s_0}{s_1-s_0}\right)$ is a smooth function from f_1 to f_2 on the interval $[s_0, s_1]$. In addition, the transformed function $\tilde{f}(s, t) = f_1(s)I\{t \leq T^* - \delta T\} + g(s; f_1, f_2, s_0, s_1)I\{T^* - \delta T < t < T^* + \delta T\} + f_2(s)I\{t > T^*\}$ is smooth in s . Here δ controls the smoothness of the transformation; smaller δ leads to more abrupt change and larger δ leads to smoother change. An example of $\tilde{f}(s, t)$ is shown in Figure 7.

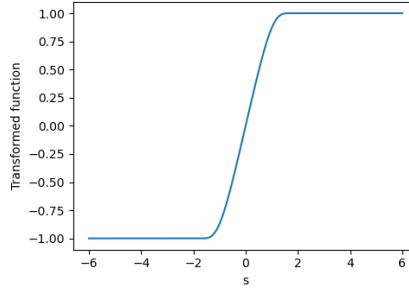


Fig 7: Smooth transformation of piecewise constant function: $f_1(s) = -I\{s \leq -2\}$ and $f_2(s) = I\{s \geq 2\}$.

The four simulations settings in Section 5.1 are specified as the following.

- (1) Time-homogeneous state transition function and piecewise constant reward function:

$$S_{0,t+1} = 0.5A_{0,t}S_{0,t} + z_{0,t}, t \in [0, T].$$

$$R_{0,t} = \begin{cases} r_1(S_{0,t}, A_{0,t}; t) \equiv -1.5A_{0,t}S_{0,t}, & \text{if } t \in [0, T^*) \\ r_2(S_{0,t}, A_{0,t}; t) \equiv A_{0,t}S_{0,t}, & \text{if } t \in [T^*, T], \end{cases}$$

- (2) Time-homogeneous state transition function and smooth reward function:

$$S_{0,t+1} = 0.5A_{0,t}S_{0,t} + z_{0,t}, t \in [0, T].$$

$$R_{0,t} = \begin{cases} r_1(S_{0,t}, A_{0,t}; t), & \text{if } t \in [0, T^* - \delta T), \\ g(S_{0,t}; r_1, r_2, T^* - \delta T, T^*), & \text{if } t \in [T^* - \delta T, T^*), \\ r_2(S_{0,t}, A_{0,t}; t), & \text{if } t \in [T^*, T]. \end{cases}$$

- (3) Piecewise constant state transition and time-homogeneous reward function:

$$S_{0,t+1} = \begin{cases} F_1(S_{0,t}, A_{0,t}; t) \equiv -0.5A_{0,t}S_{0,t} + z_{0,t}, & \text{if } t \in [0, T^*), \\ F_2(S_{0,t}, A_{0,t}; t) \equiv 0.5A_{0,t}S_{0,t} + z_{0,t}, & \text{if } t \in [T^*, T]. \end{cases}$$

$$R_{0,t} = 0.25A_{0,t}S_{0,t}^2 + 4S_{0,t}, t \in [0, T].$$

- (4) Smooth state transition and time-homogeneous reward function:

$$S_{0,t+1} = \begin{cases} F_1(S_{0,t}, A_{0,t}; t), & \text{if } t \in [0, T^*), \\ g(S_{0,t}; F_1, F_2, T^* - \delta T, T^*), & \text{if } t \in [T^* - \delta T, T^*), \\ F_2(S_{0,t}, A_{0,t}; t), & \text{if } t \in [T^*, T]. \end{cases}$$

$$R_{0,t} = 0.25A_{0,t}S_{0,t}^2 + 4S_{0,t}, t \in [0, T].$$

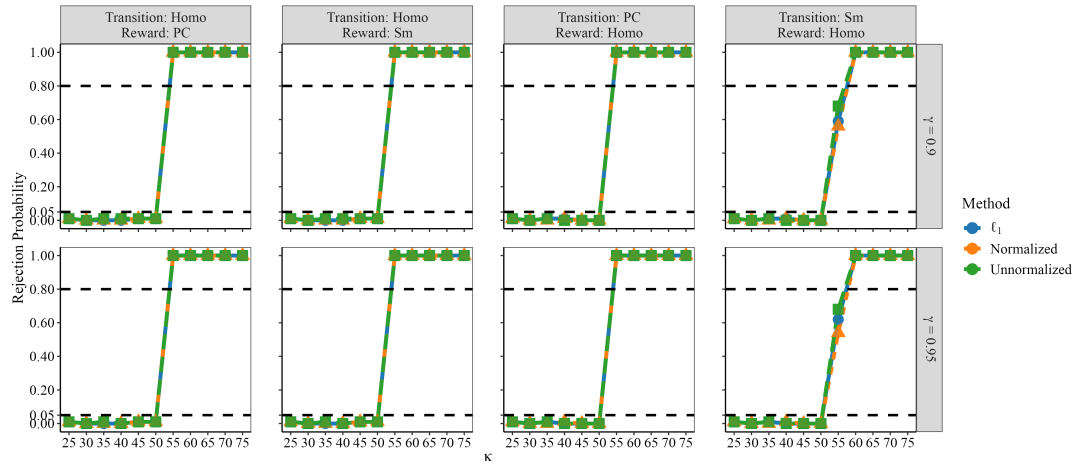


Fig 8: Empirical type I errors and powers of the proposed test and their associated 95% confidence intervals under settings described in Section 5.1, with $N = 100$. Abbreviations: Homo for homogeneous, PC for piecewise constant, and Sm for smooth.

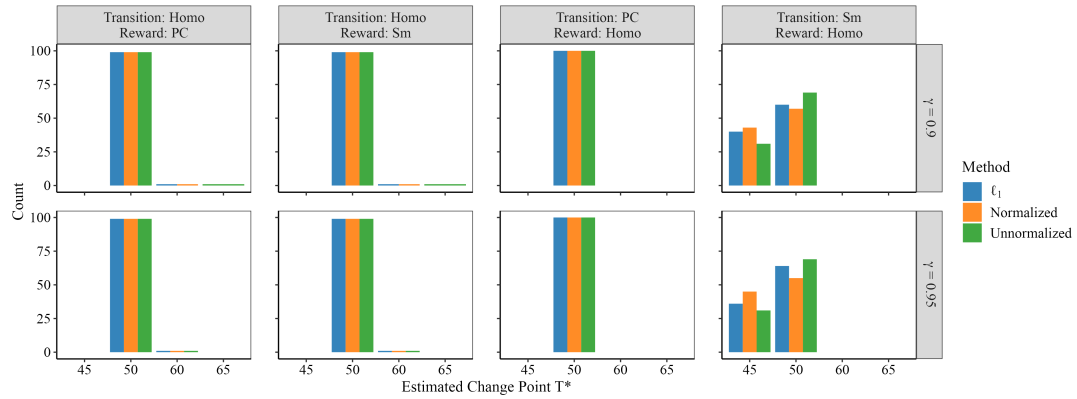
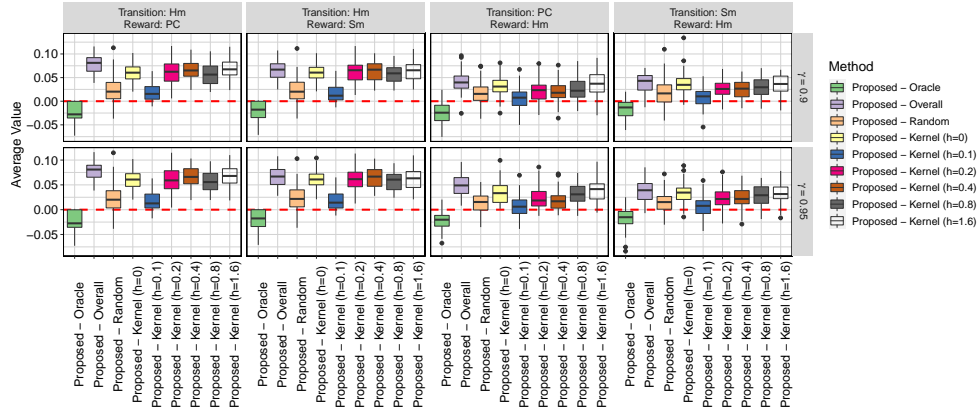
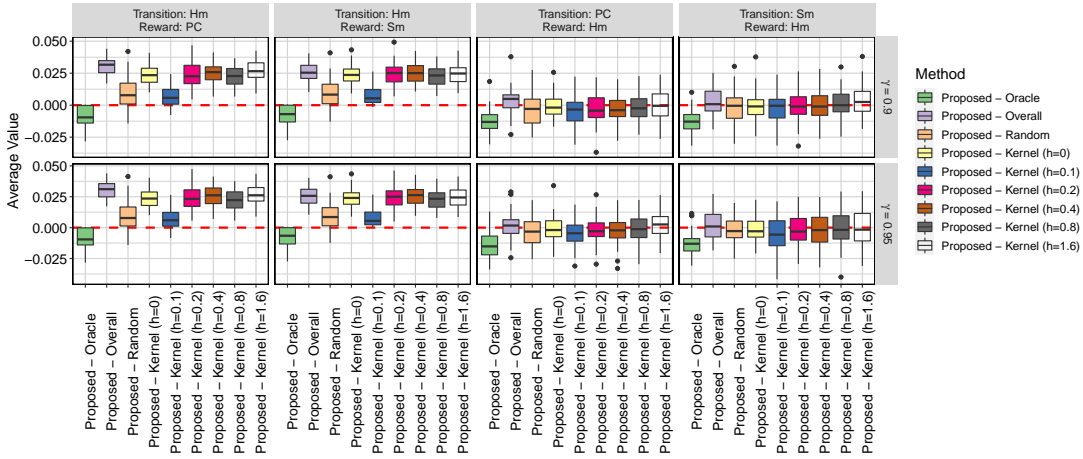


Fig 9: Distribution of detected change points under simulation settings in Section 5.1 with $N = 100$.



(a) Moderate signal.



(b) Weak signal.

Fig 10: Distribution of the difference between the expected return under the proposed policy and those under policies computed by other baseline methods, under settings in Section 5.1 with moderate and weak signal-to-noise ratios. The proposed policy is based on the change point detected by the ℓ_1 type test statistic. In all scenarios, we find the value results based on the normalized or unnormalized test statistics are similar to those of the integral test statistic.

D.4. Additional Simulation Results.